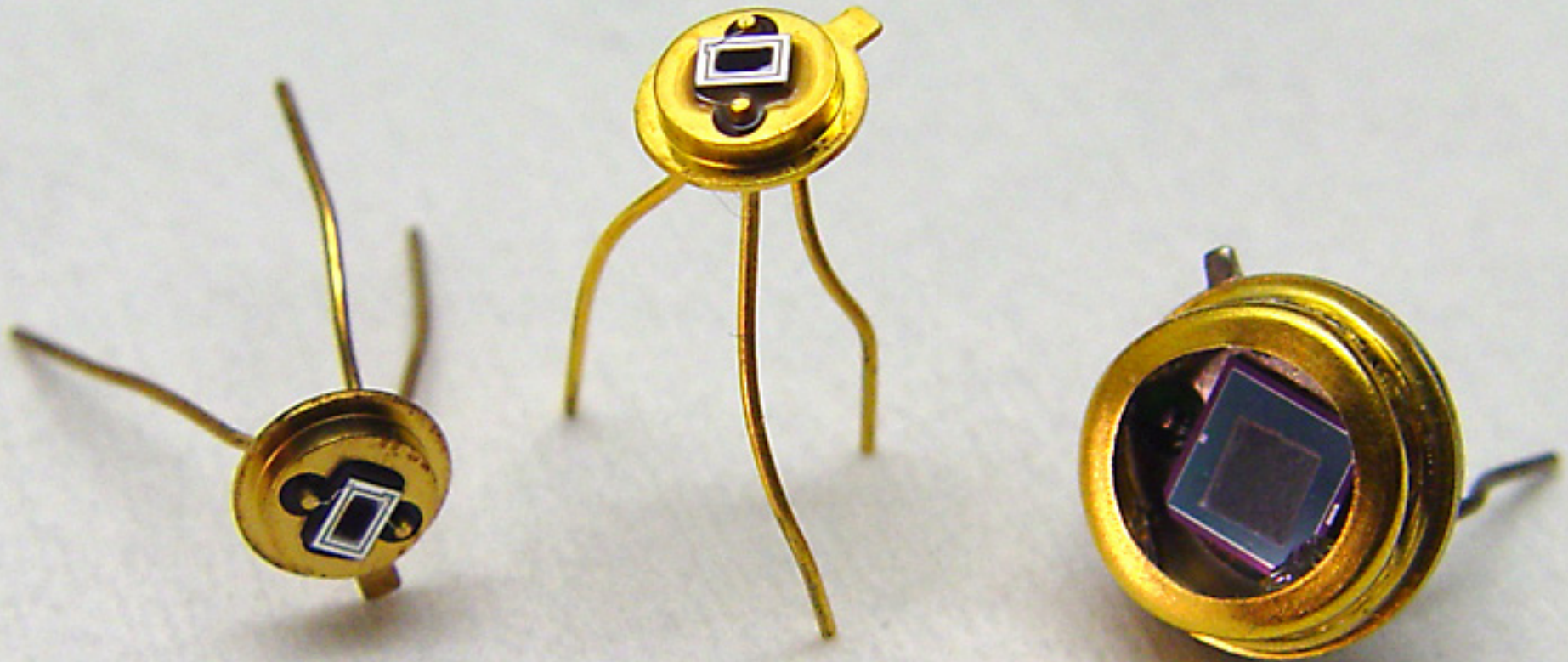


# Laser doping and texturing of silicon for advanced optoelectronic devices



Tsing Hua University  
Hsinchu, Republic of China, 29 June 2016



# Laser doping and texturing of silicon for advanced optoelectronic devices



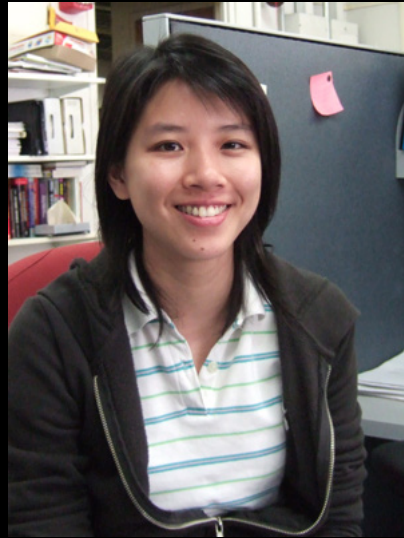
**@eric\_mazur**

Tsing Hua University  
Hsinchu, Republic of China, 29 June 2016





**Renee Sher**



**Yu-Ting Lin**



**Kasey Philips**



**Ben Franta**



**eric\_mazur**

**and also....**

**Hemi Gandhi**  
**Alexander Raymond**  
**Marc Winkler**  
**Eric Diebold**  
**Haifei Albert Zhang**  
**Dr. Brian Tull**  
**Dr. Jim Carey (SiOnyx)**  
**Prof. Tsing-Hua Her (UNC Charlotte)**  
**Dr. Shrenik Deliwala**  
**Dr. Richard Finlay**  
**Dr. Michael Sheehy**  
**Dr. Claudia Wu**  
**Dr. Rebecca Younkin**  
**Prof. Catherine Crouch (Swarthmore)**  
**Prof. Mengyan Shen (Lowell U)**  
**Prof. Li Zhao (Fudan U)**  
  
**Prof. Alan Aspuru-Guzik**  
**Prof. Michael Aziz**  
**Prof. Michael Brenner**  
**Prof. Cynthia Friend**  
**Prof. Howard Stone**

**Dr. Martin Pralle (SiOnyx)**  
**and everyone else at SiOnyx...**

**Prof. Tonio Buonassisi (MIT)**  
**Prof. Silvija Gradecak (MIT)**  
**Prof. Jeff Grossman (MIT)**  
**Dr. Bonna Newman (MIT)**  
**Joe Sullivan (MIT)**  
**Matthew Smith (MIT)**

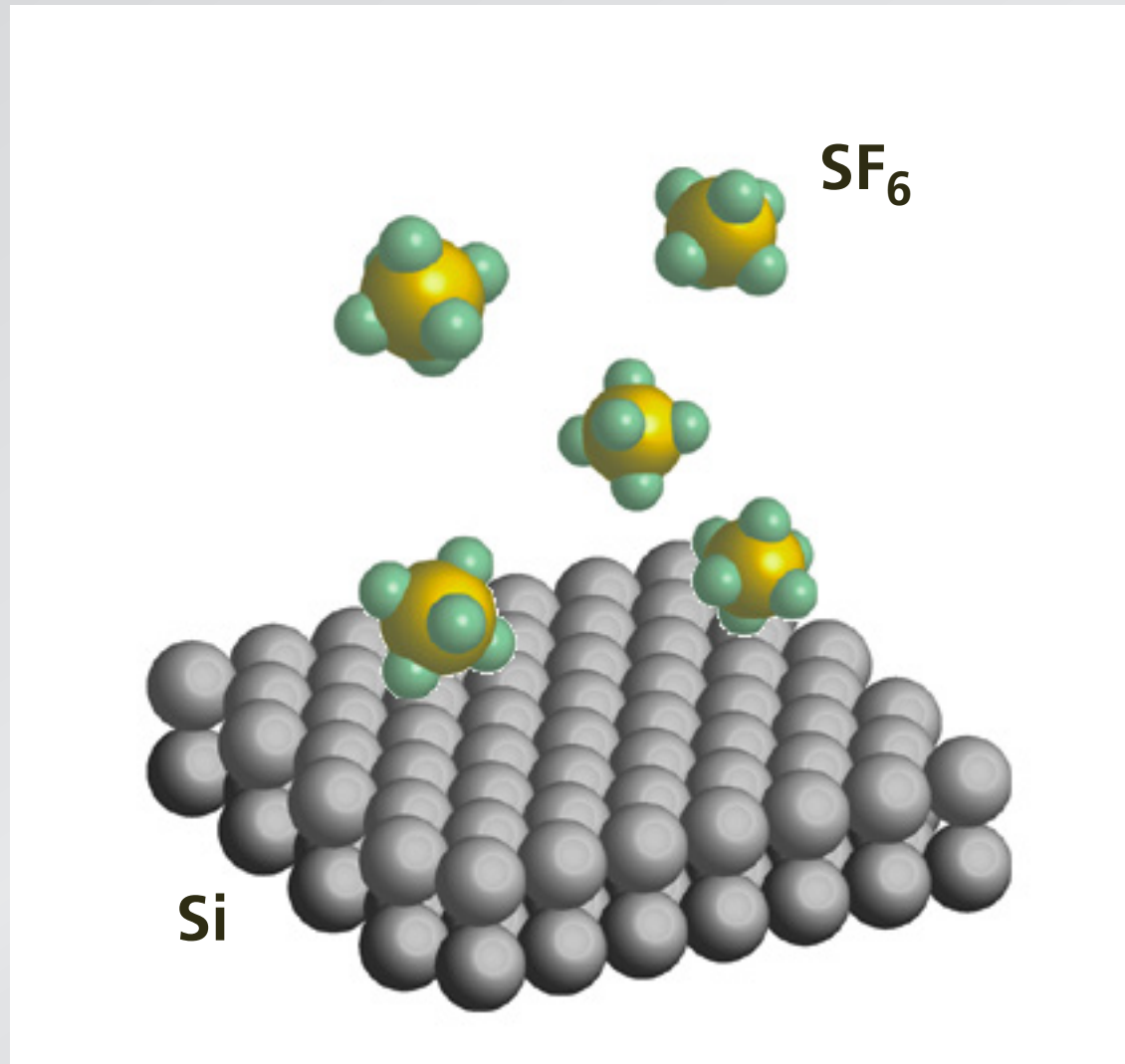
**Prof. Augustinus Asenbaum (Vienna)**

**Dr. François Génin (LLNL)**  
**Mark Wall (LLNL)**

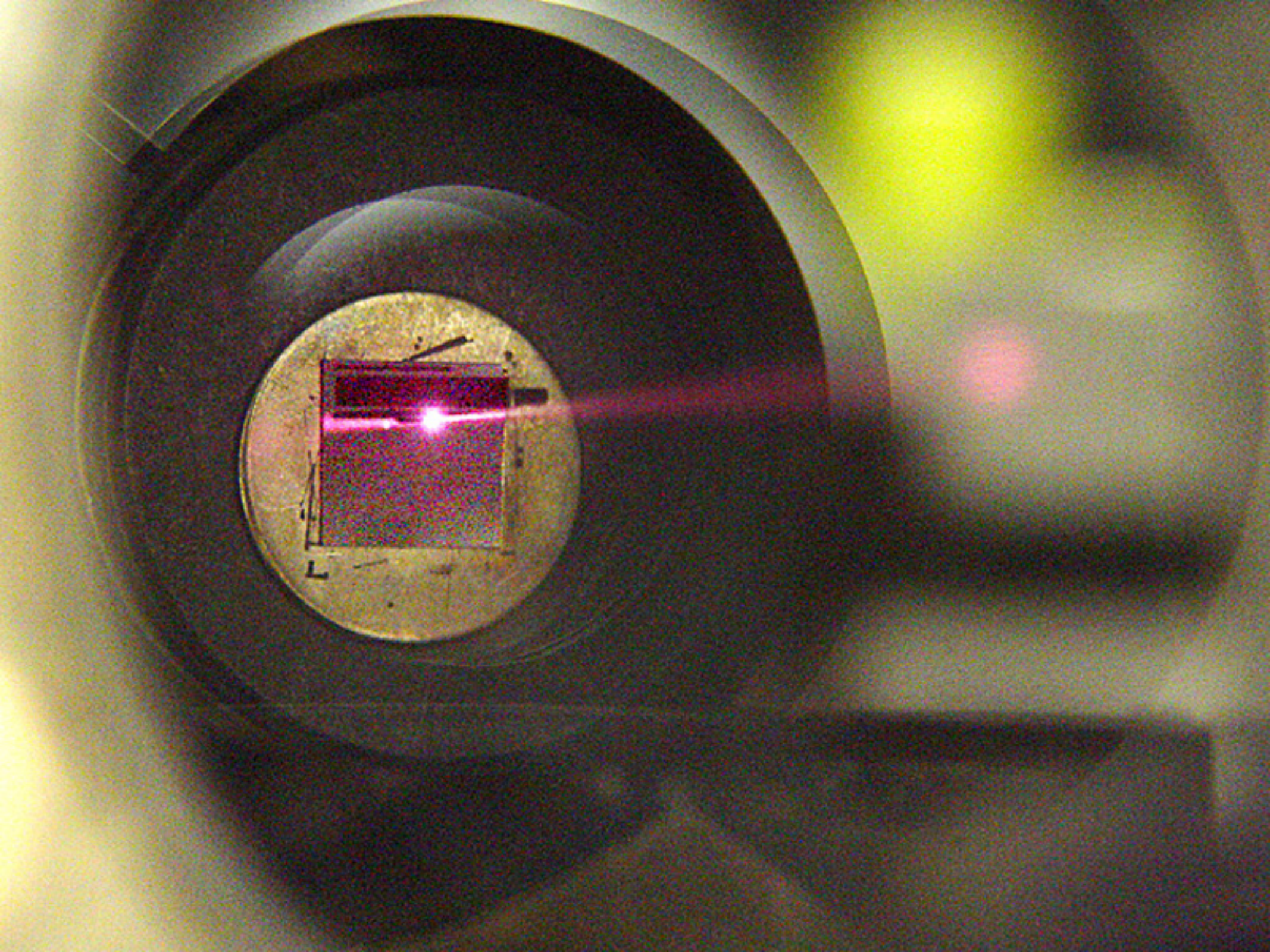
**Dr. Richard Farrell (RMD)**  
**Dr. Arie Karger (RMD)**  
**Dr. Richard Meyers (RMD)**

**Dr. Pat Maloney (NVSED)**

**Dr. Jeffrey Warrander (ARDEC)**

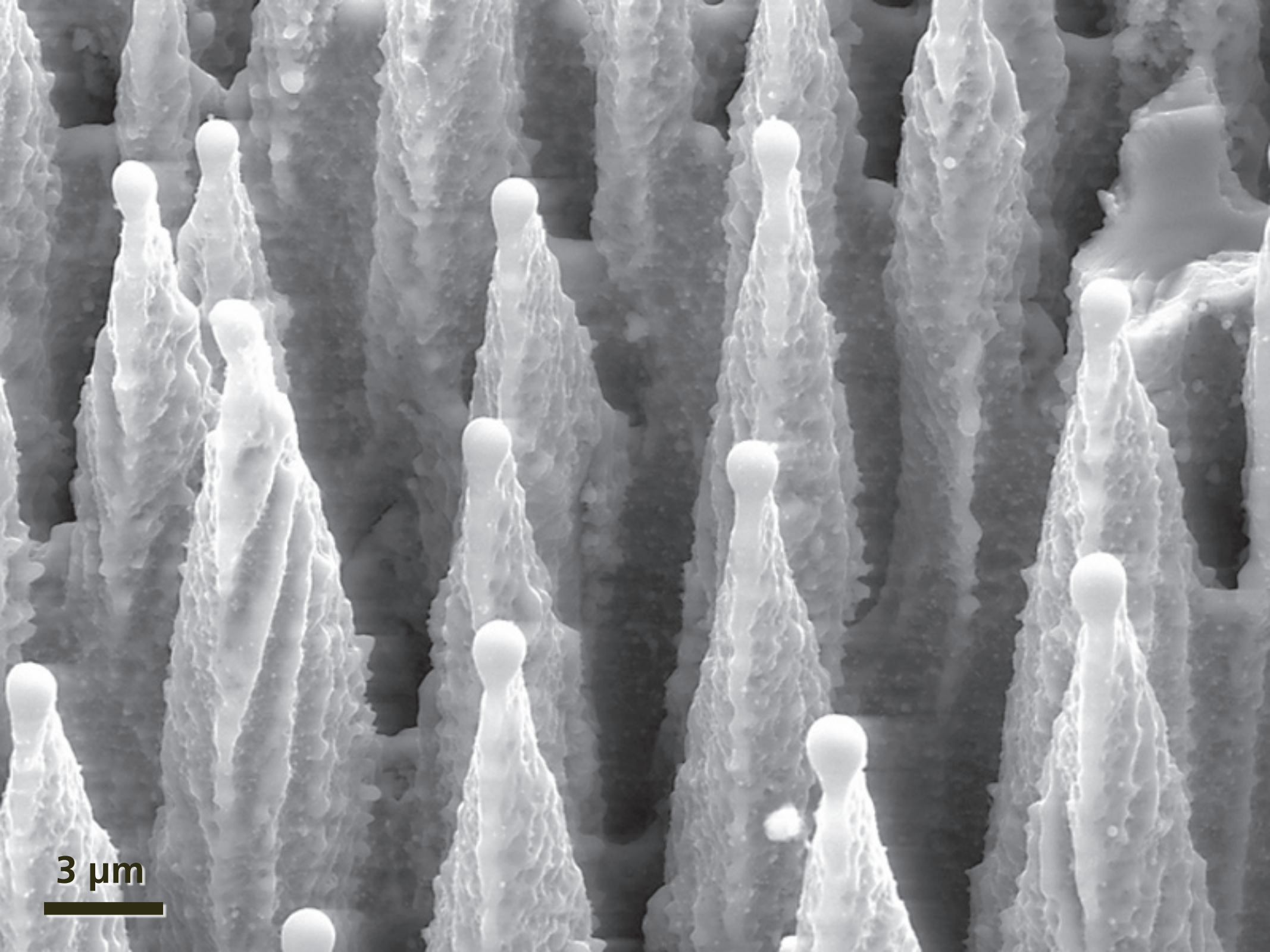


irradiate with 100-fs 10 kJ/m<sup>2</sup> pulses





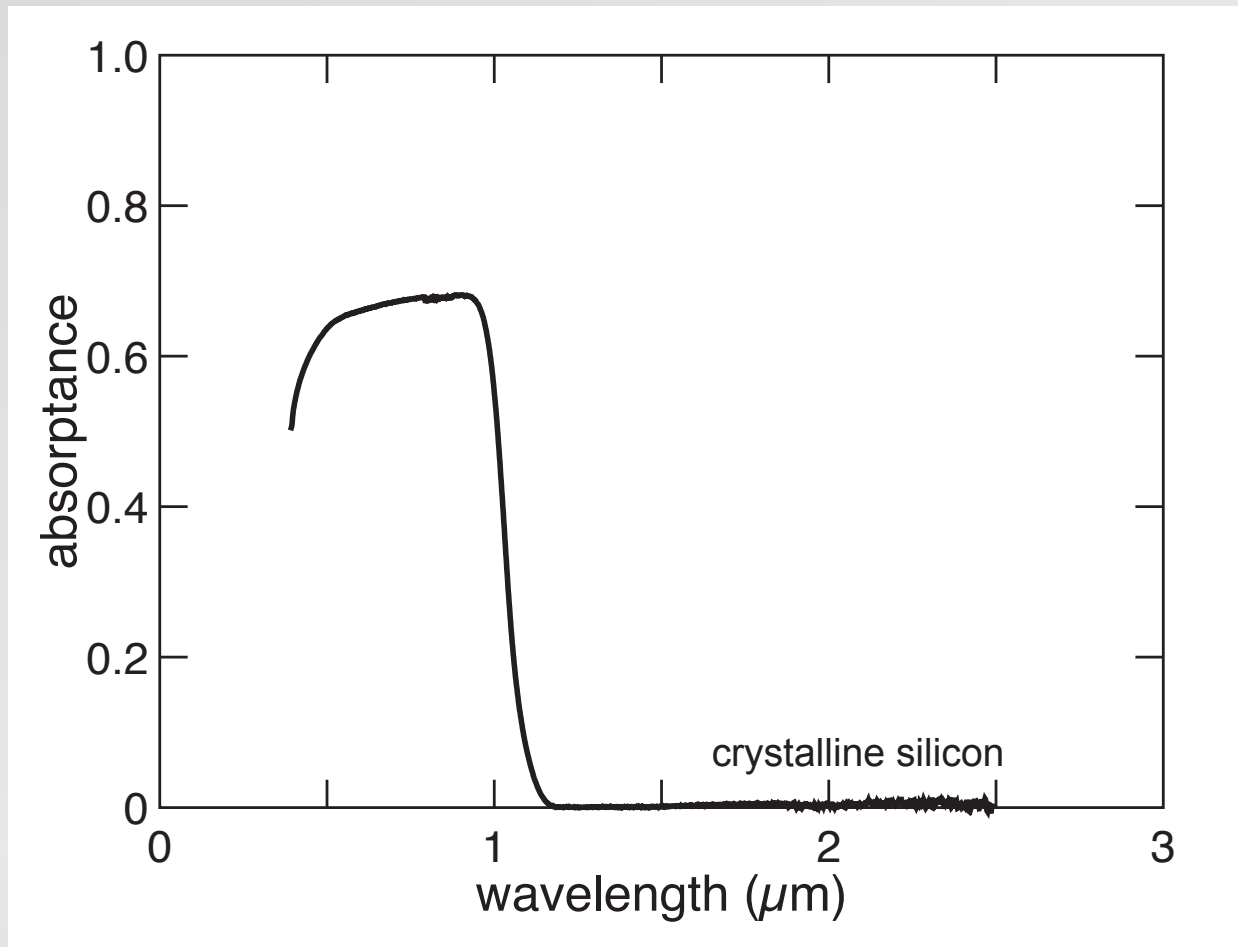
**"black silicon"**



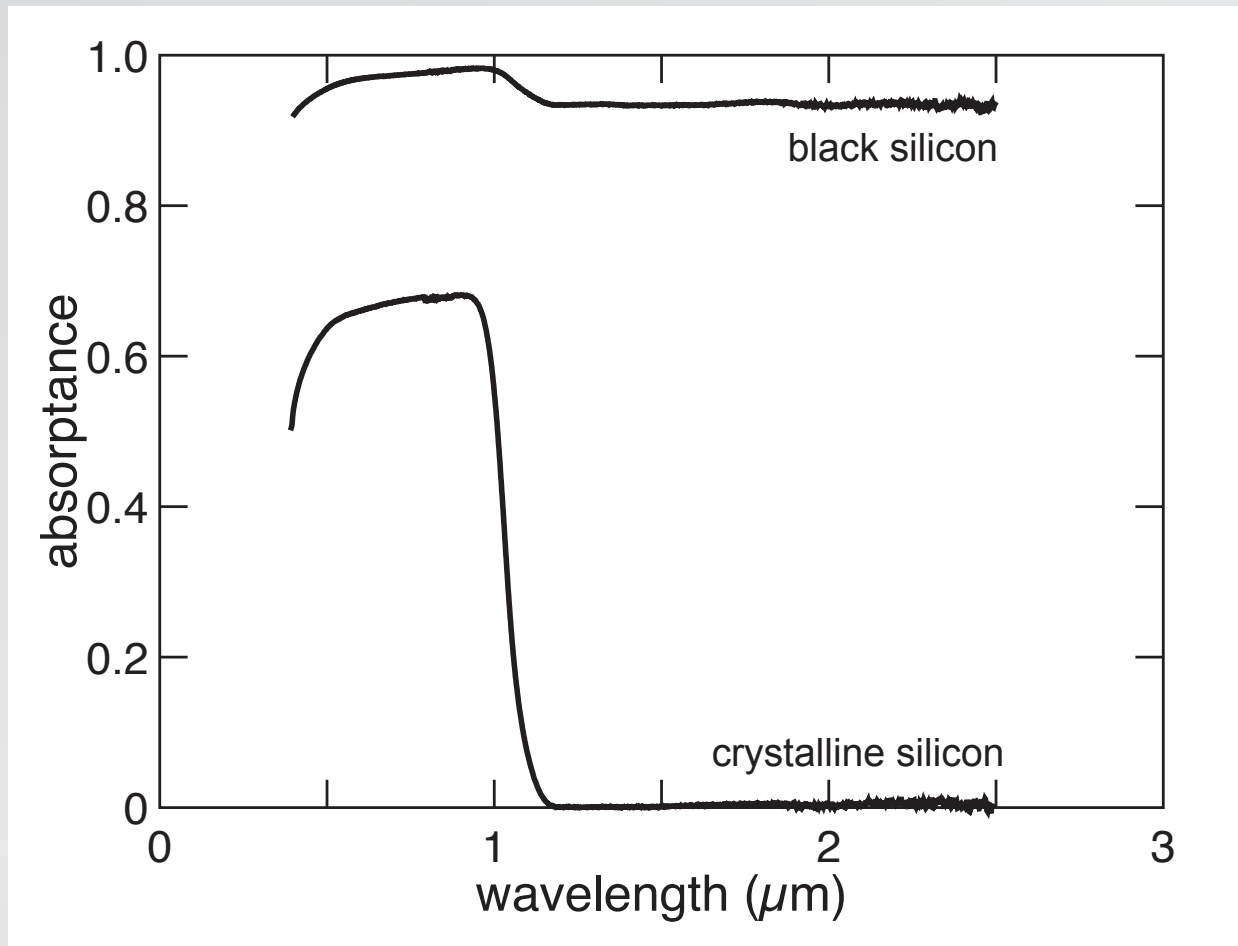
3  $\mu\text{m}$

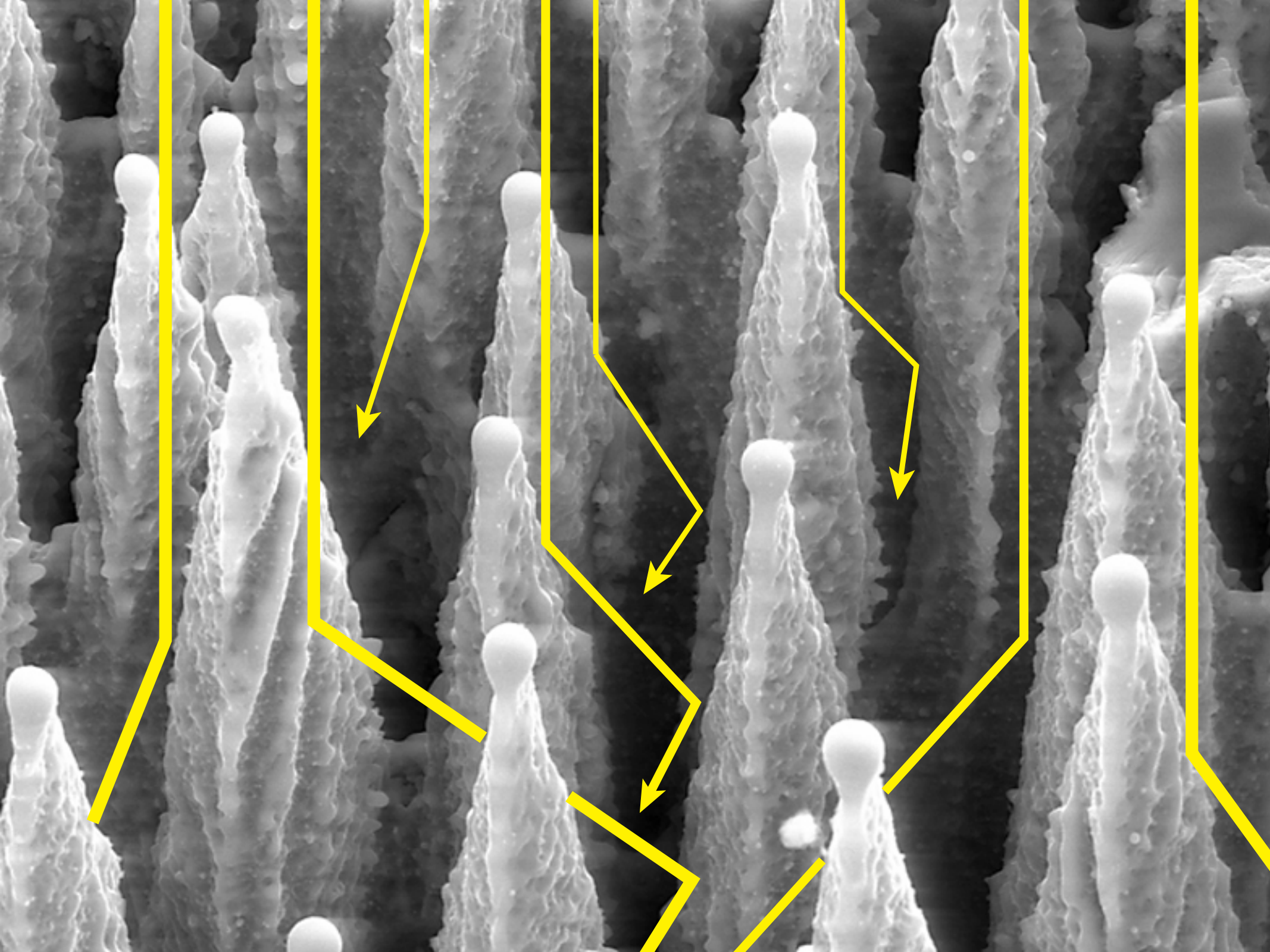


absorptance  $(1 - R_{int} - T_{int})$

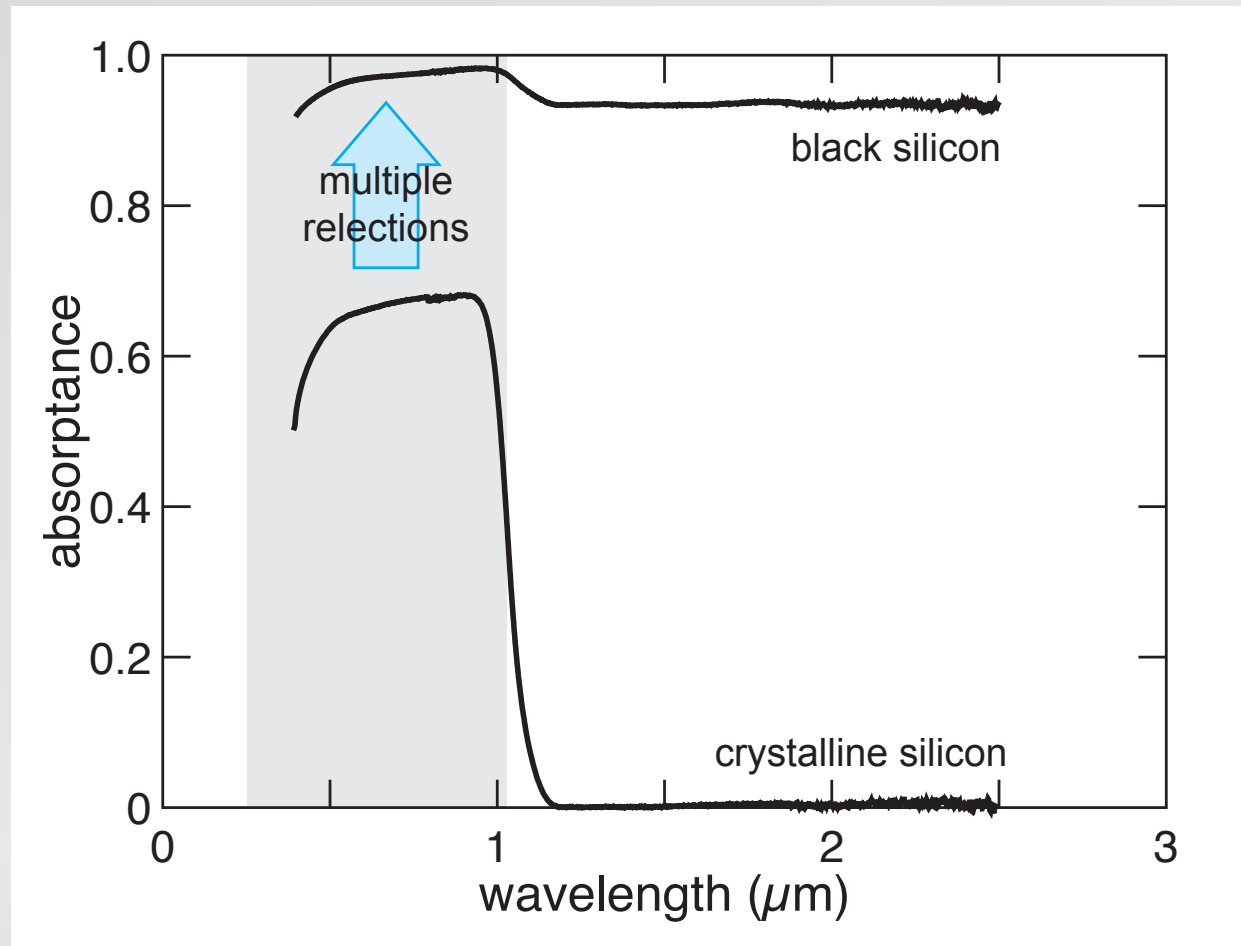


absorptance  $(1 - R_{int} - T_{int})$

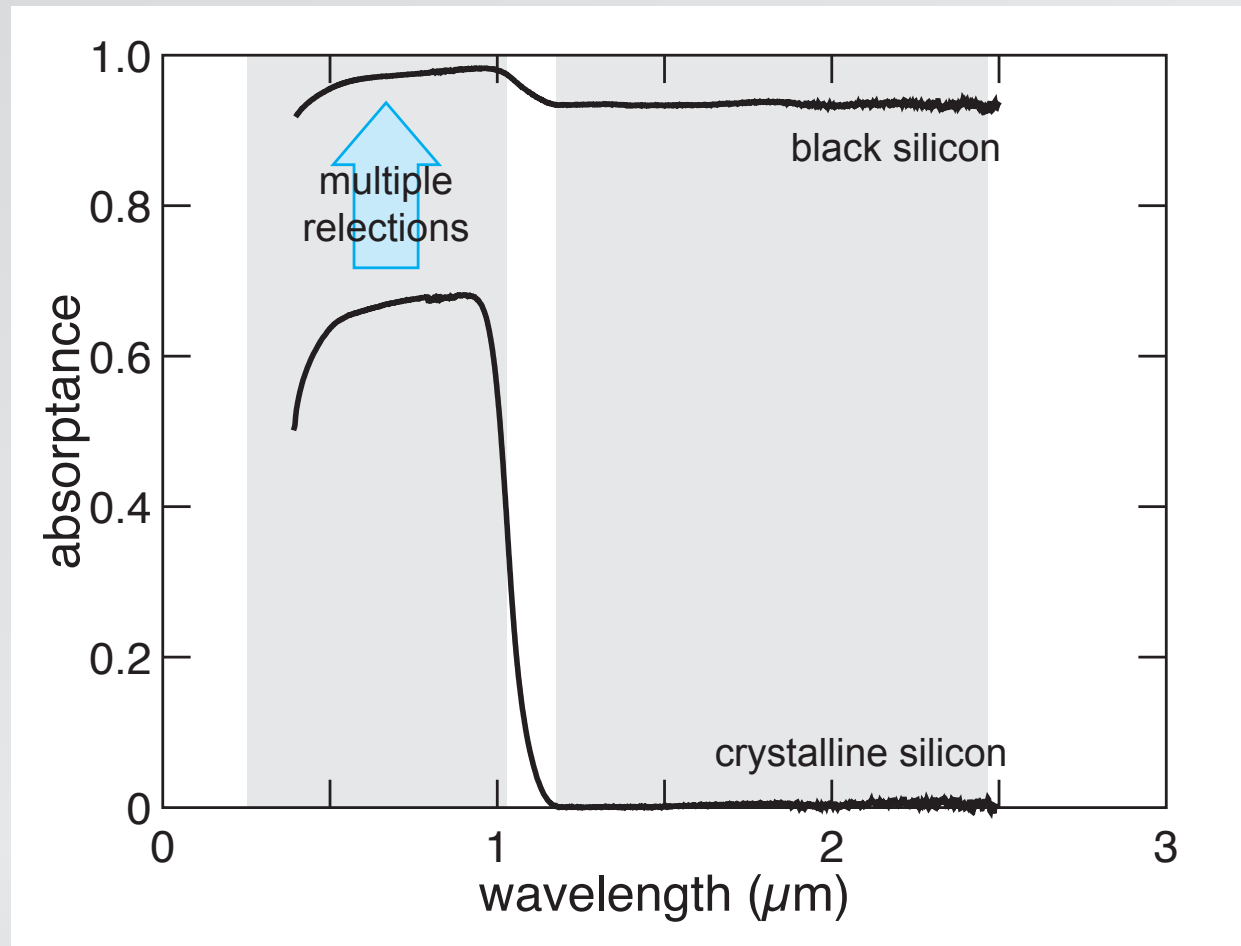




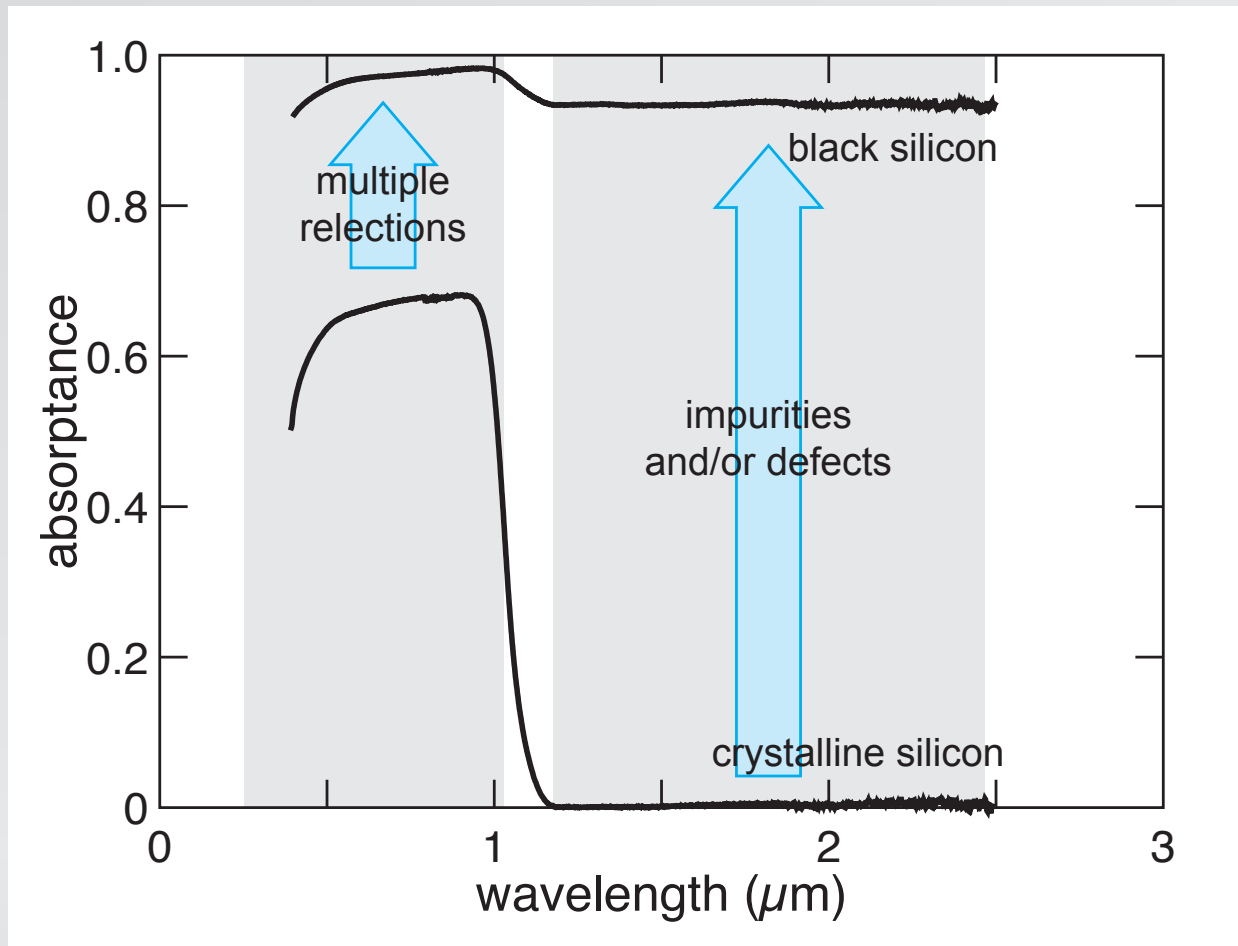
absorptance  $(1 - R_{int} - T_{int})$



absorptance ( $1 - R_{int} - T_{int}$ )



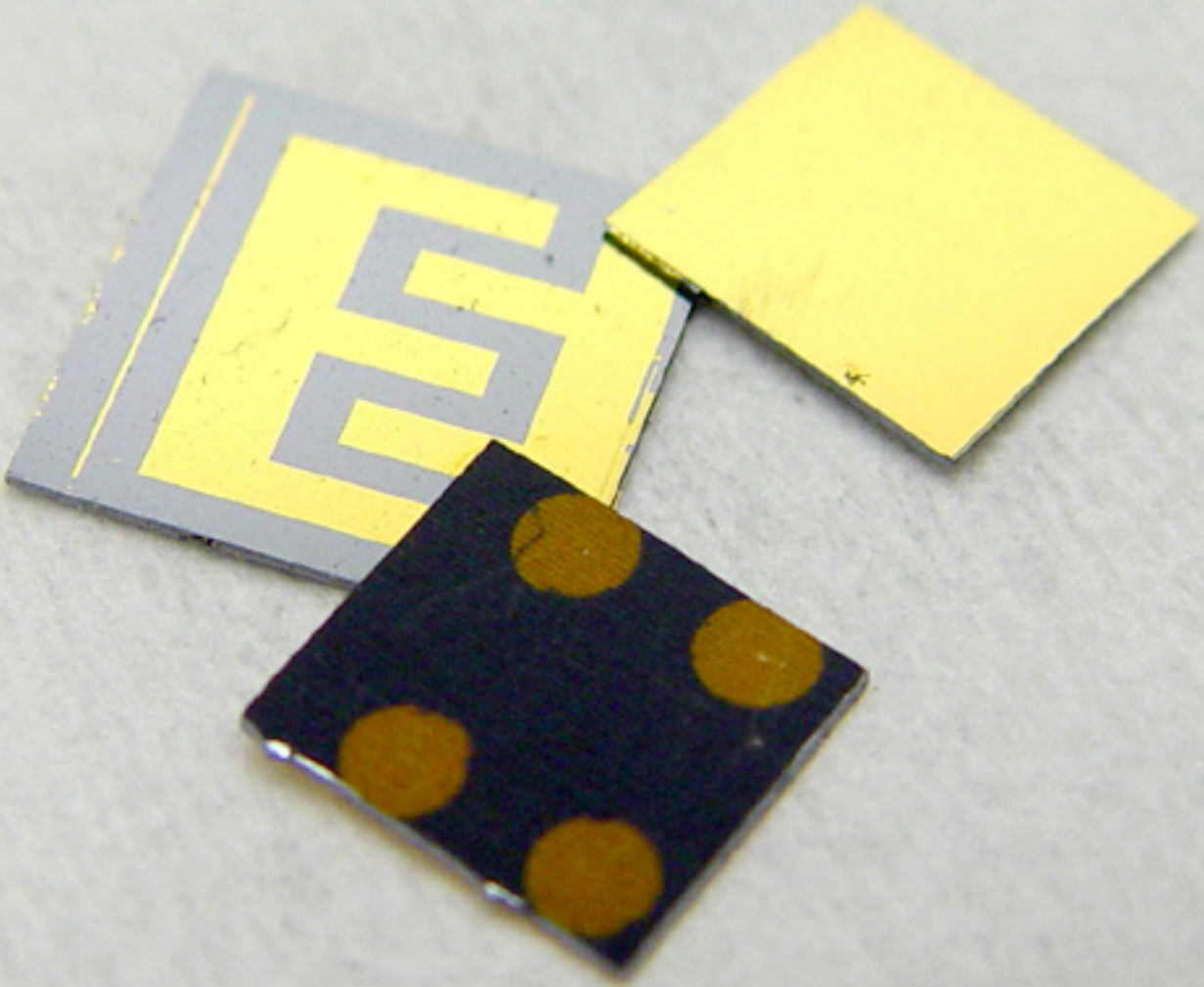
absorptance ( $1 - R_{int} - T_{int}$ )



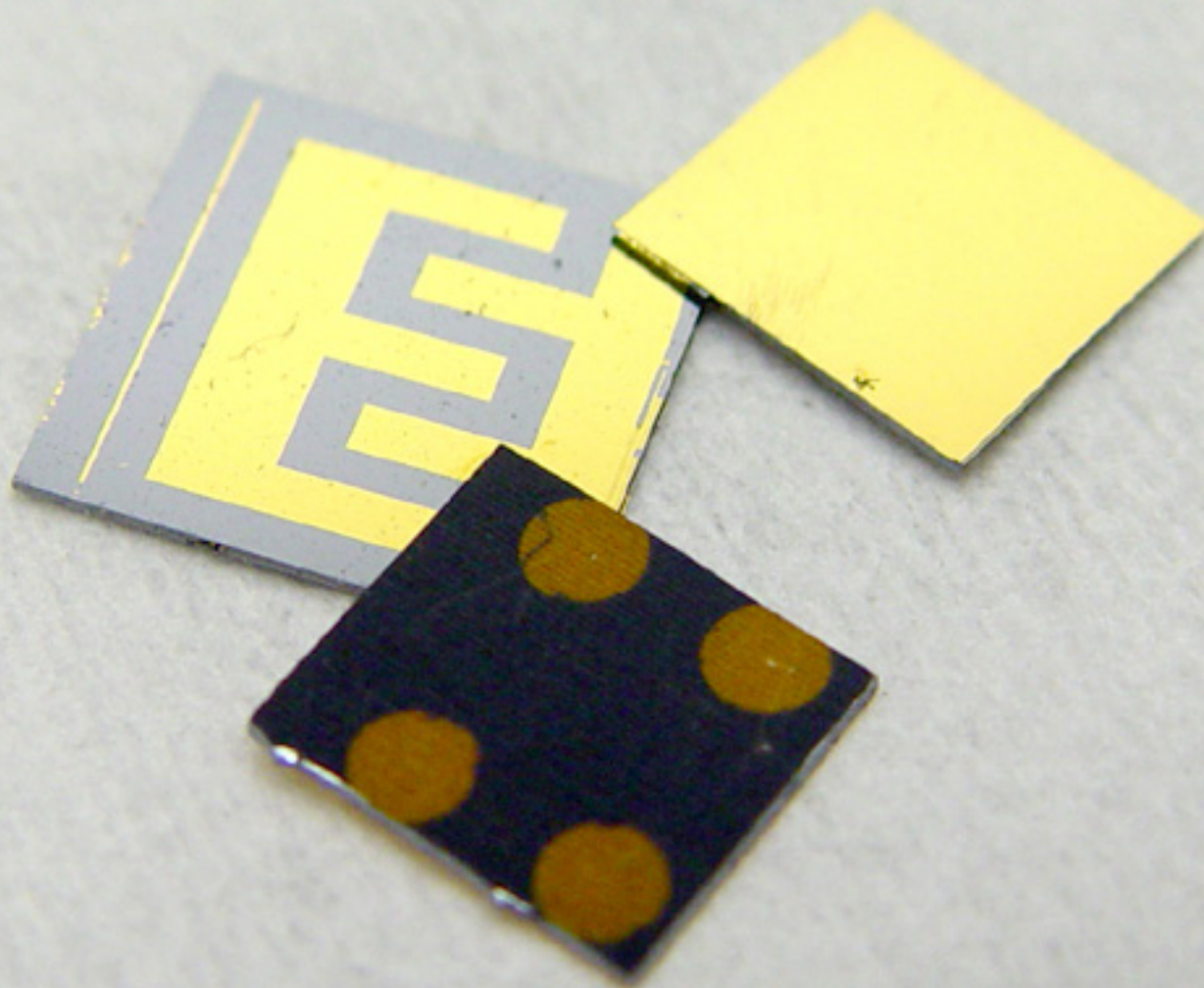
A scanning electron micrograph (SEM) showing a surface with a dense, regular array of small, conical structures. The structures are arranged in a grid-like pattern, with each structure having a rounded, conical top and a narrower base. The overall appearance is that of a highly textured, porous surface.

**laser treatment causes:**

- **surface structuring**
- **inclusion of dopants**

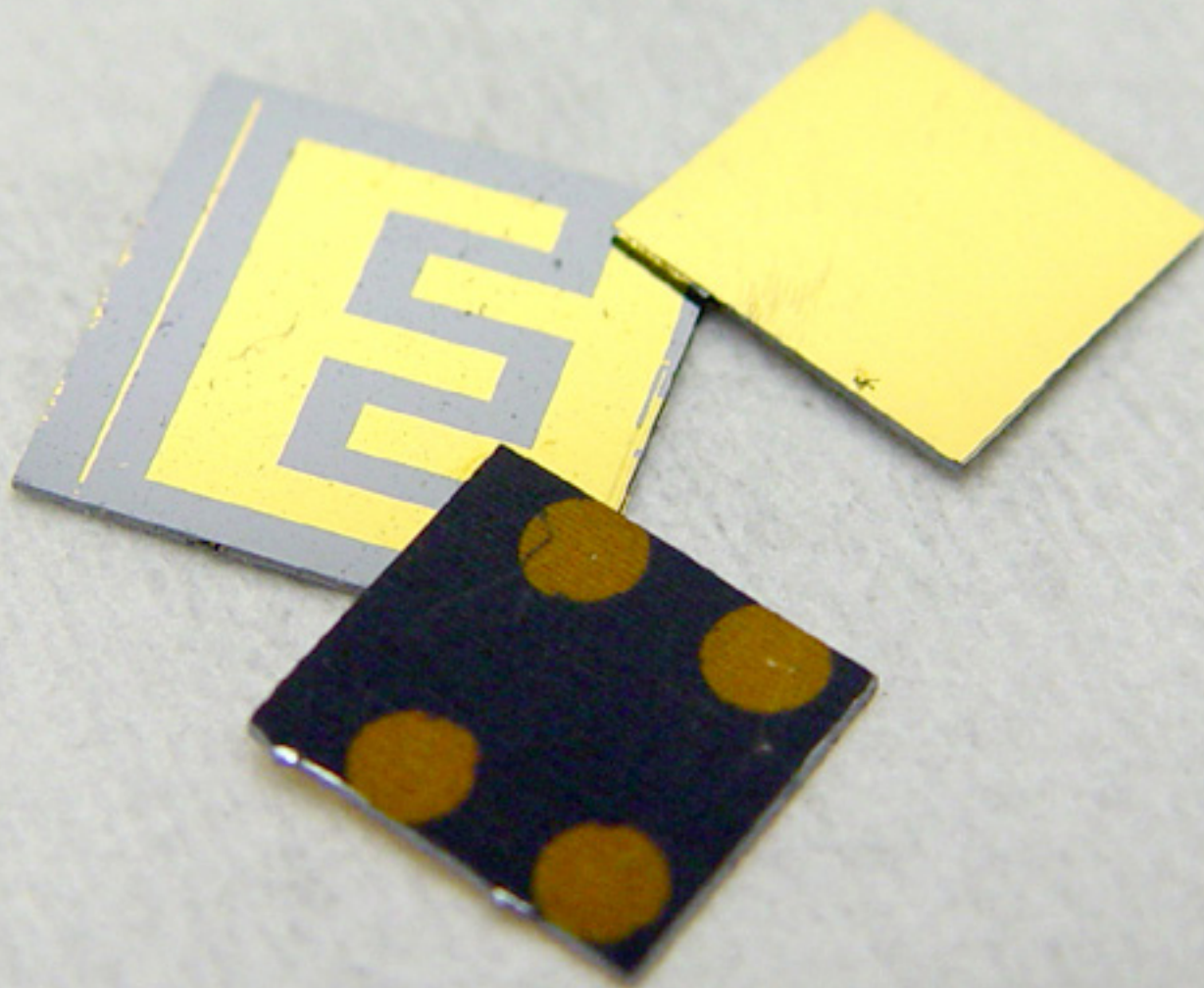






**1** properties

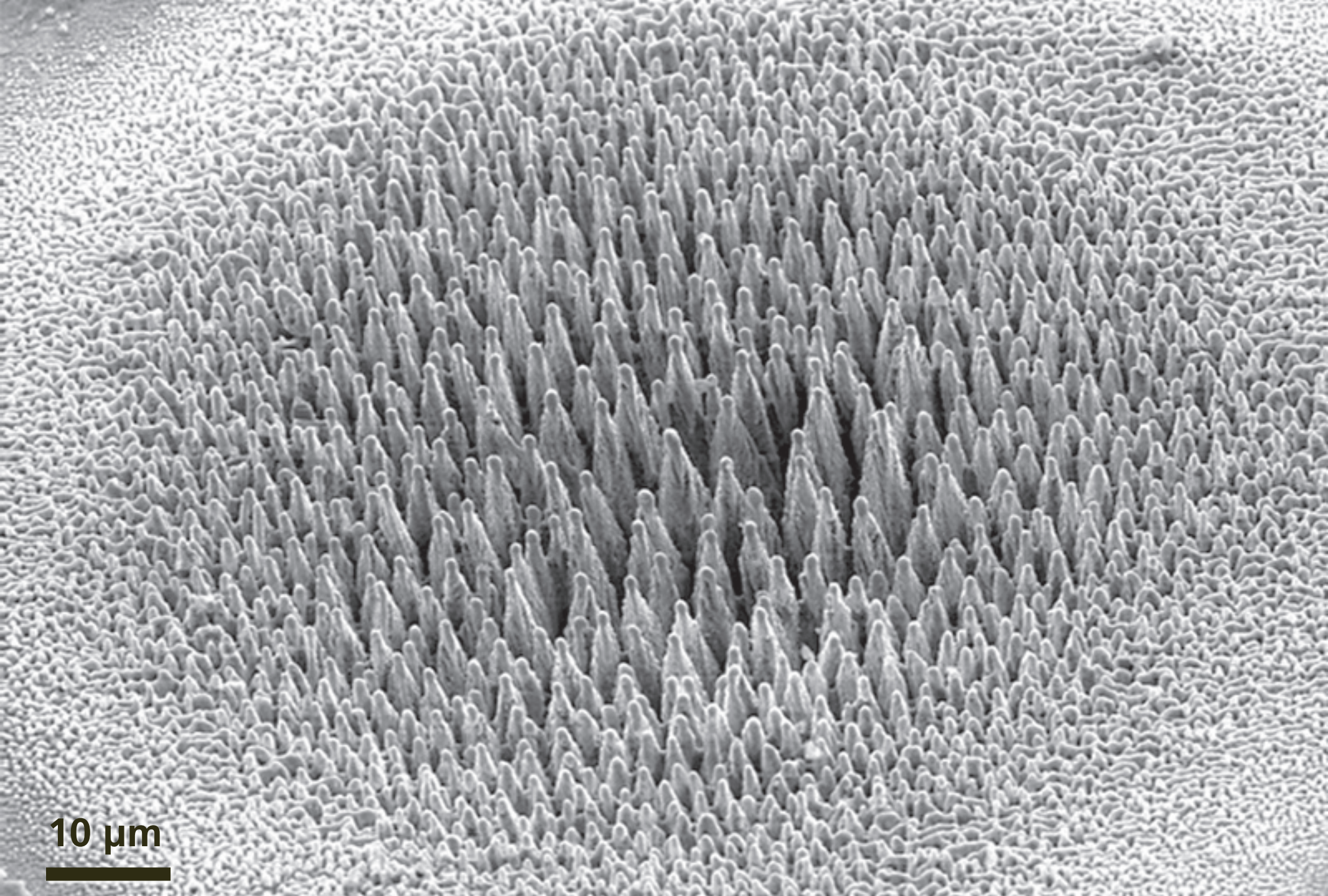
**2** intermediate band



**1** properties

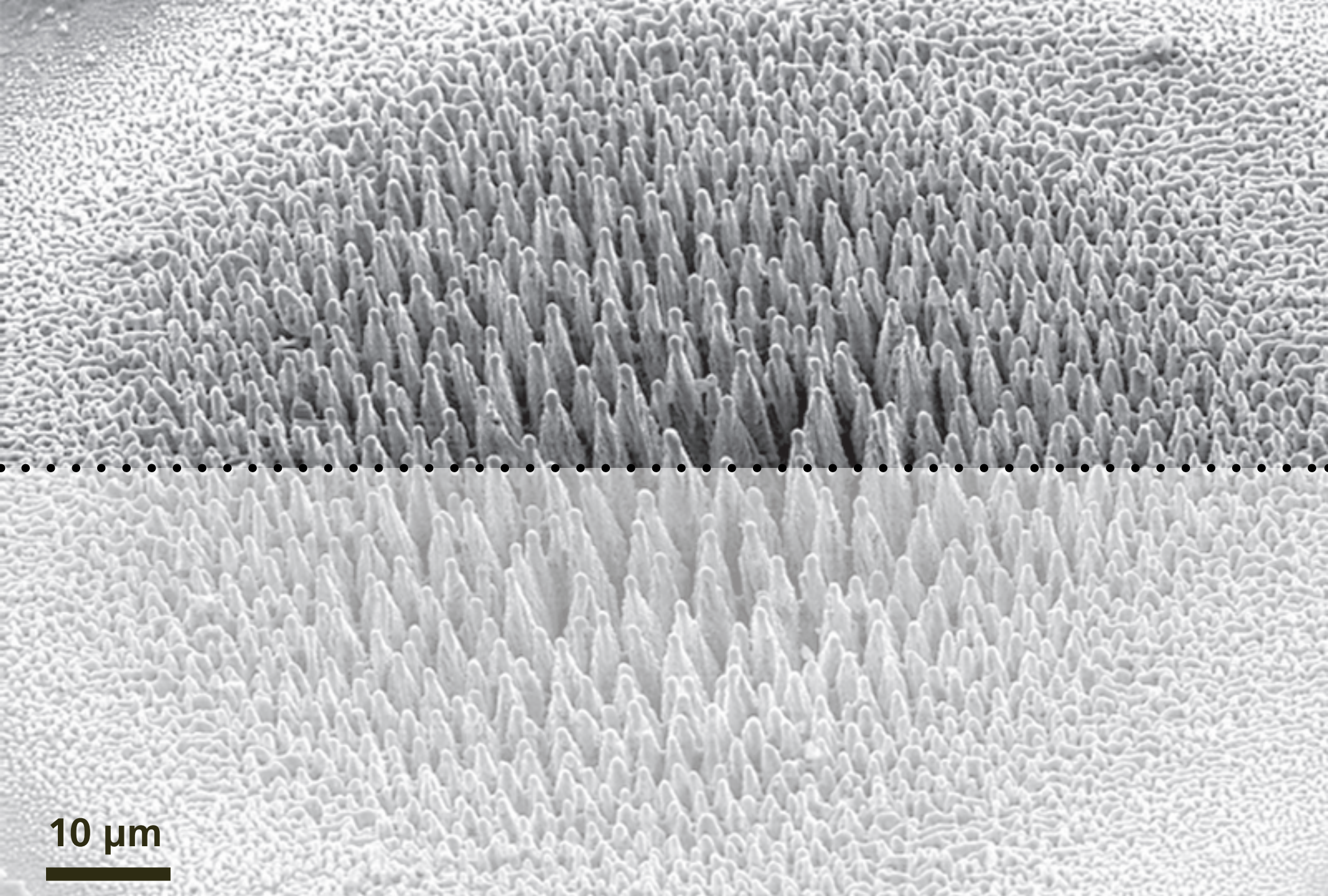
**2** intermediate band

**3** devices



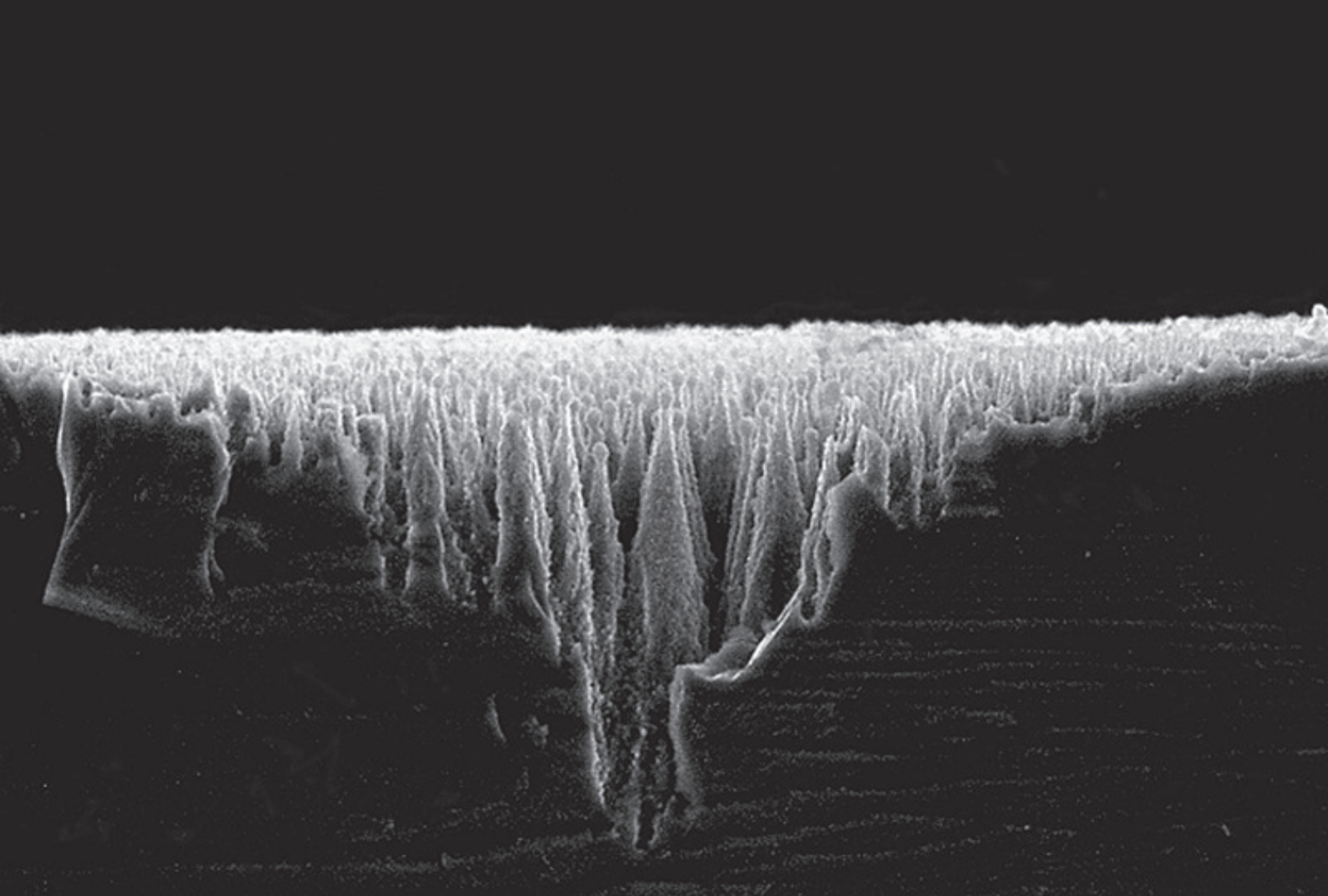
10  $\mu\text{m}$

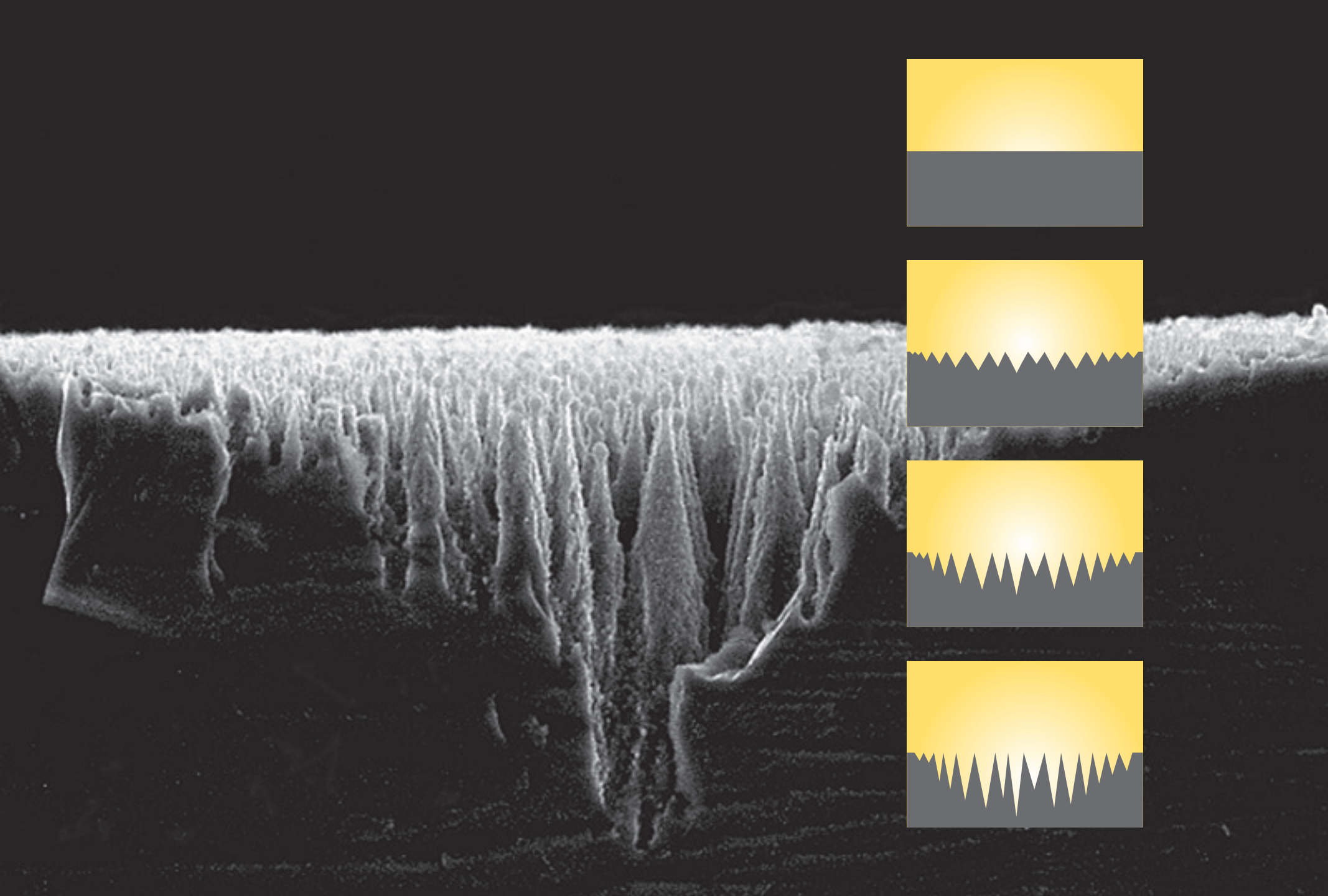
**1** properties



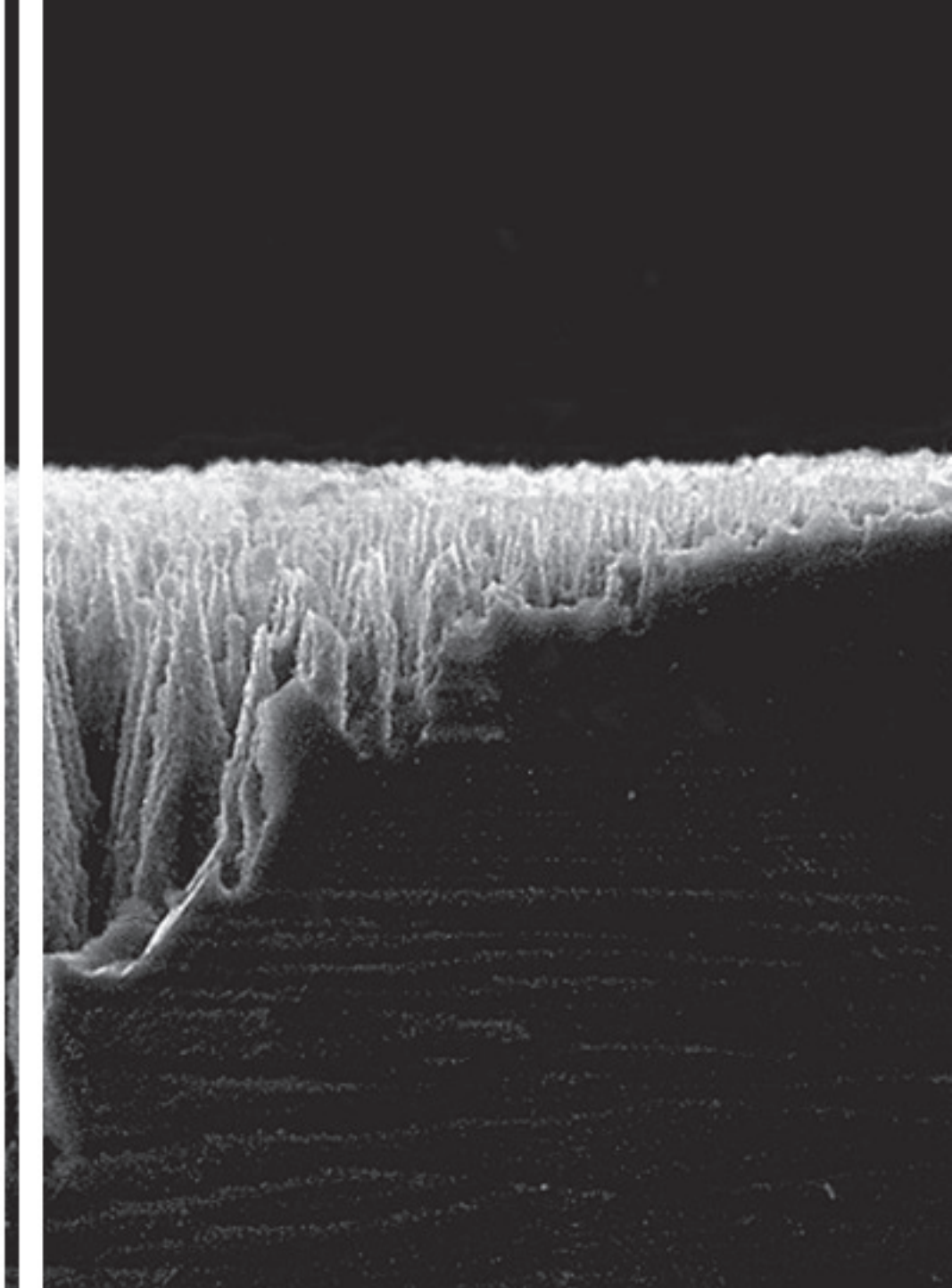
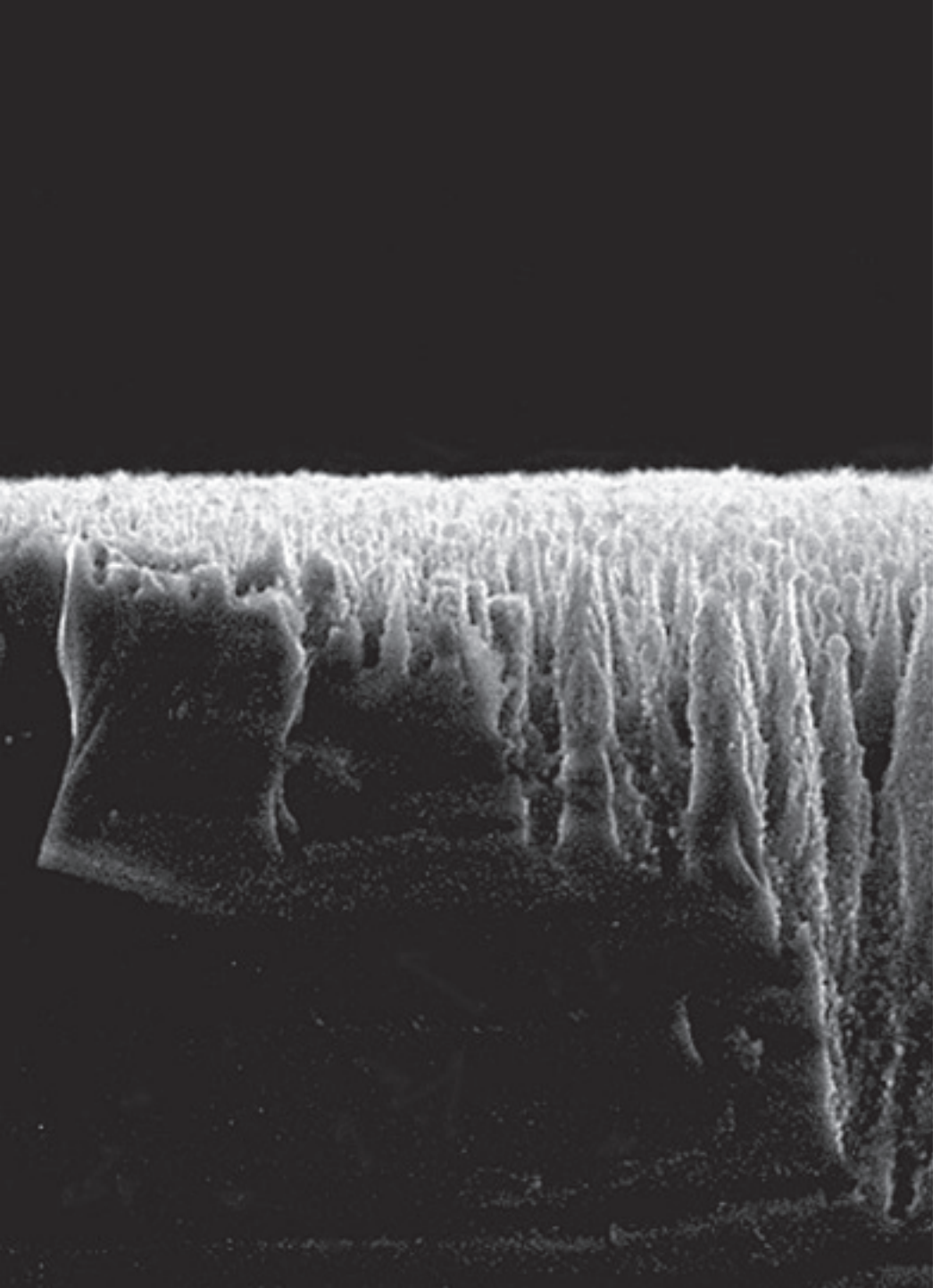
10 μm

**1** properties

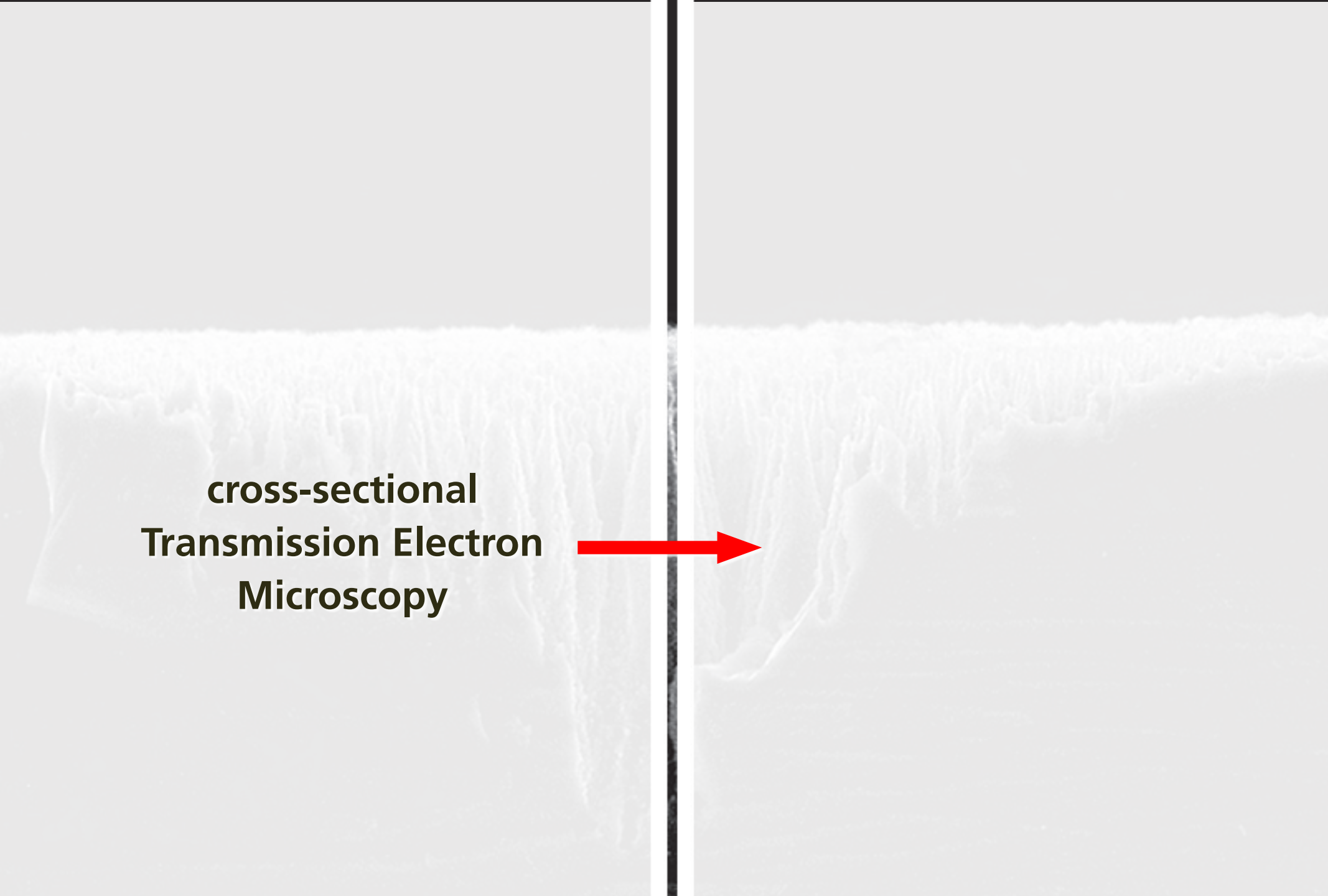




**1** properties



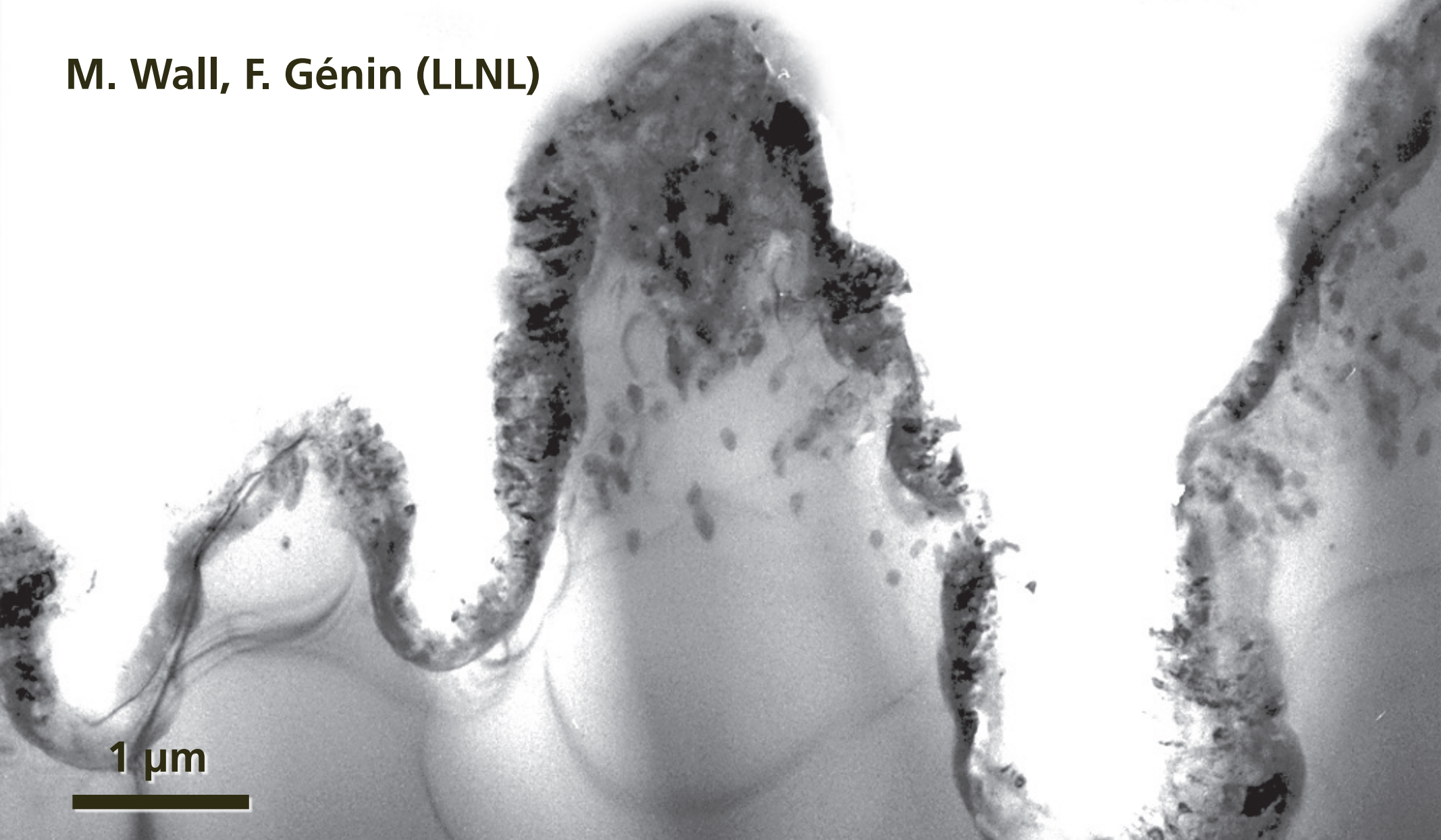
**1** properties



**cross-sectional  
Transmission Electron  
Microscopy**

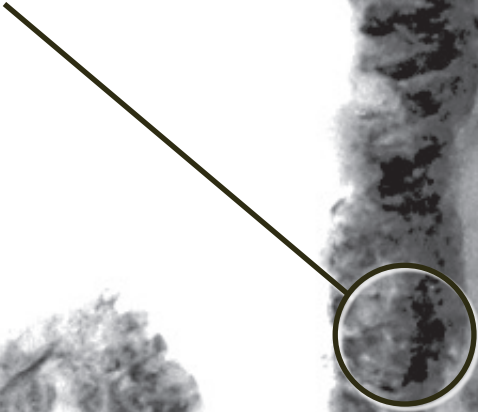


M. Wall, F. Génin (LLNL)

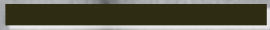


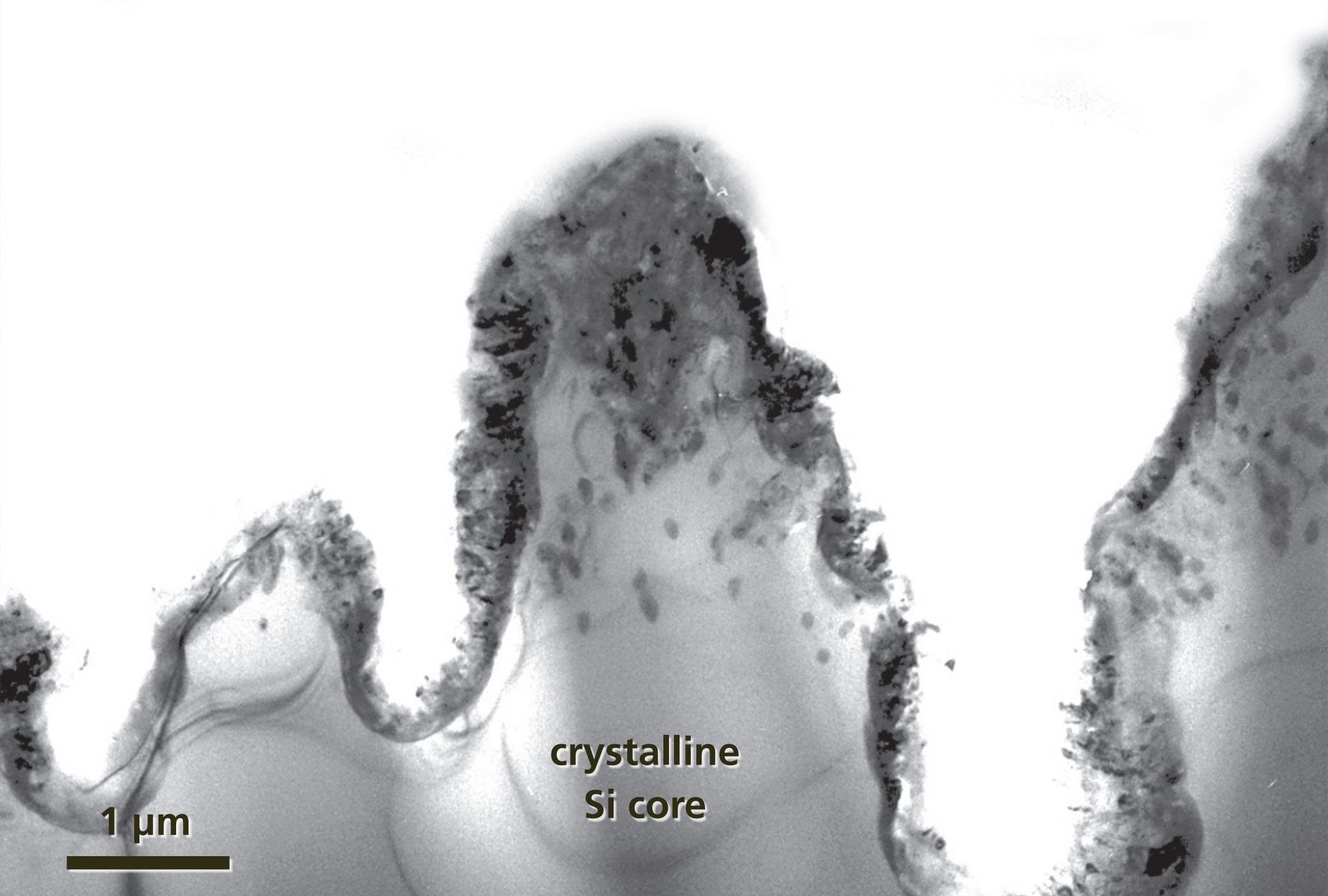
1 μm

**disordered  
surface layer**



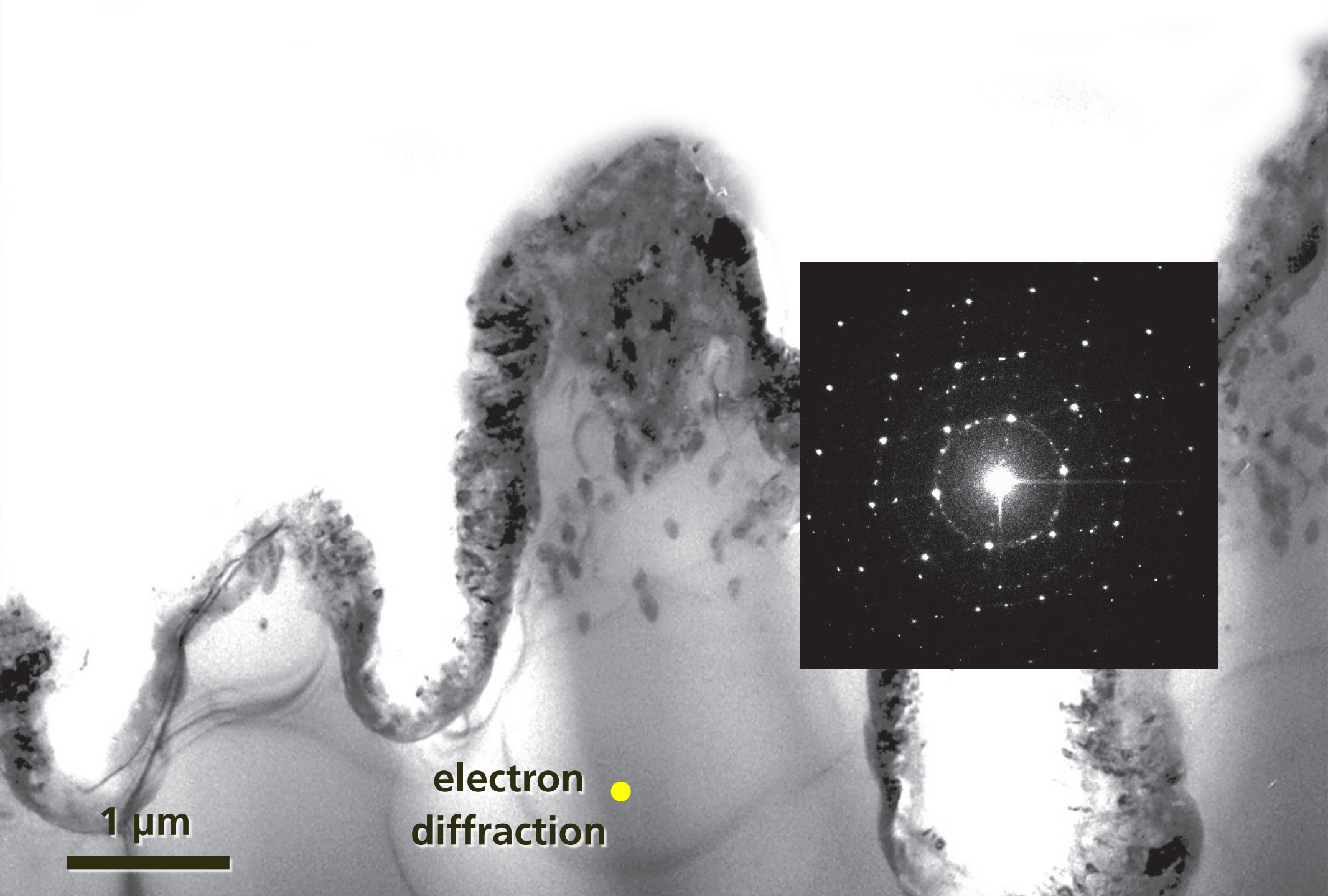
**1  $\mu\text{m}$**





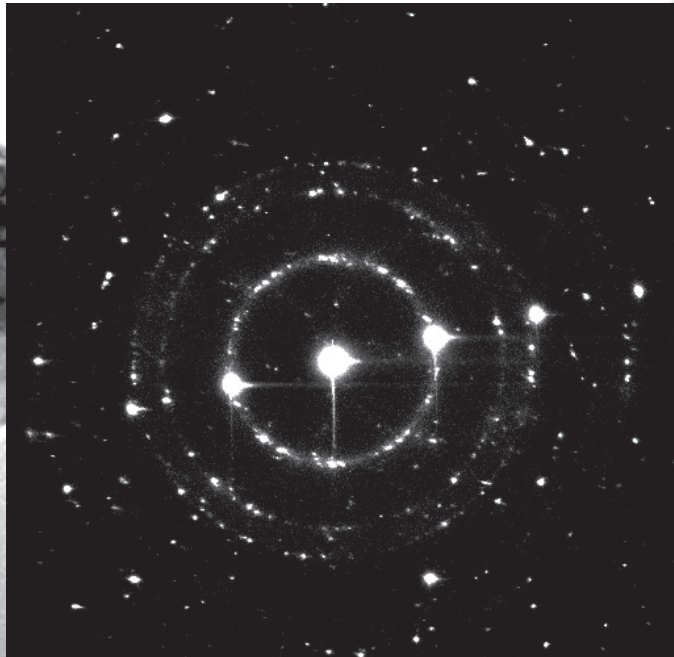
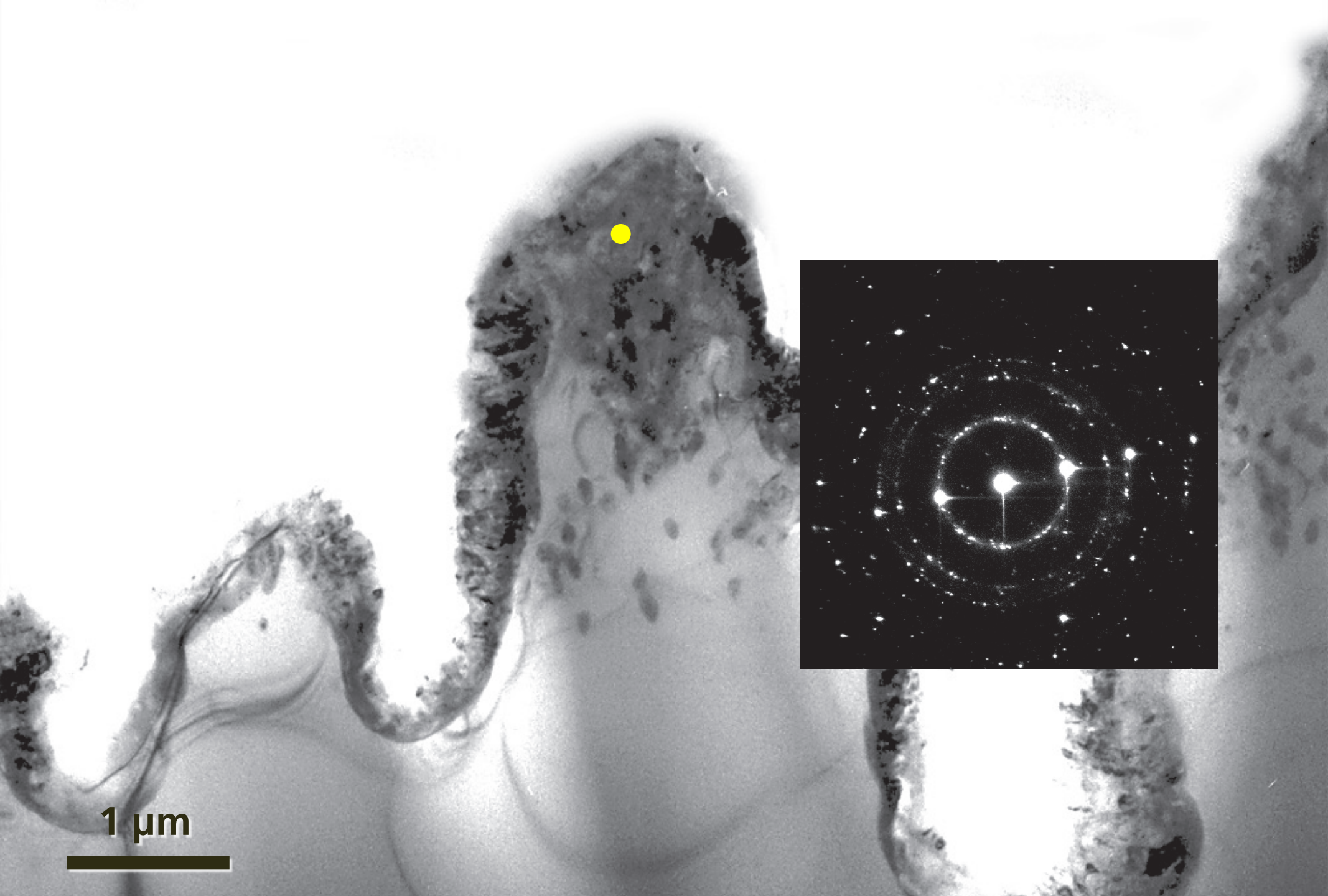
crystalline  
Si core

1 μm

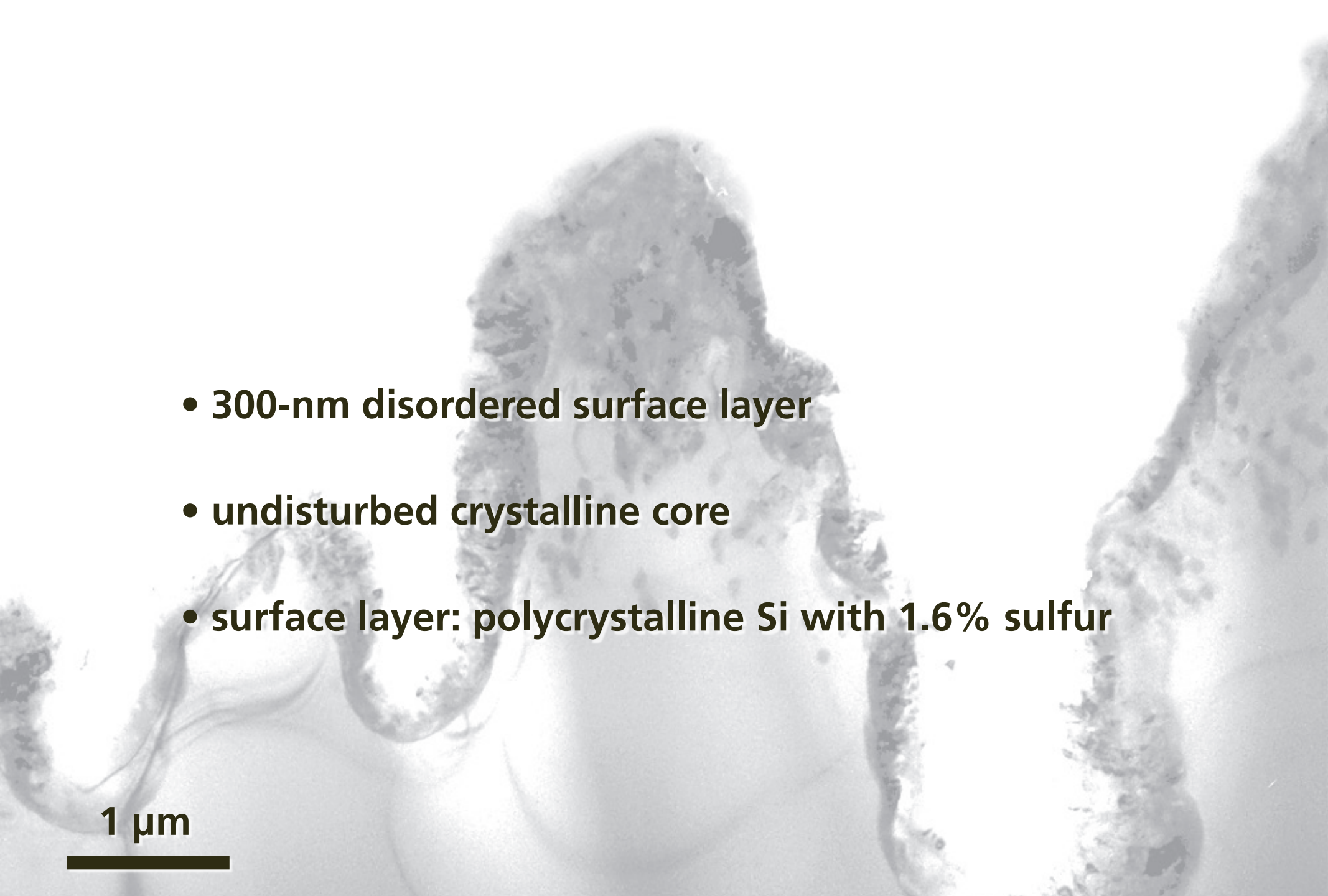


1 μm

electron •  
diffraction



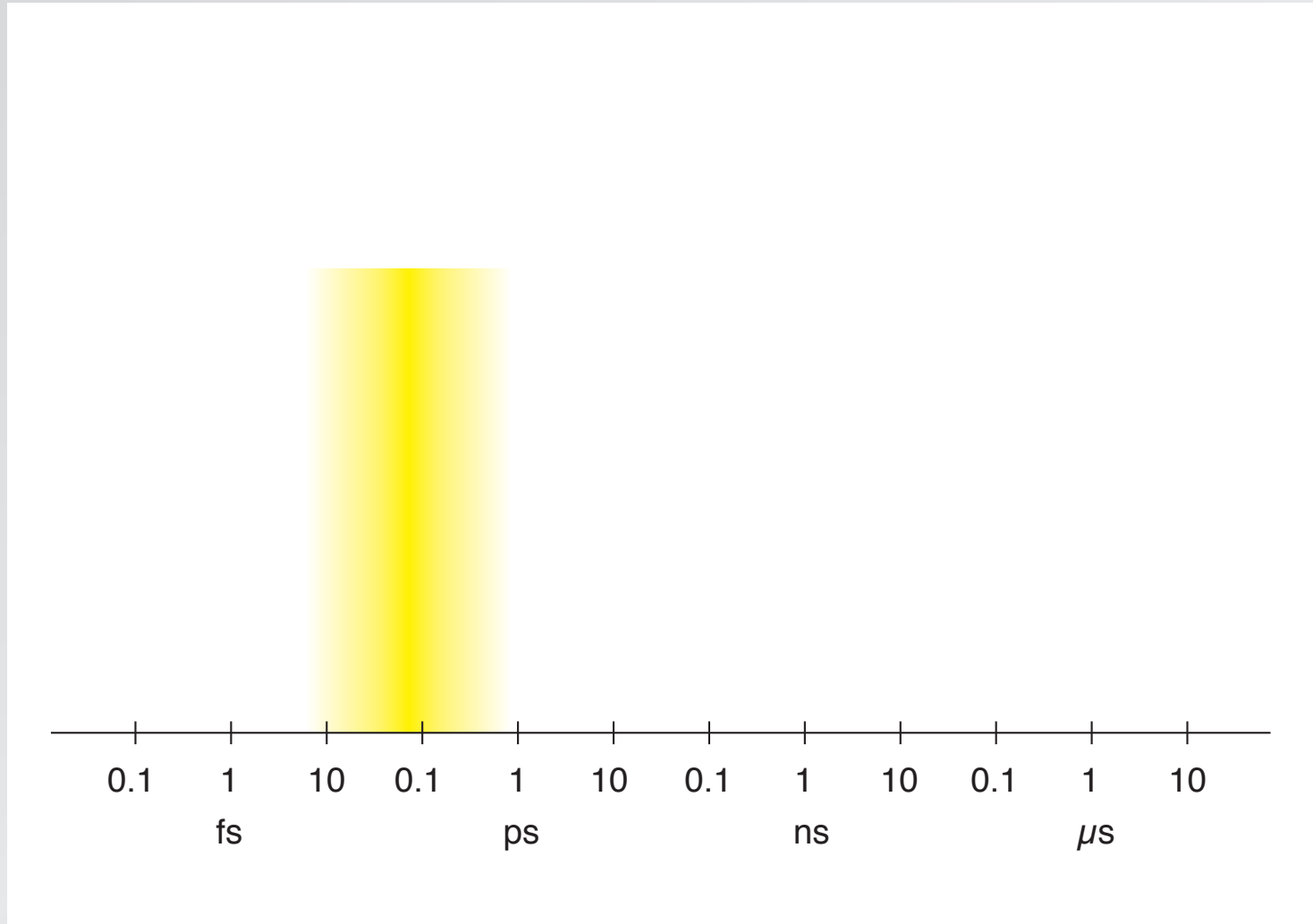
**1** properties

- 
- 300-nm disordered surface layer
  - undisturbed crystalline core
  - surface layer: polycrystalline Si with 1.6% sulfur

1  $\mu\text{m}$

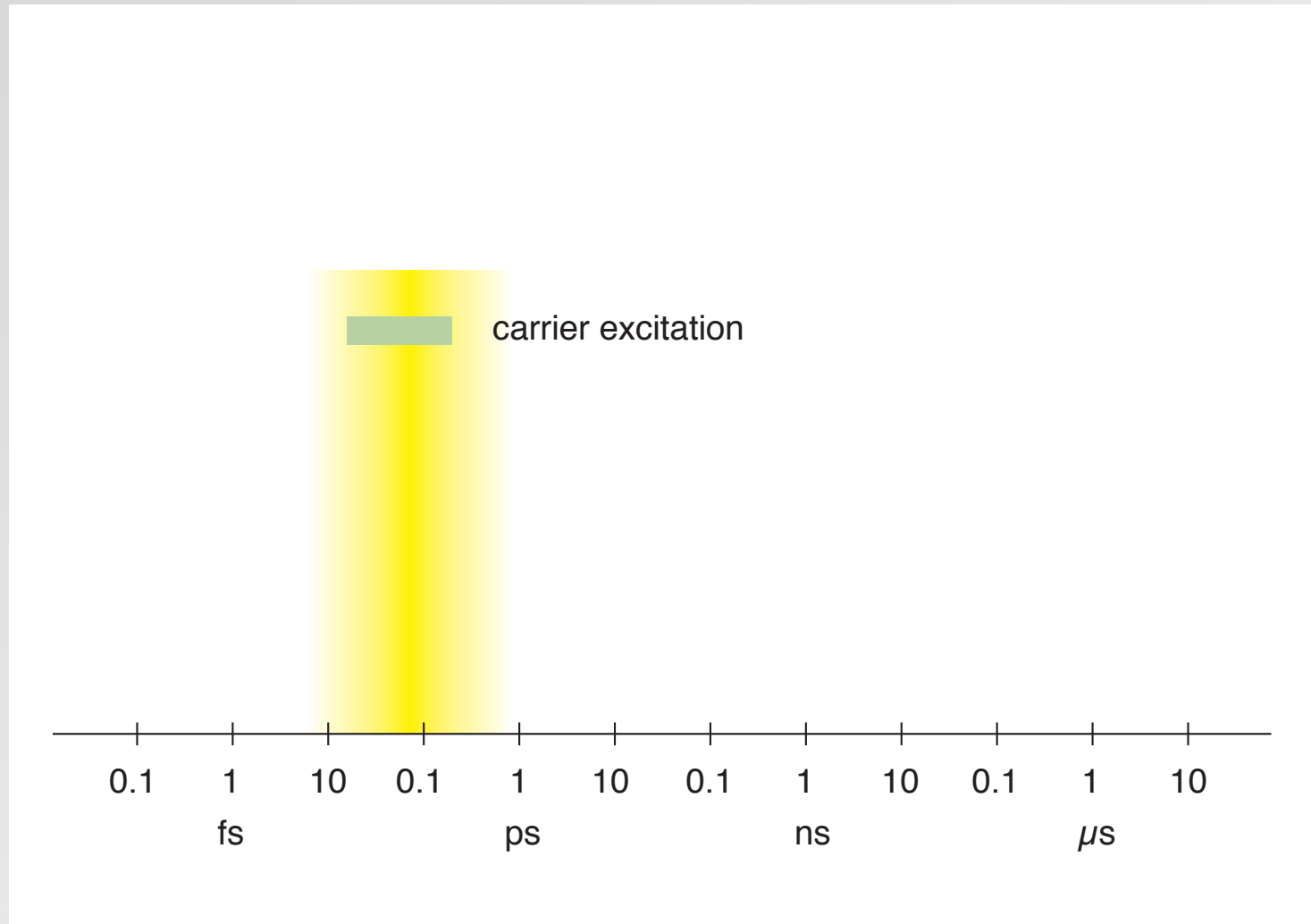
**two processes: melting and ablation**

# relevant time scales

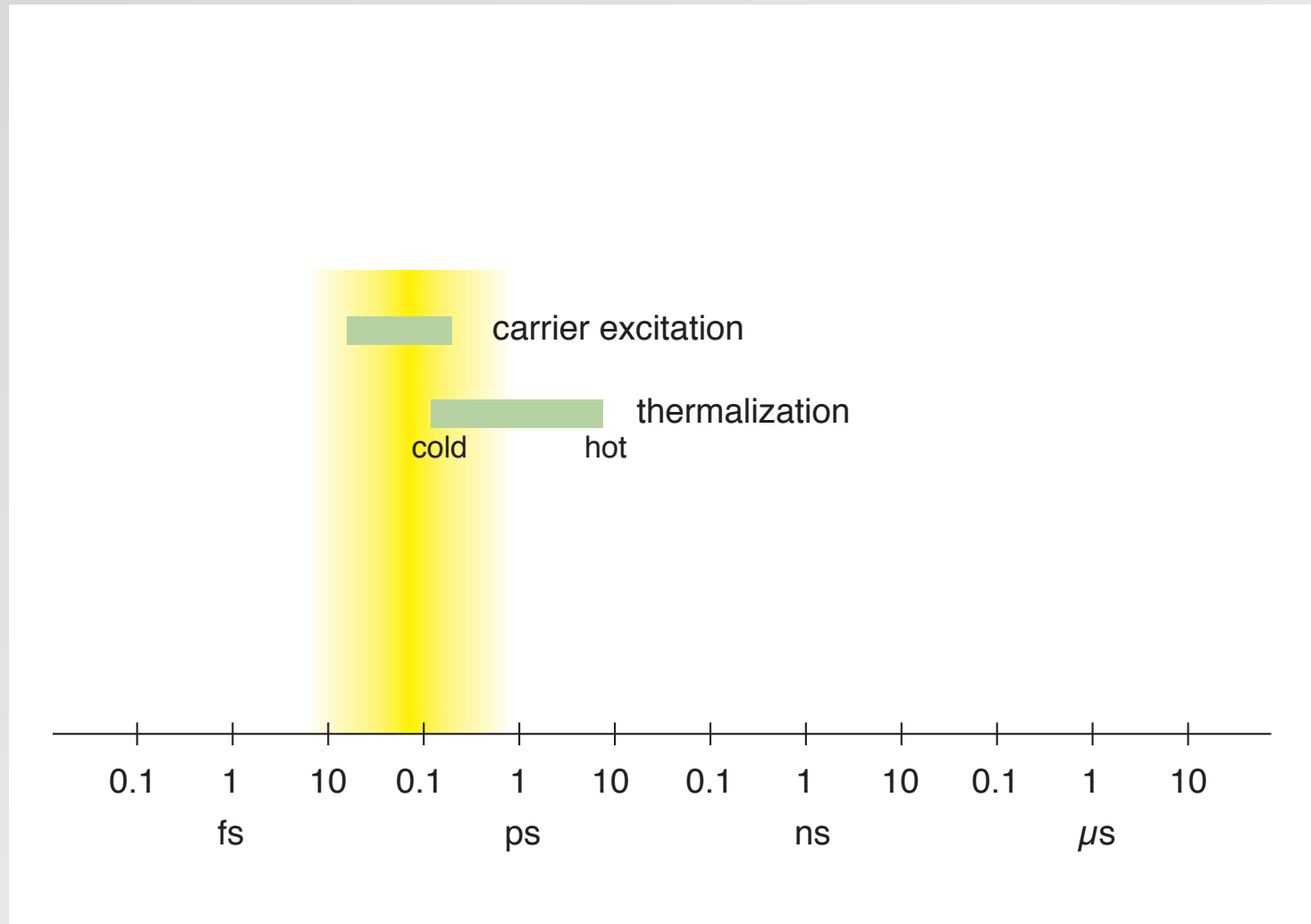




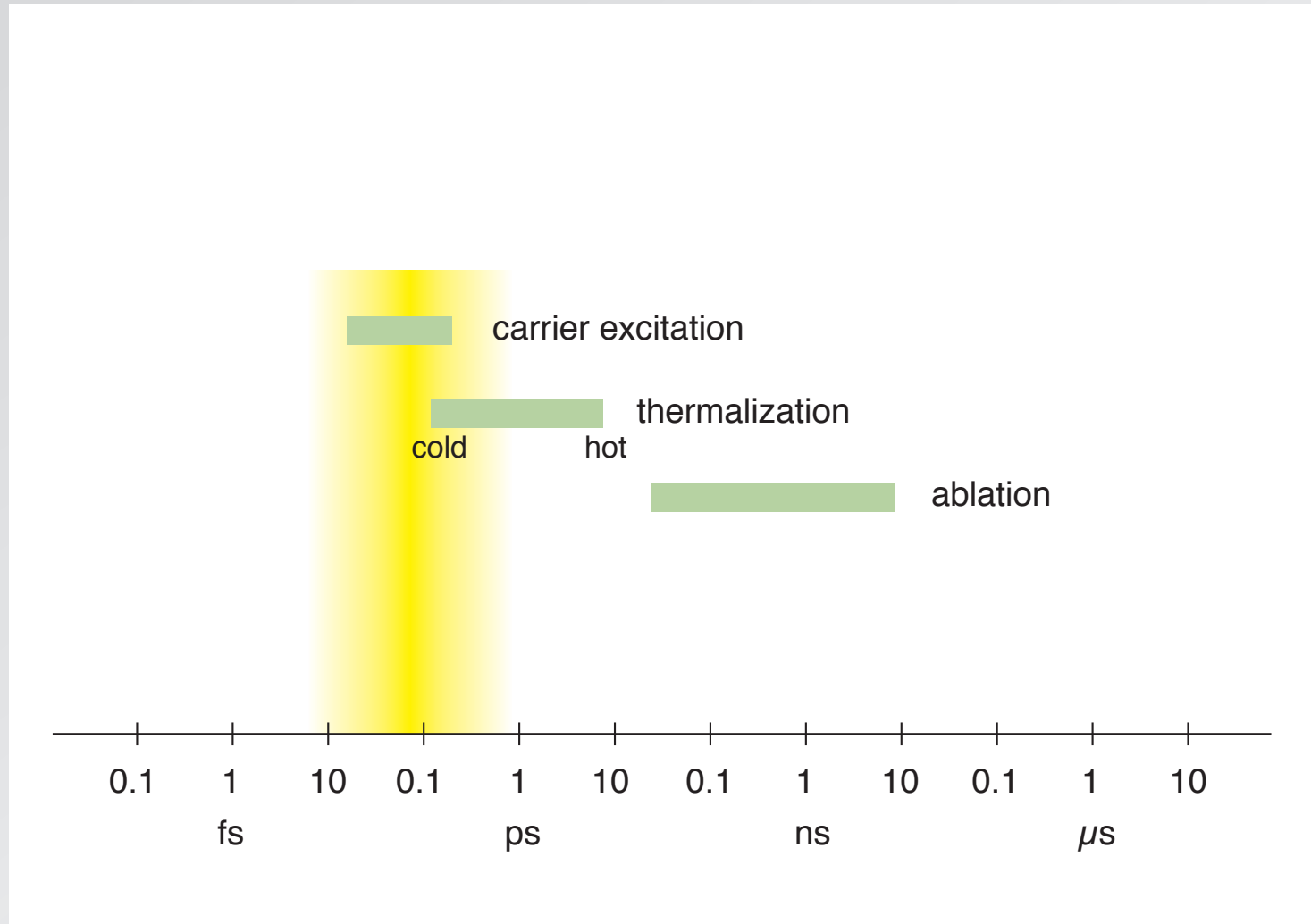
# relevant time scales



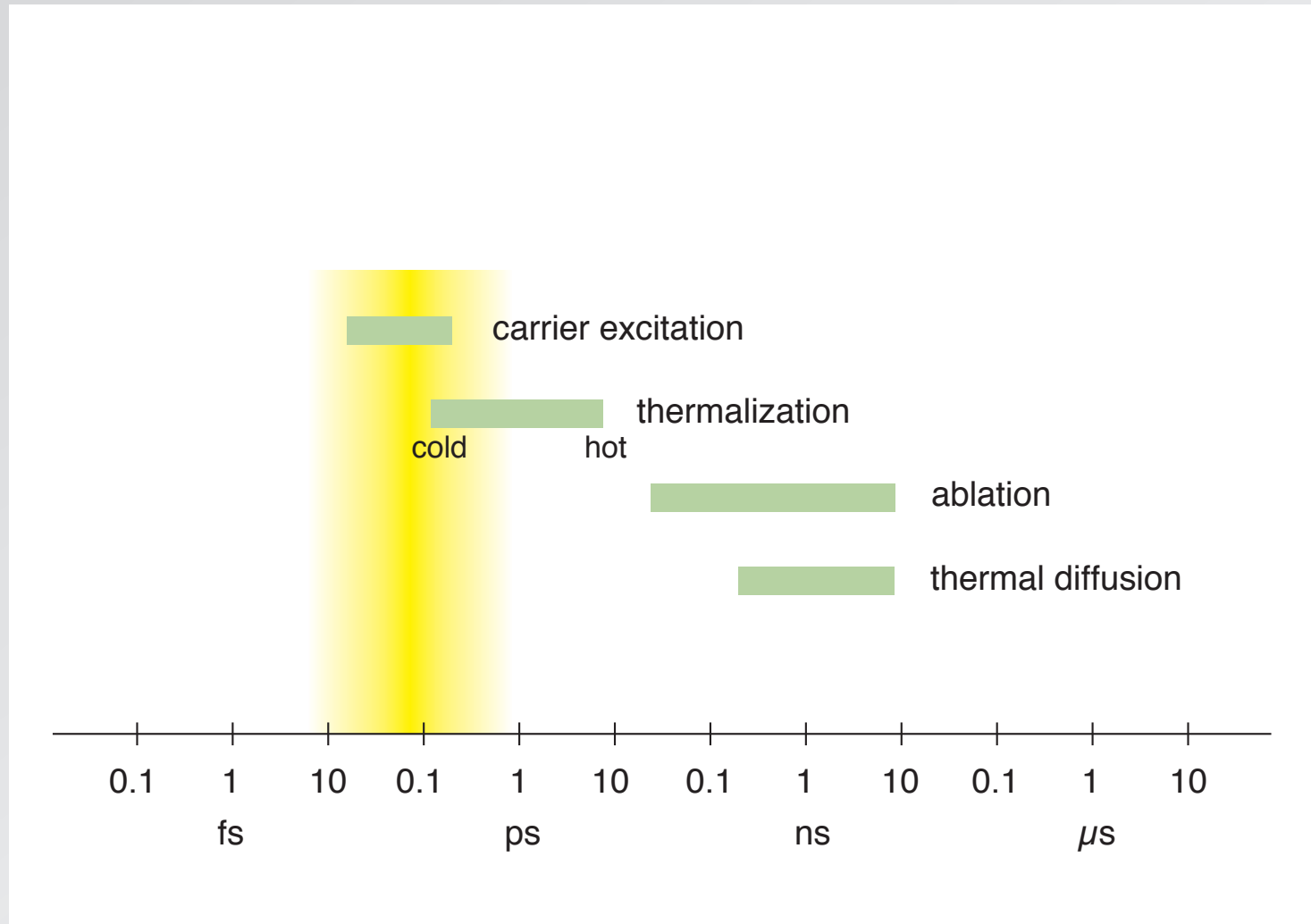
# relevant time scales



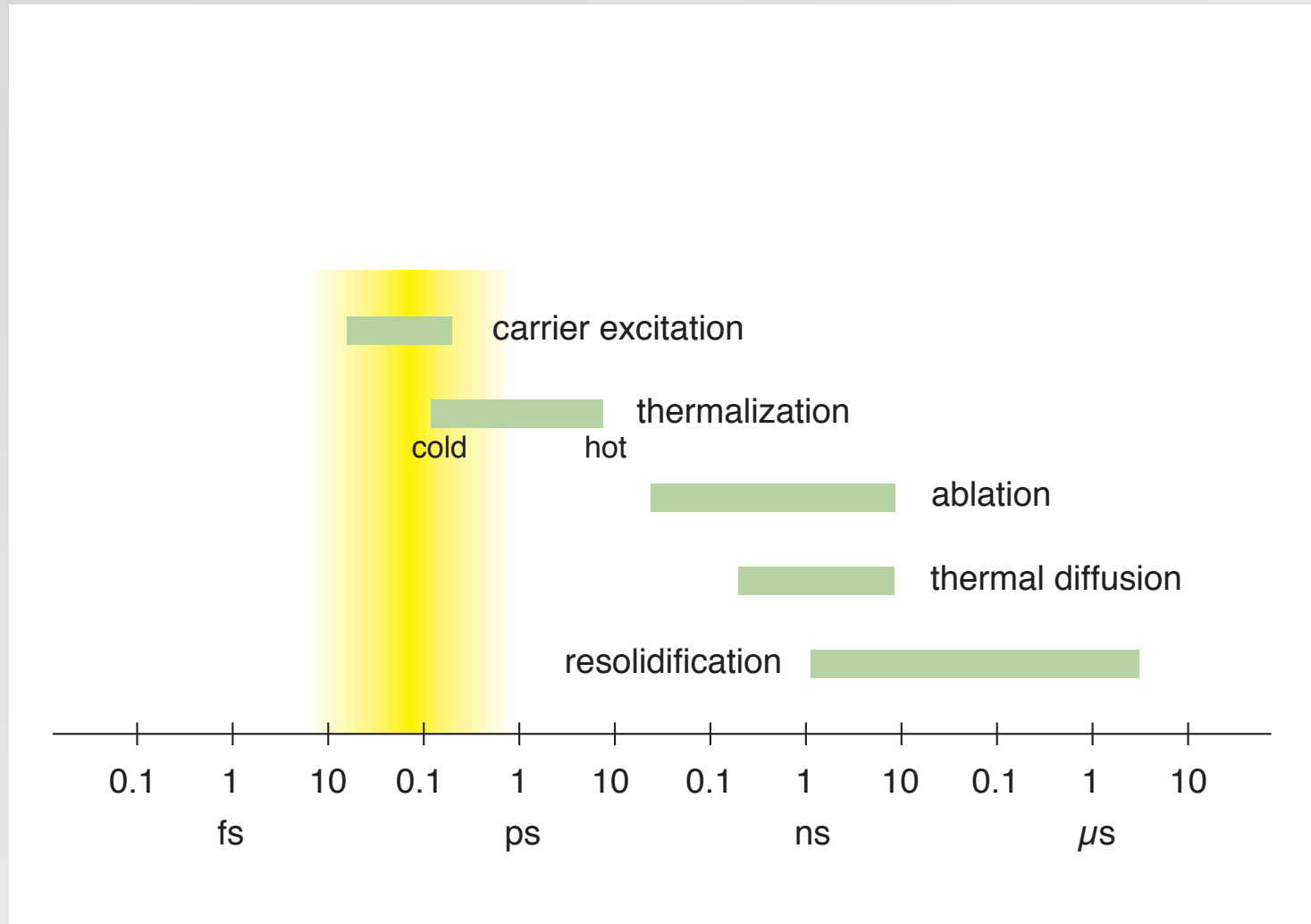
# relevant time scales



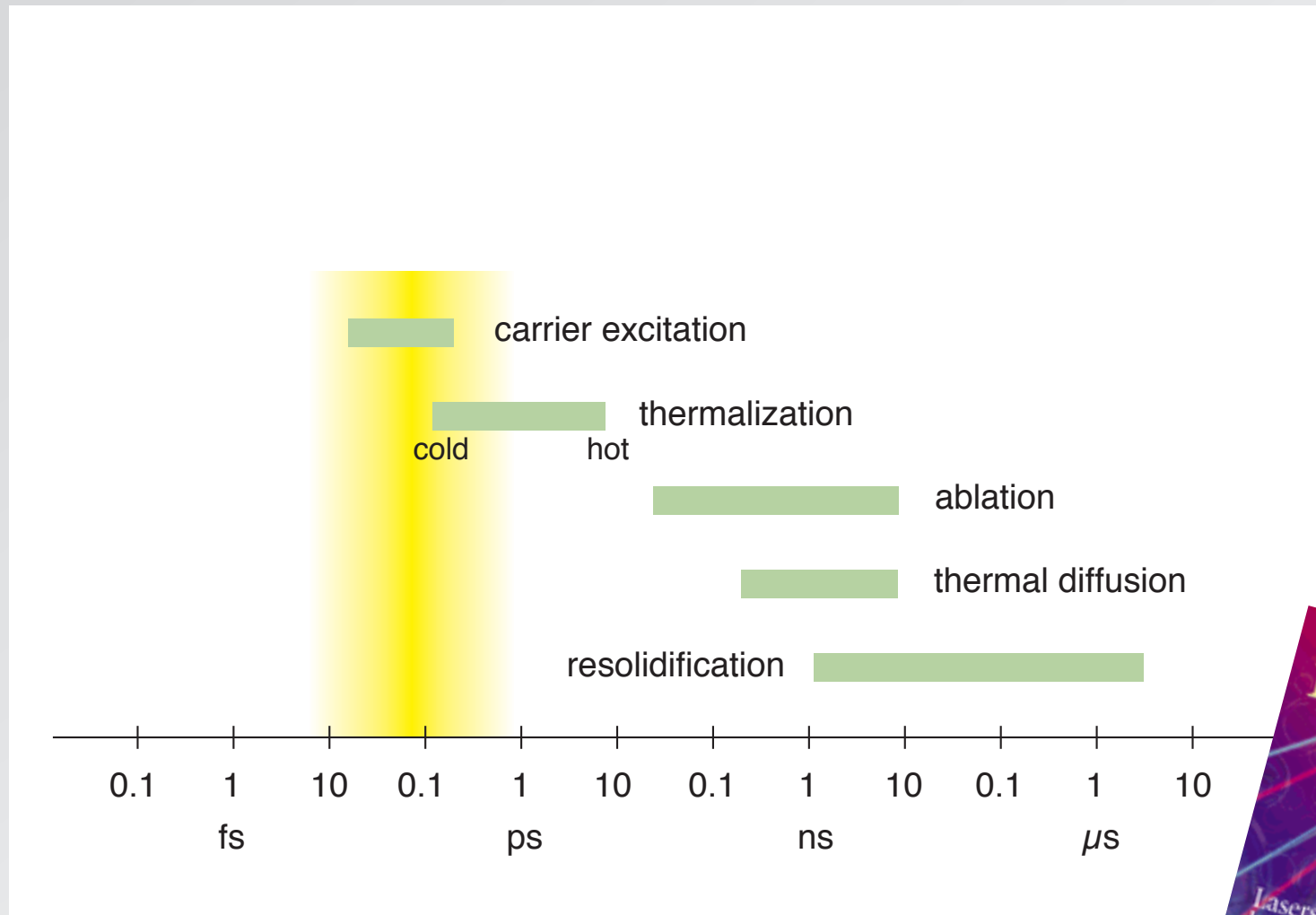
# relevant time scales



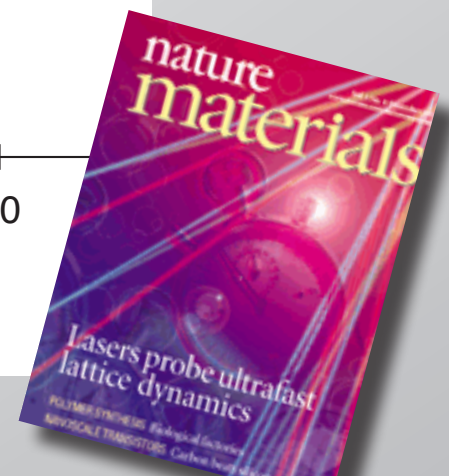
# relevant time scales



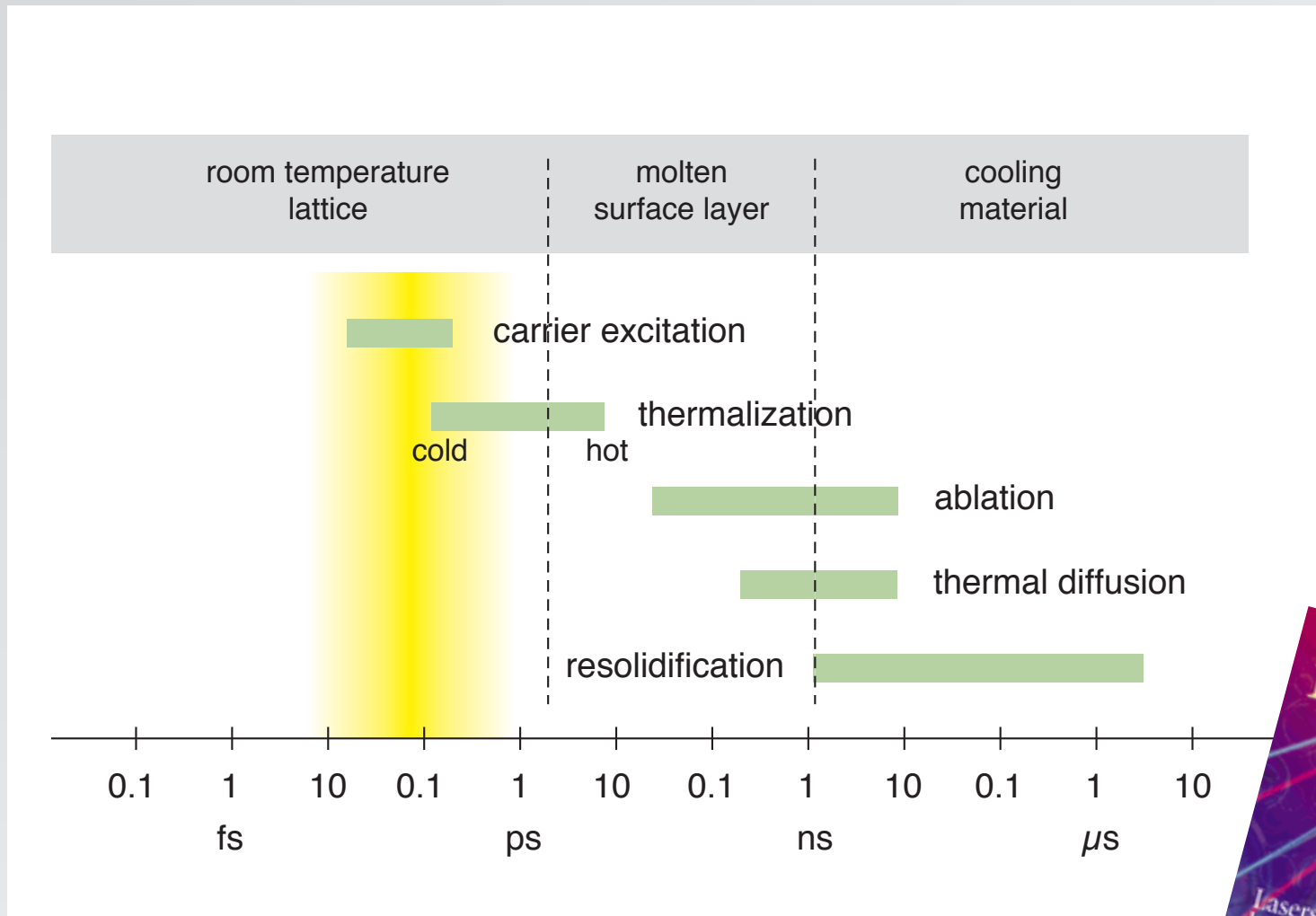
# relevant time scales



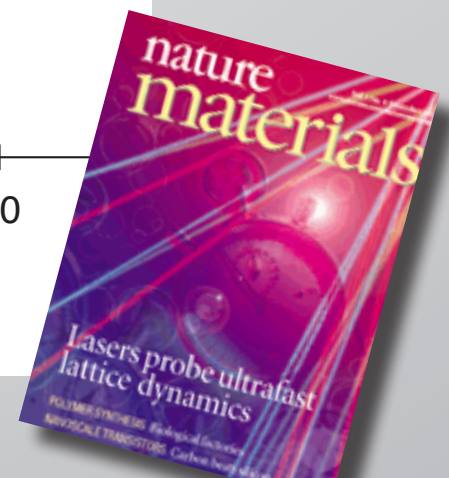
*Nature Materials* 1, 217 (2002)



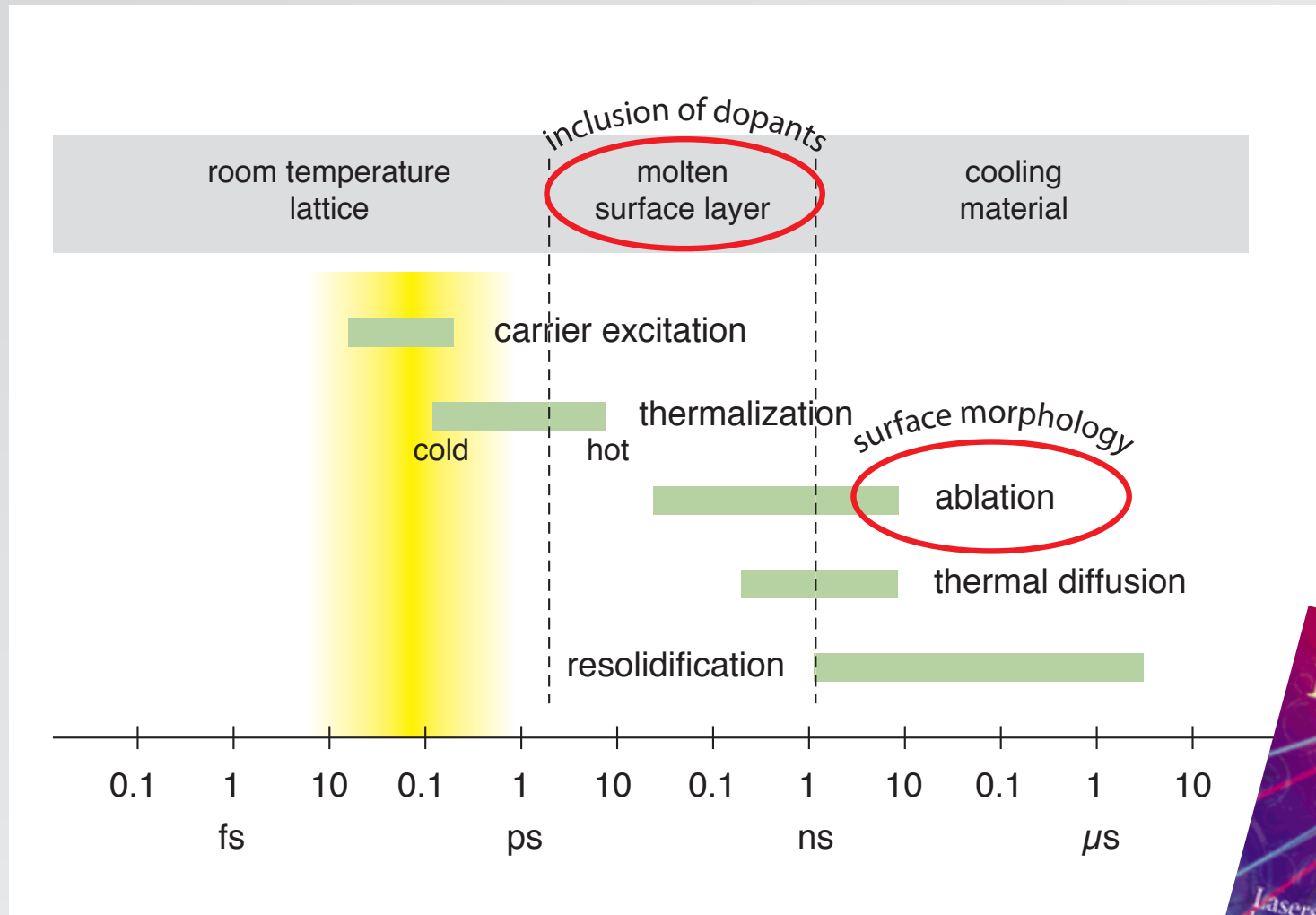
# relevant time scales



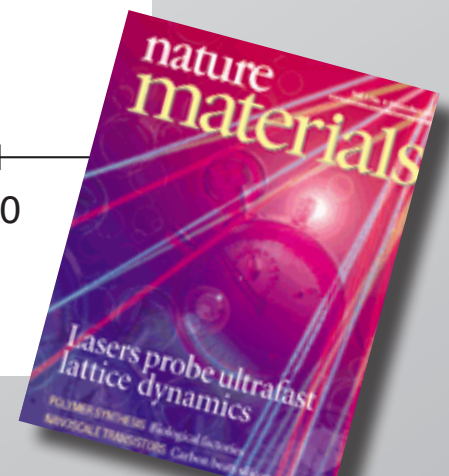
*Nature Materials* 1, 217 (2002)



# relevant time scales



*Nature Materials* 1, 217 (2002)



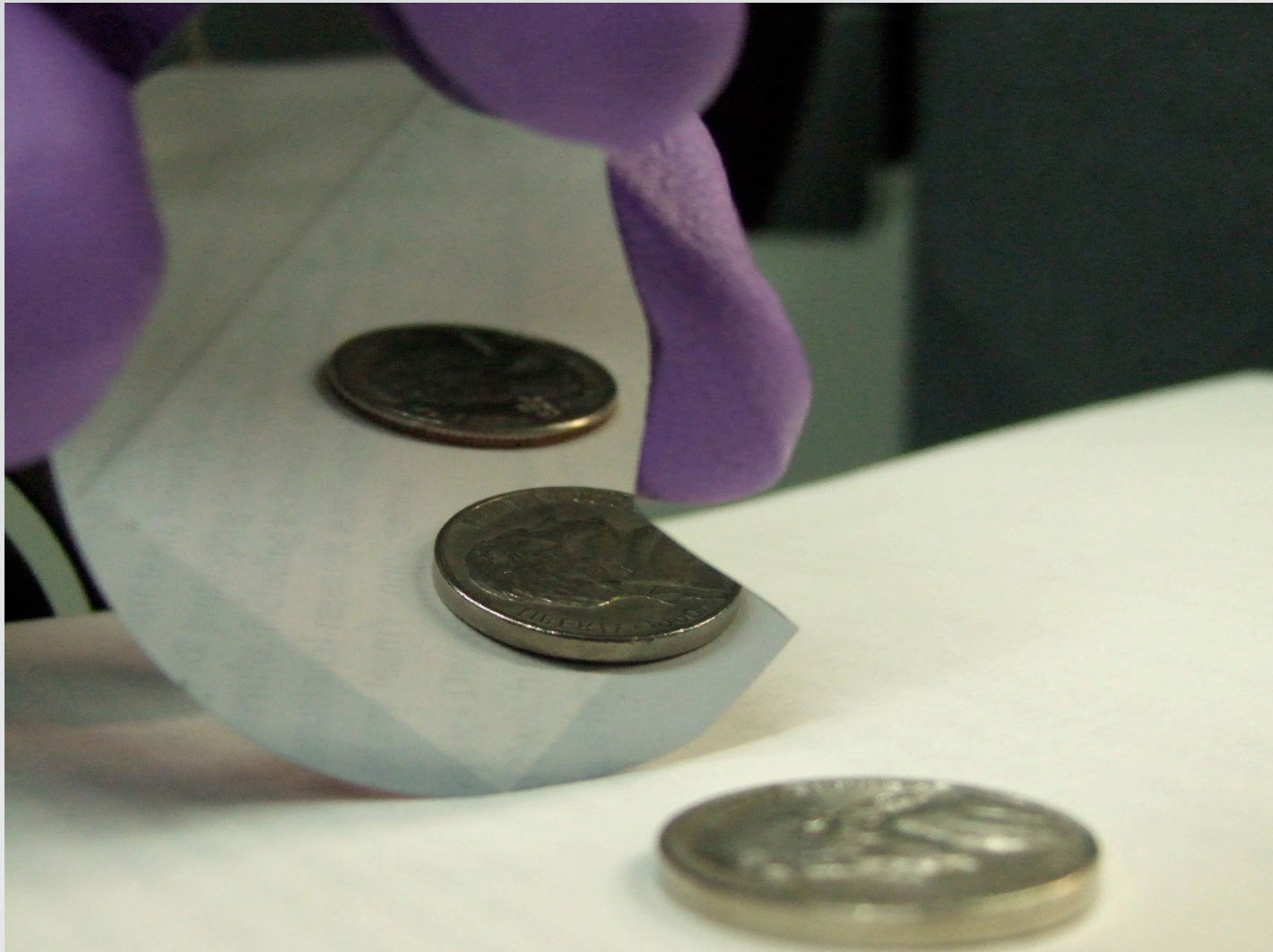


**different thresholds:**

**melting: 1.5 kJ/m<sup>2</sup>**

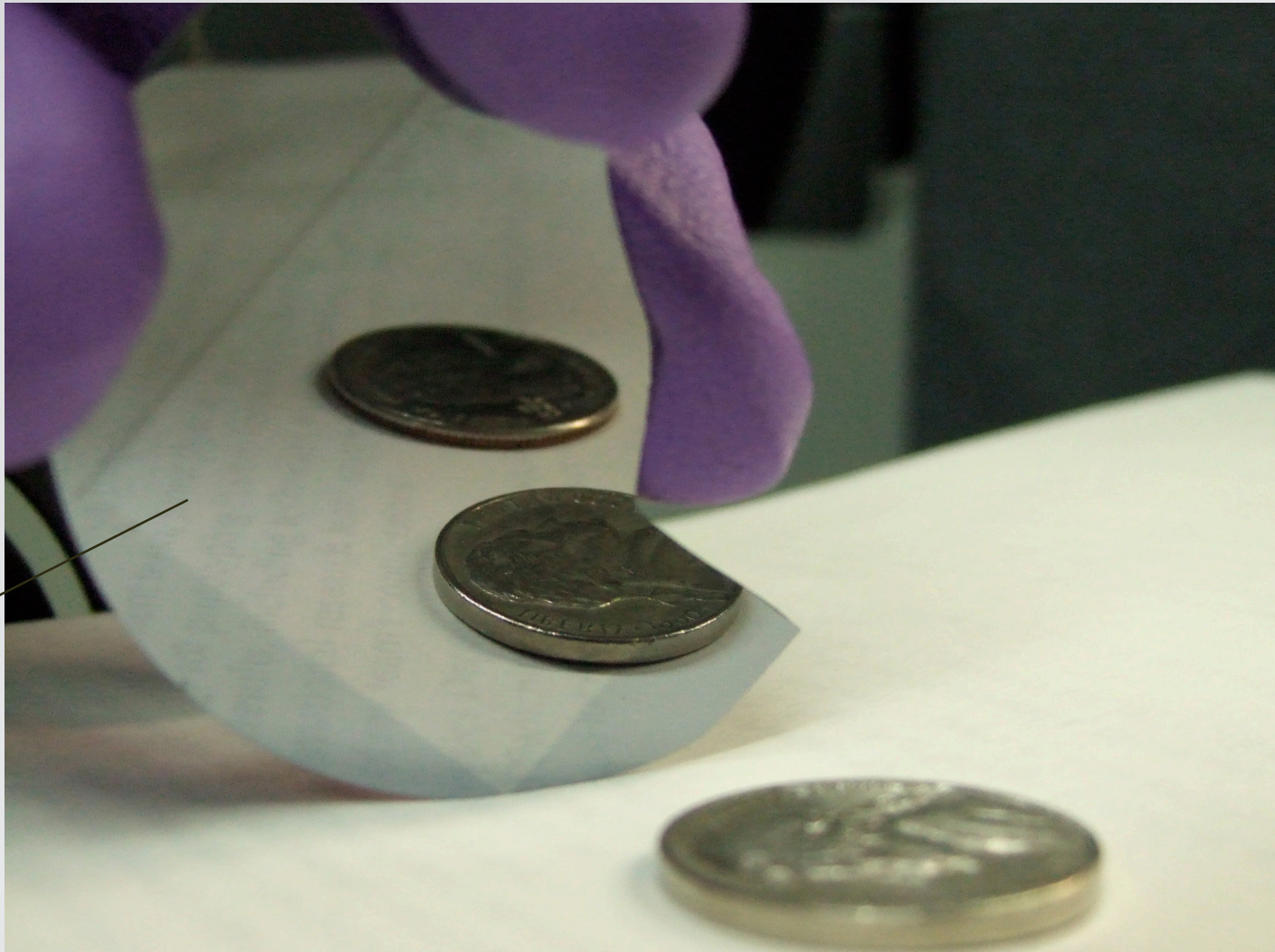
**ablation: 3.1 kJ/m<sup>2</sup>**

## decouple ablation from melting

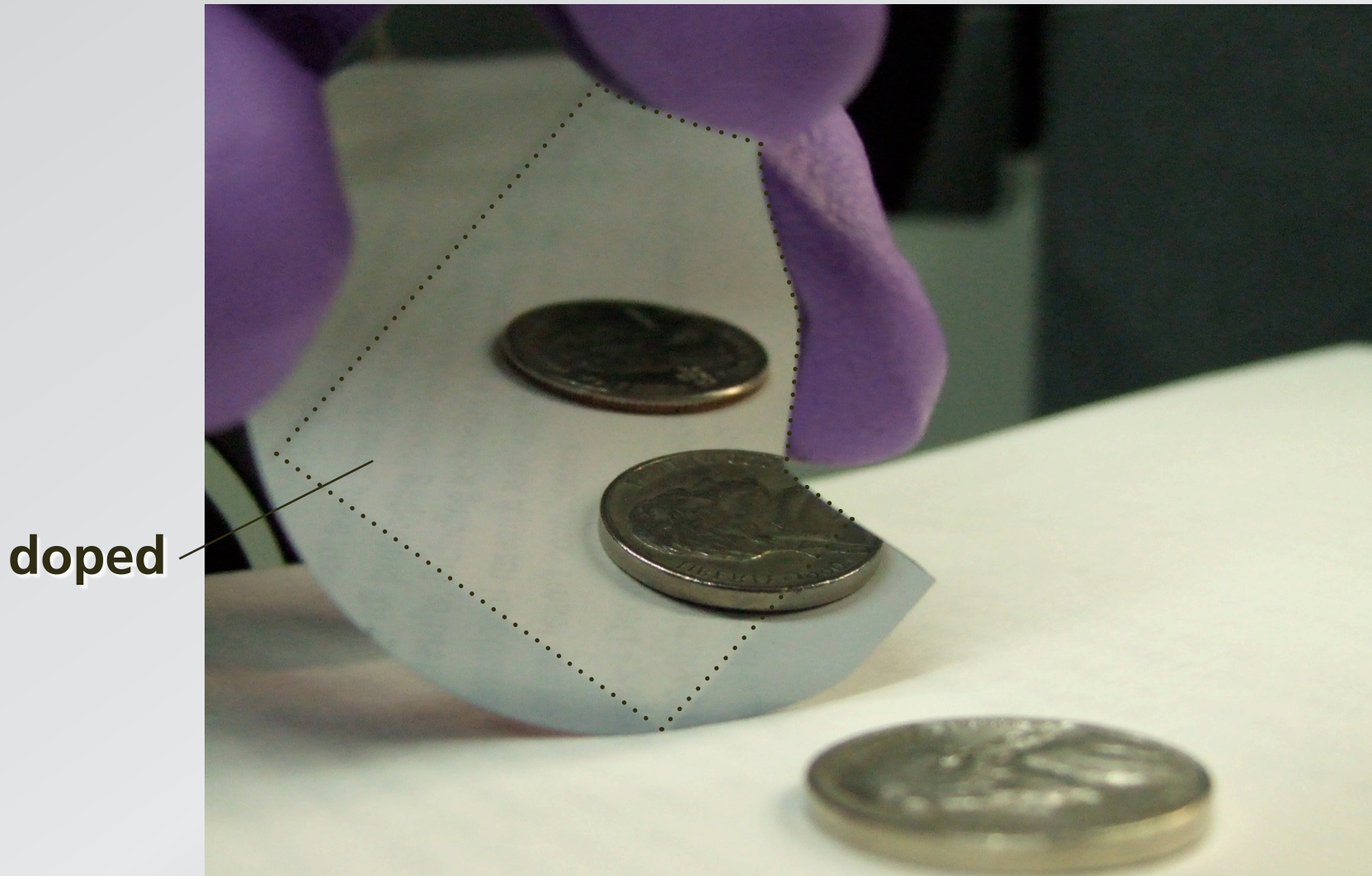


## decouple ablation from melting

doped

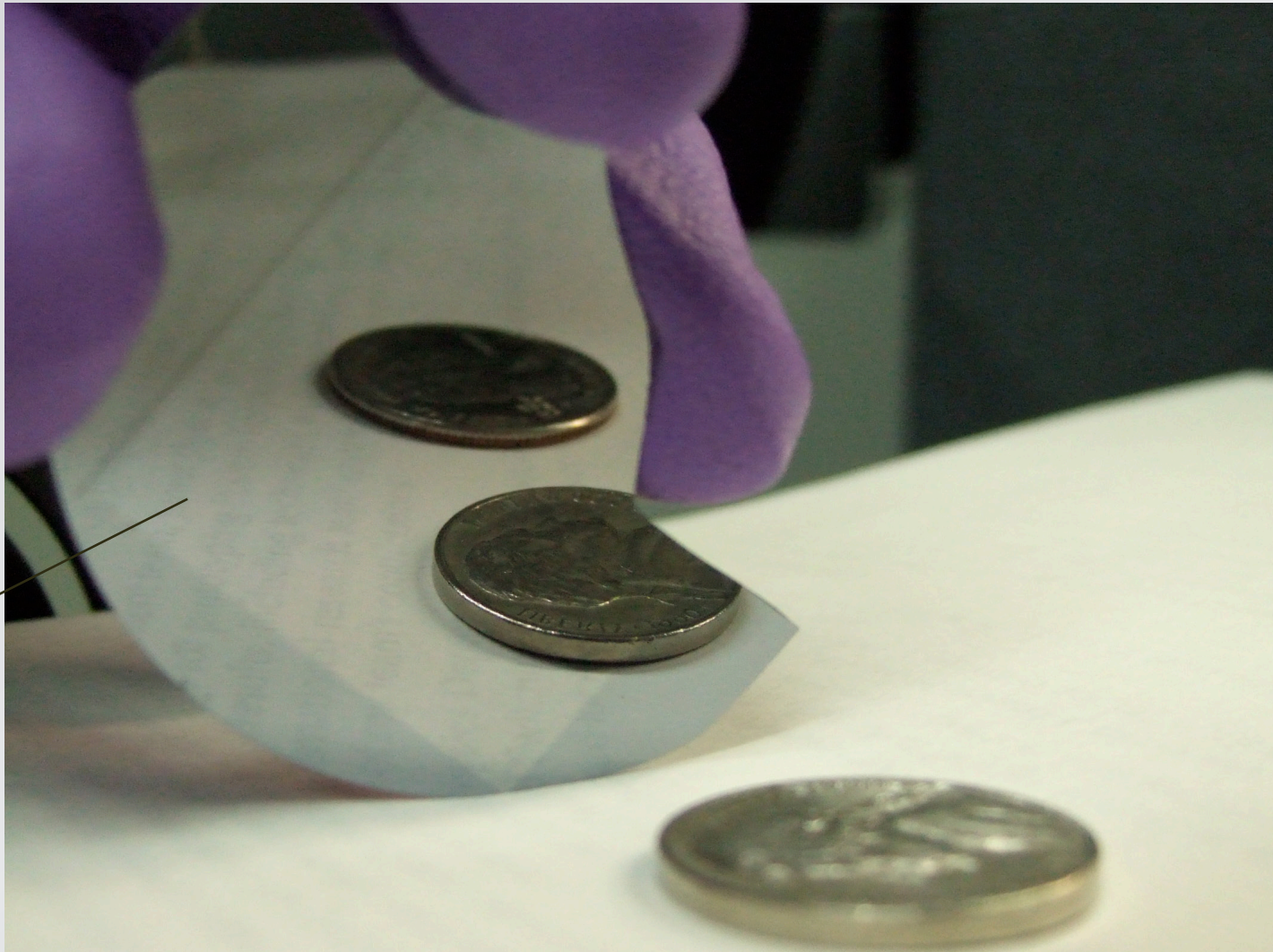


## decouple ablation from melting



## decouple ablation from melting

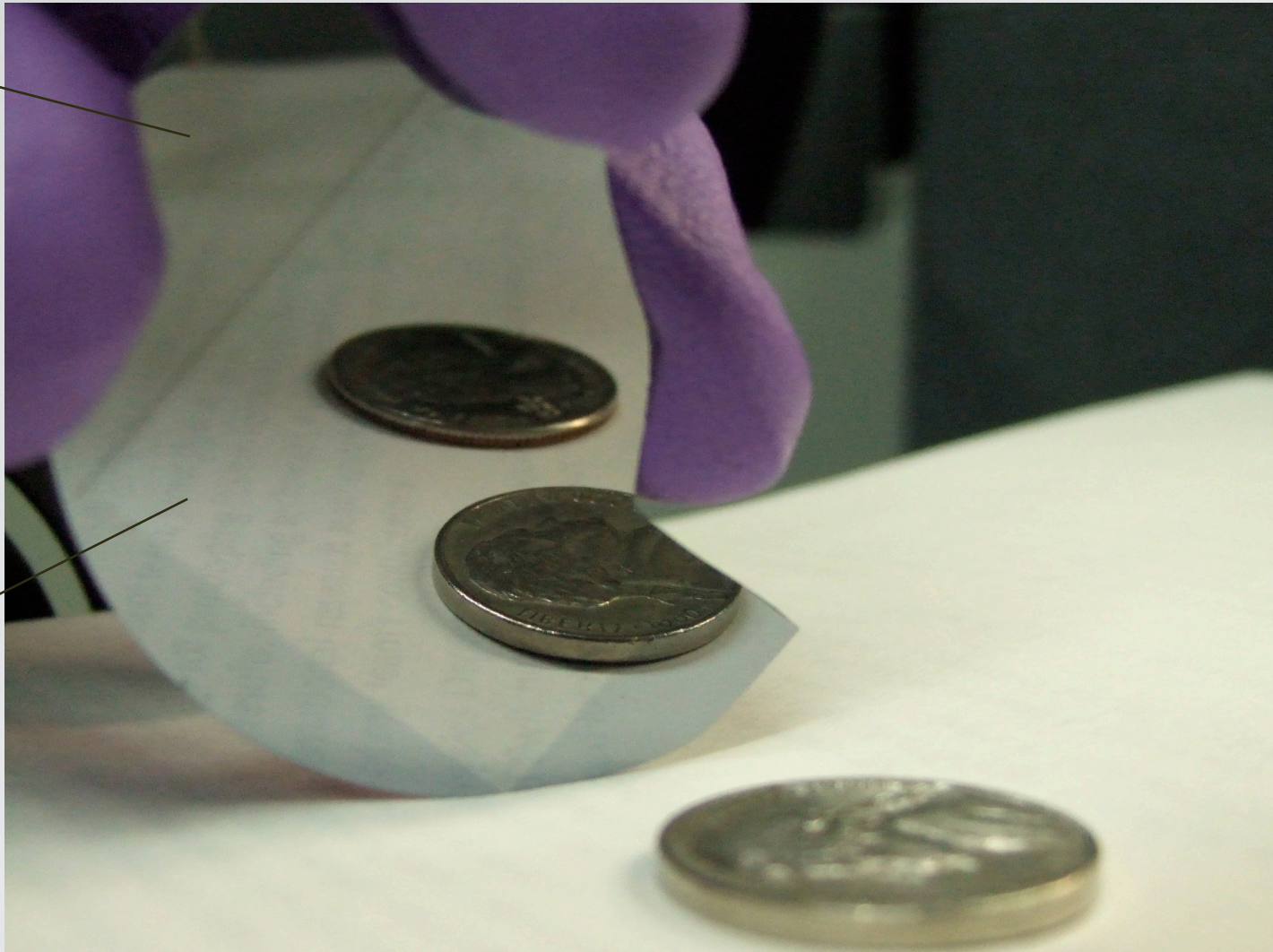
doped



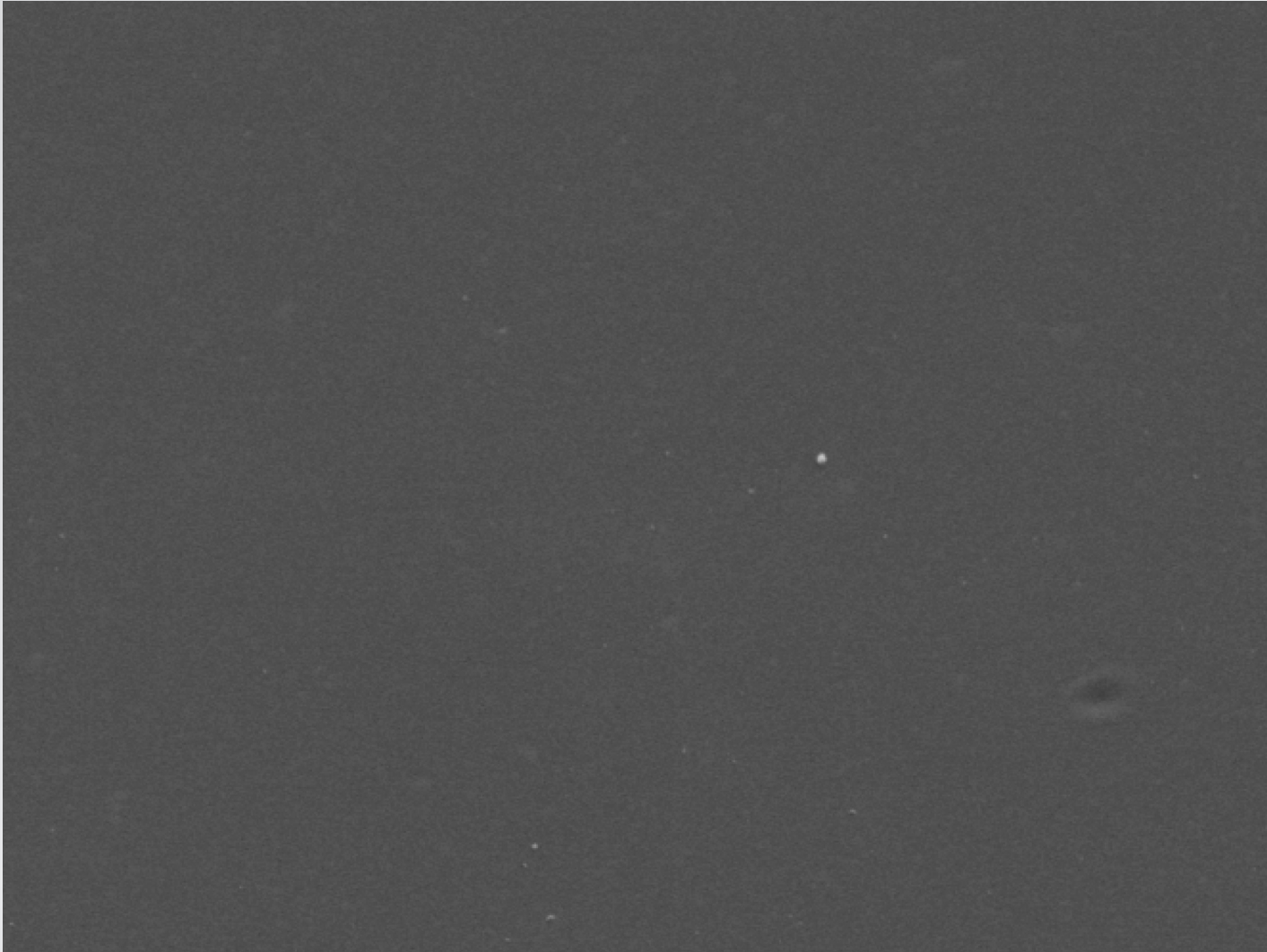
## decouple ablation from melting

undoped

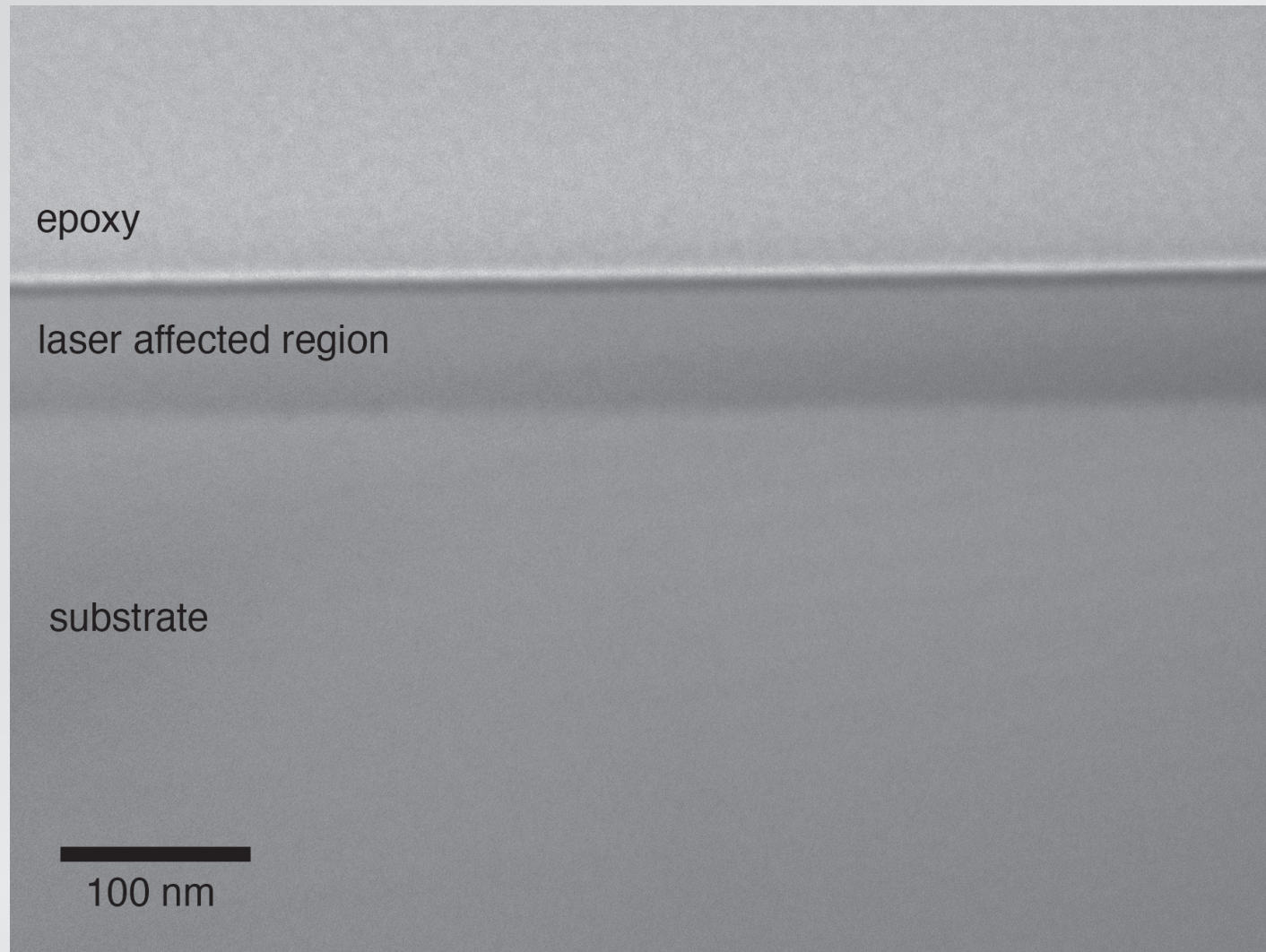
doped



## decouple ablation from melting

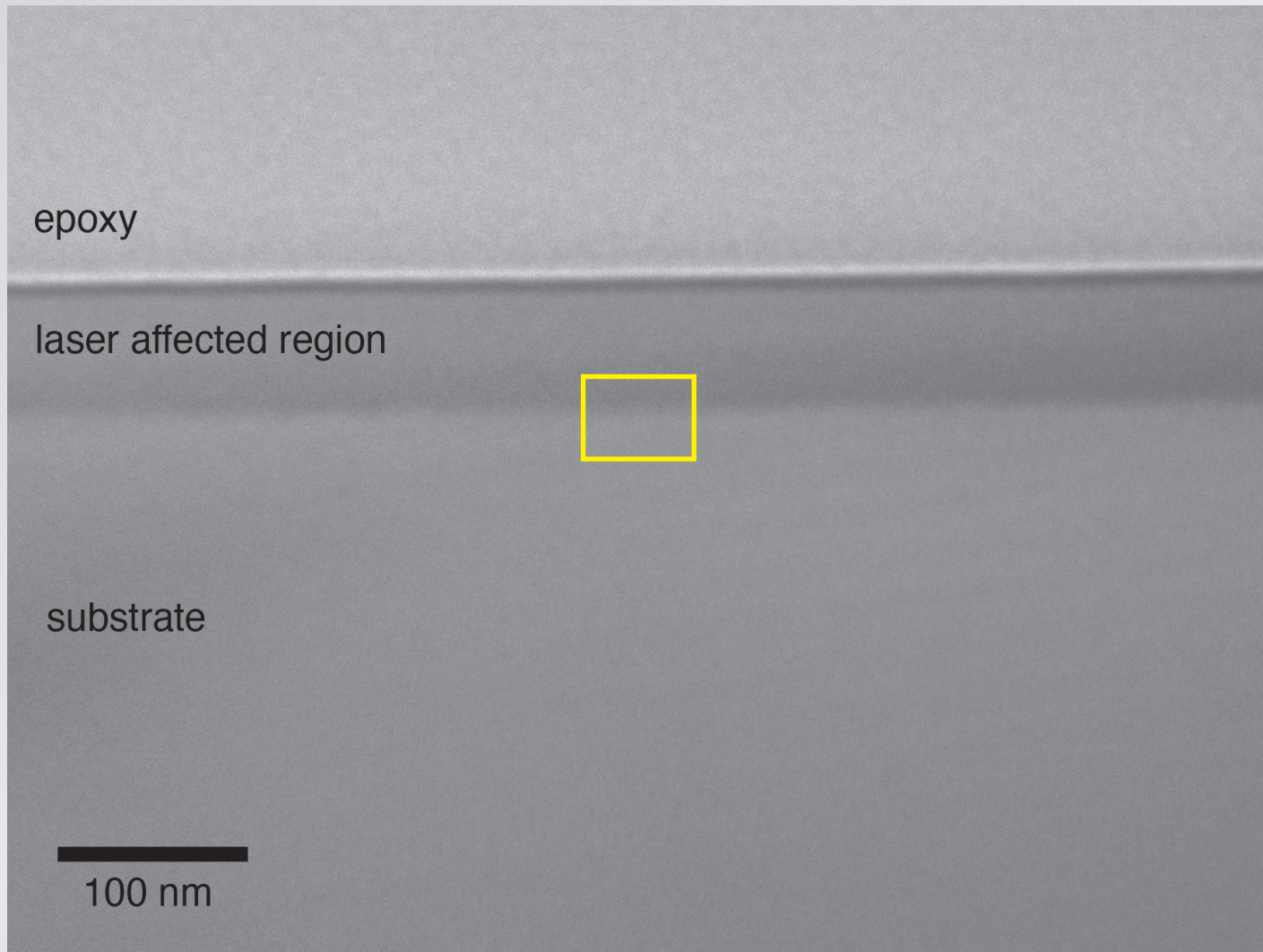


# decouple ablation from melting

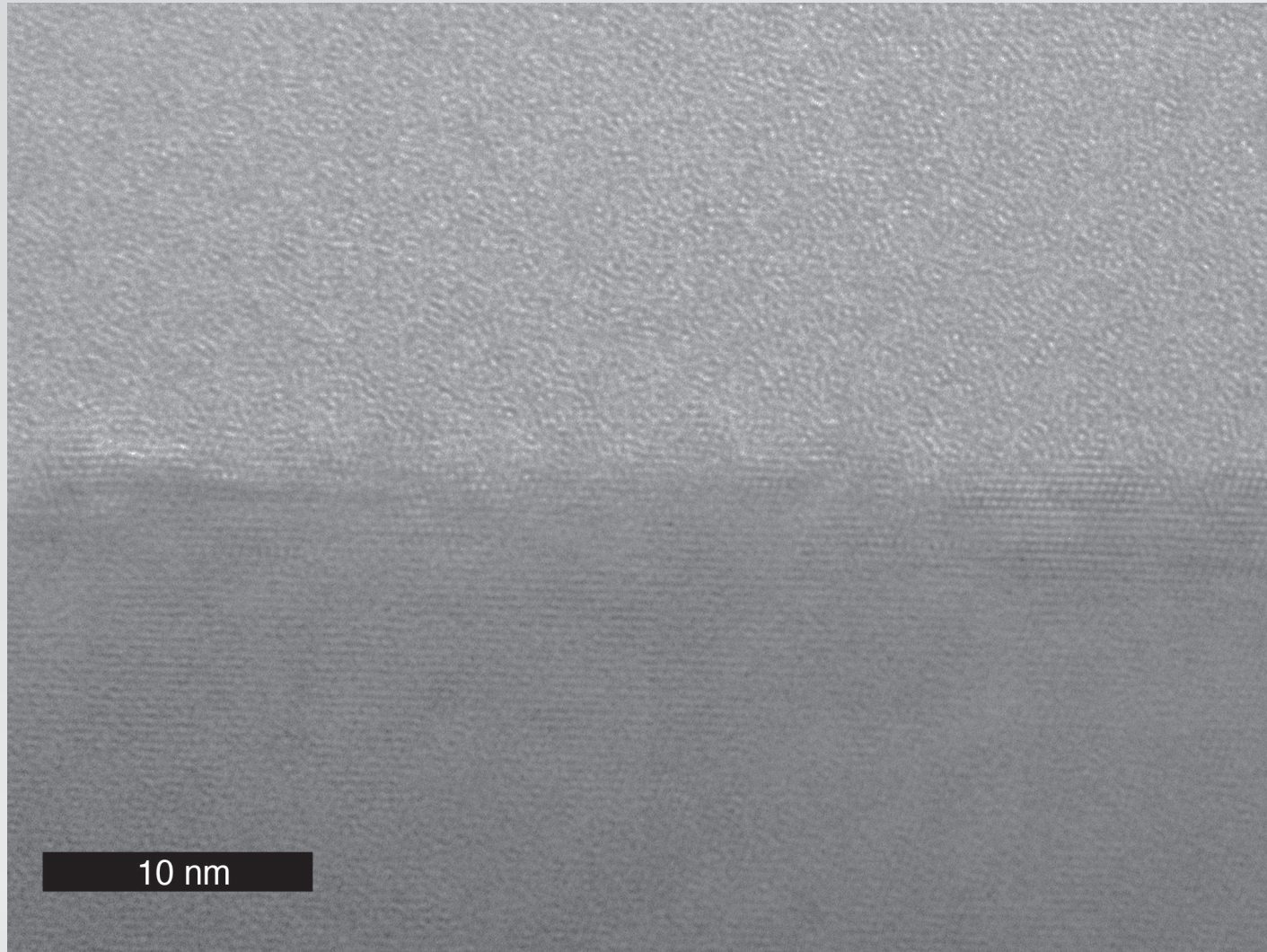




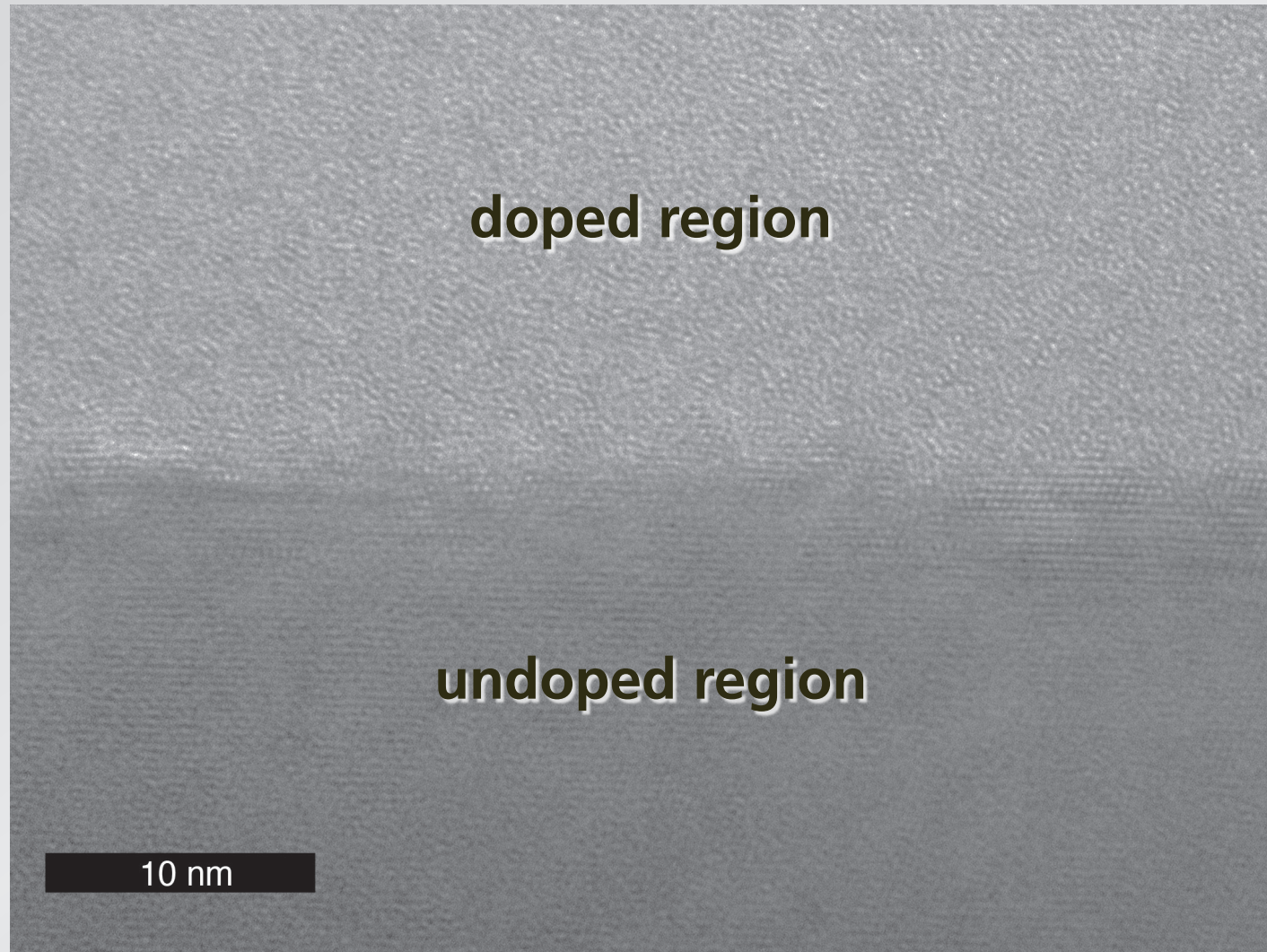
# decouple ablation from melting



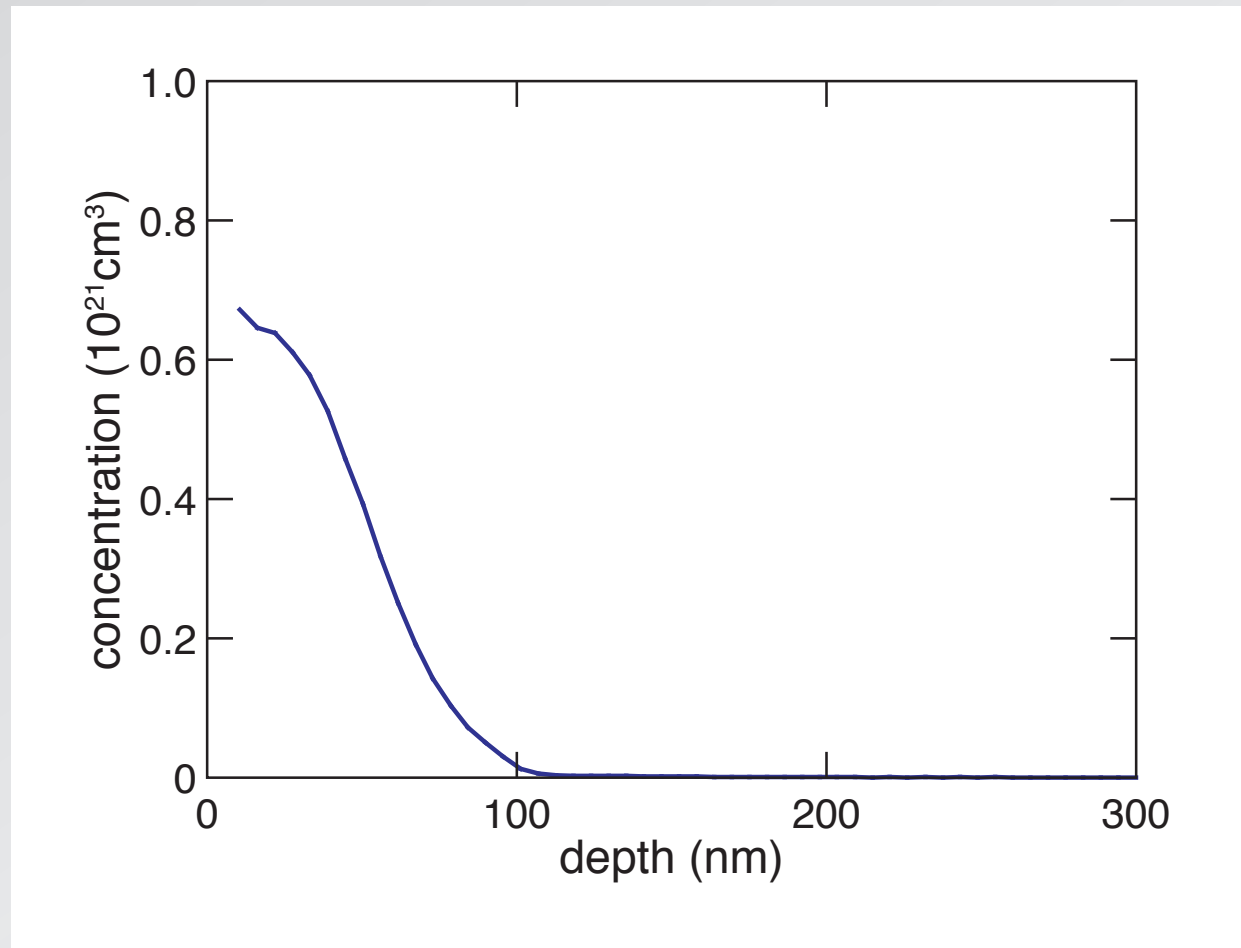
## decouple ablation from melting



# decouple ablation from melting

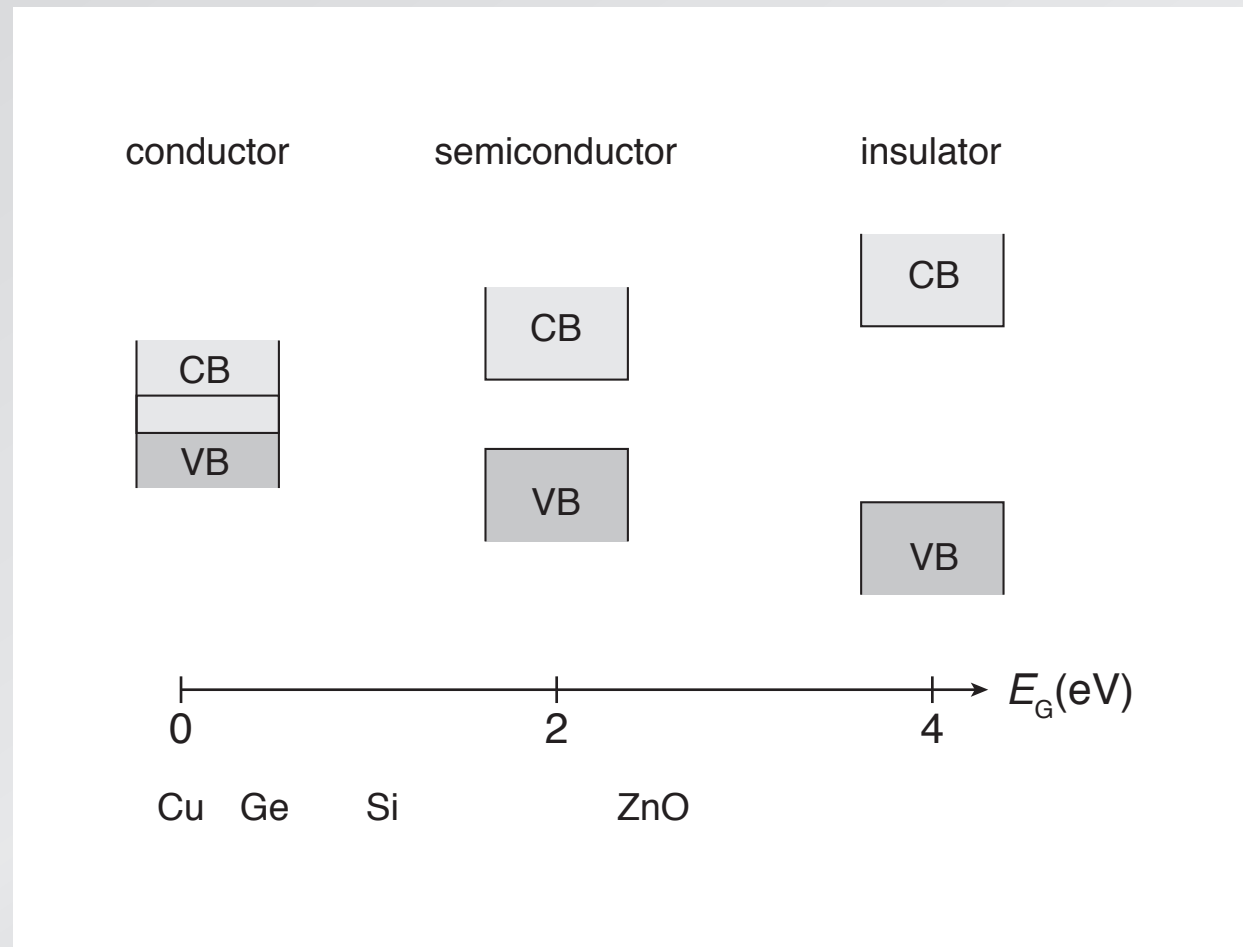


# secondary ion mass spectrometry



## Things to keep in mind

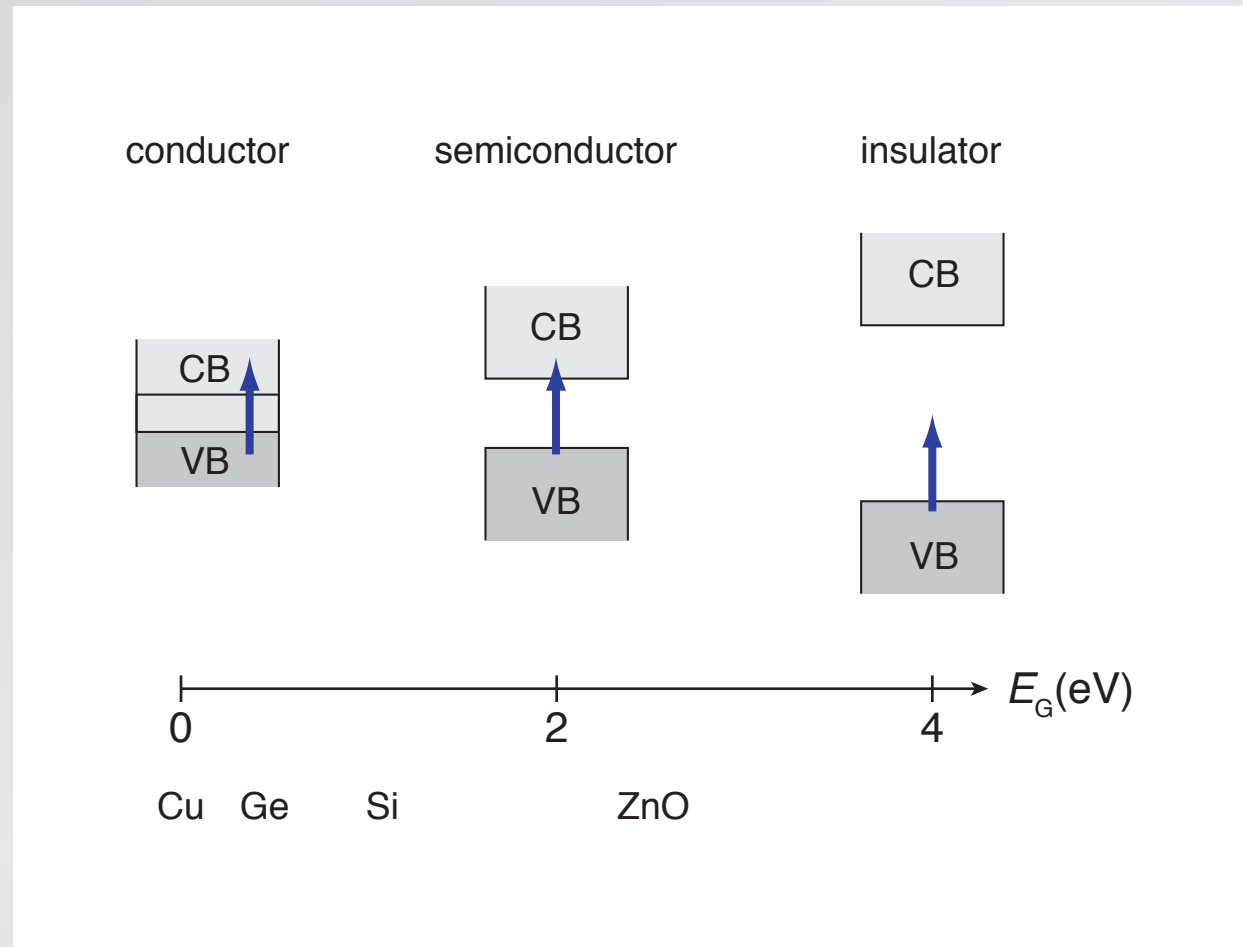
- near unit absorption extending into IR
- surface structure due to ablation
- hyperdoping due to rapid melting and resolidification
- can decouple both processes



**1** properties

**2** intermediate band

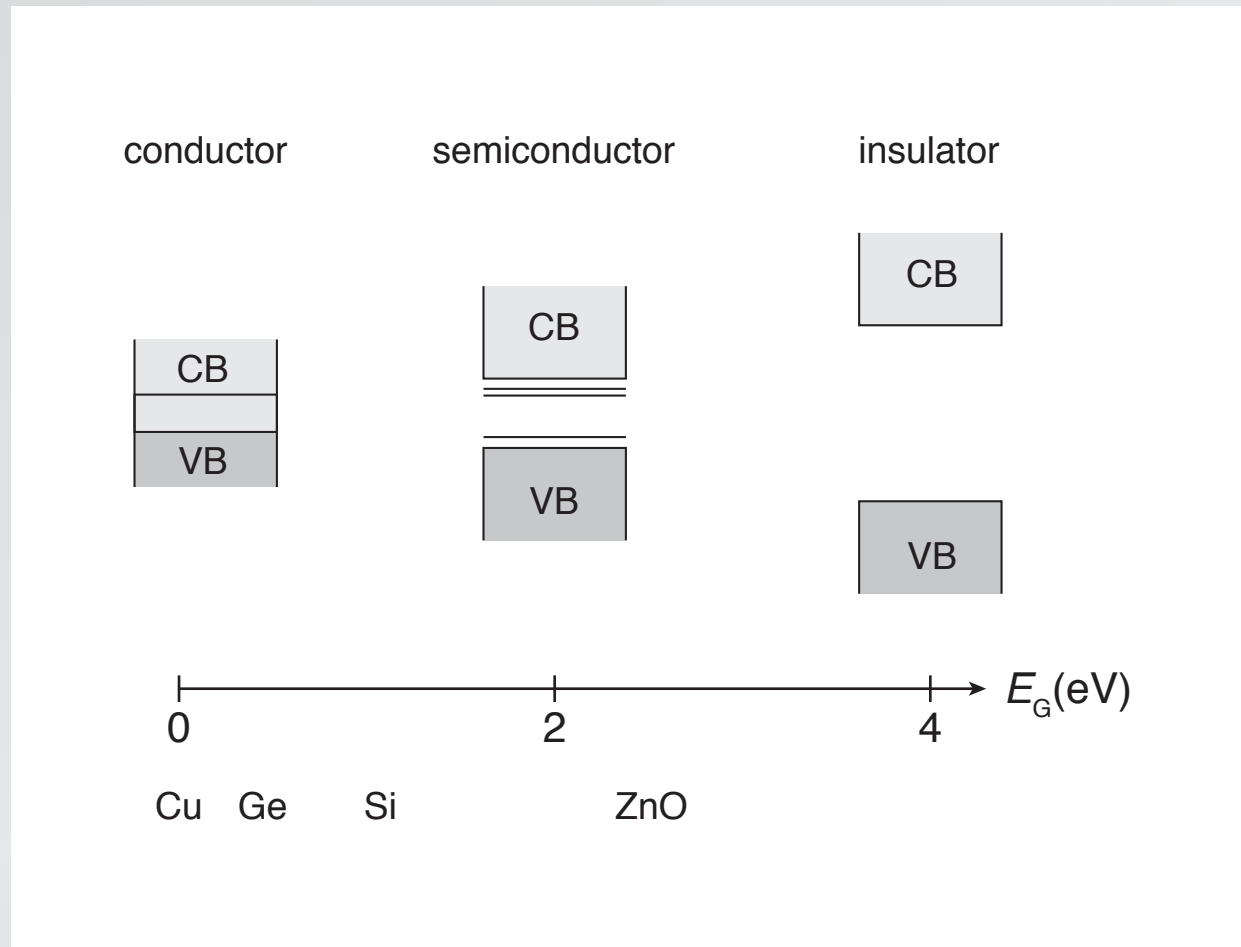
# gap determines optical and electronic properties



1 properties

2 intermediate band

# shallow-level dopants control electronic properties

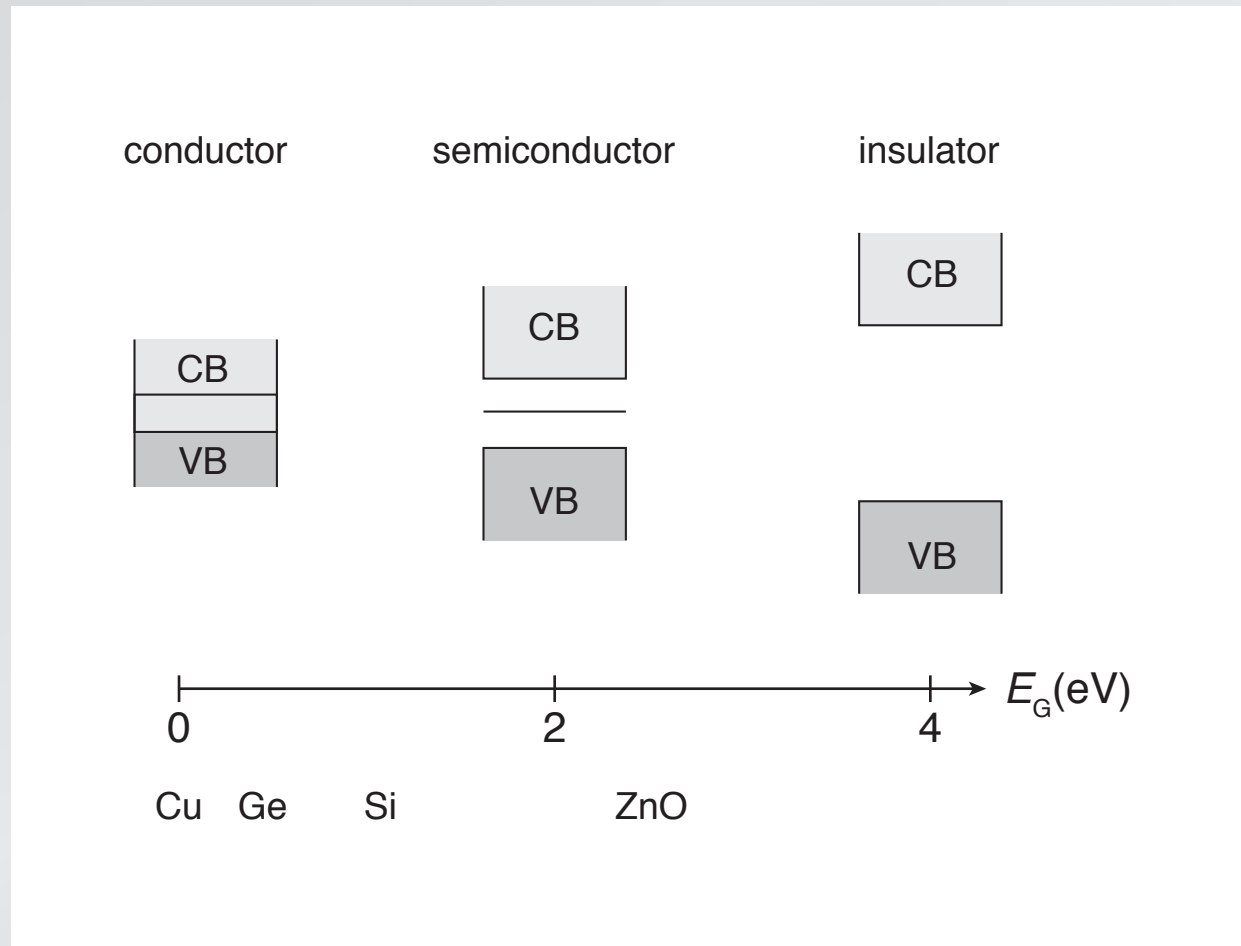


1 properties

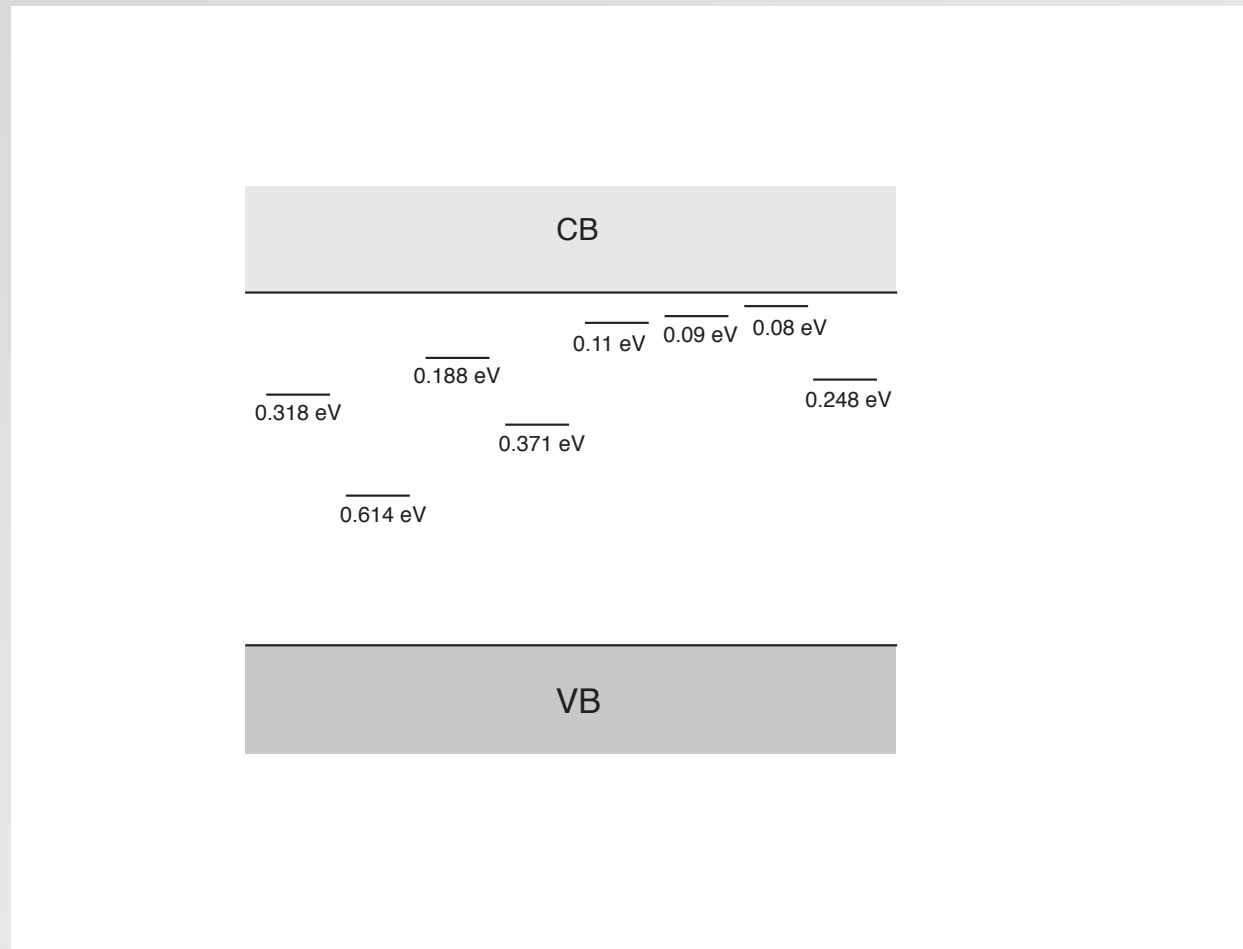
2 intermediate band



# deep-level dopants typically avoided



1 part in  $10^6$  sulfur introduces donor states in gap

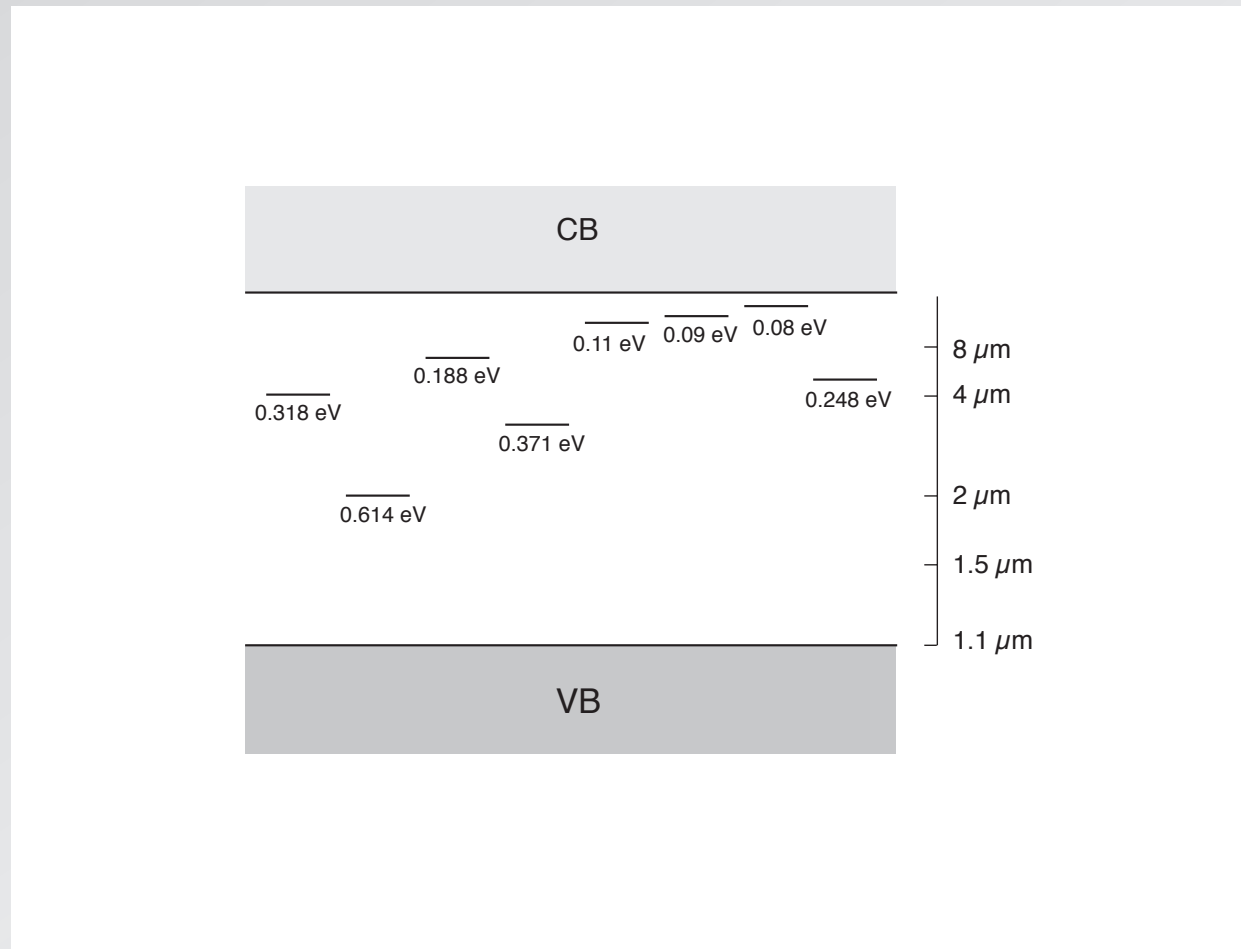


Janzén *et al.*, Phys. Rev. B 29, 1907 (1984)

1 properties

2 intermediate band

# 1 part in $10^6$ sulfur introduces donor states in gap

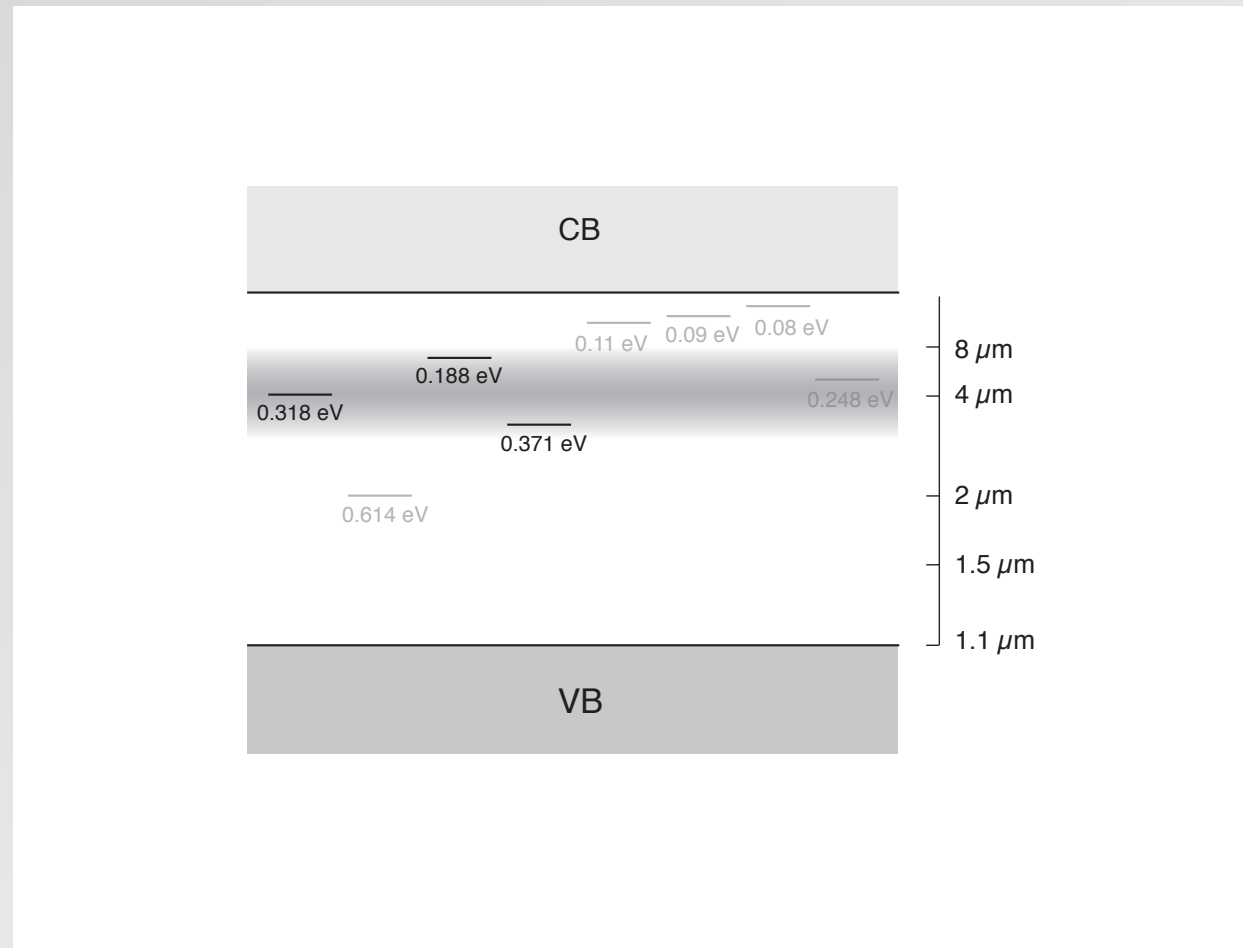


Janzén *et al.*, Phys. Rev. B 29, 1907 (1984)

1 properties

2 intermediate band

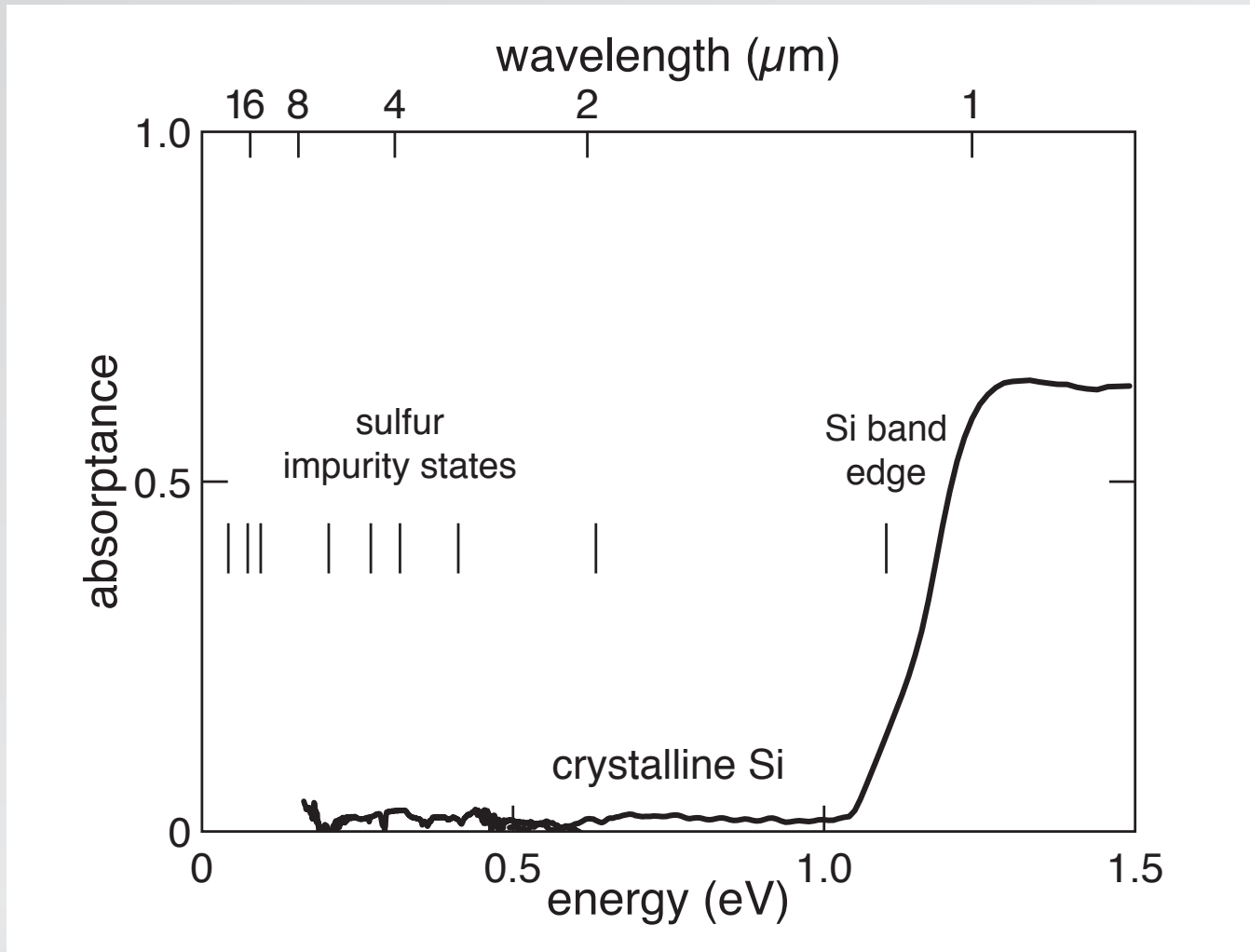
at high concentration states broaden into band



1 properties

2 intermediate band

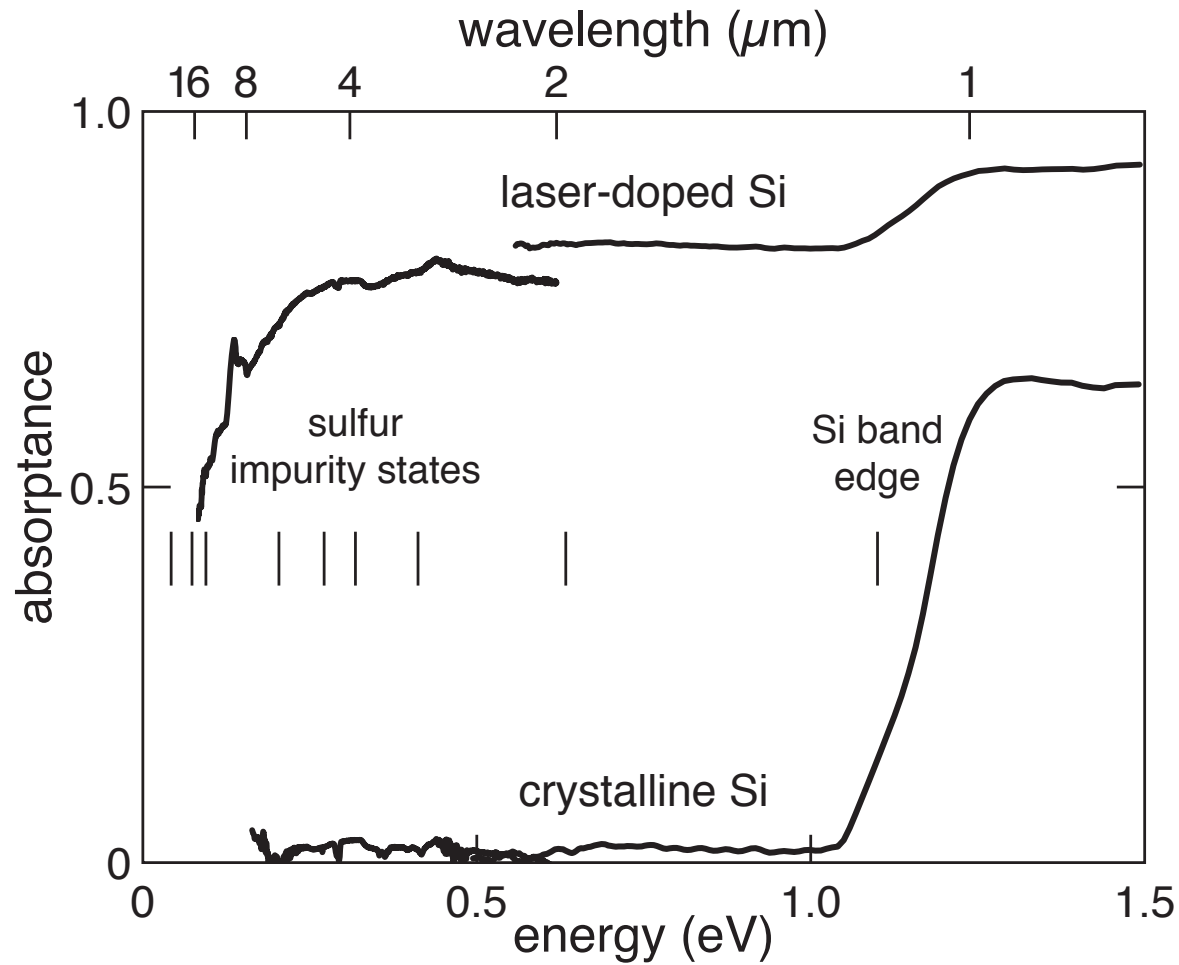
# $10^{-6}$ sulfur doping



1 properties

2 intermediate band

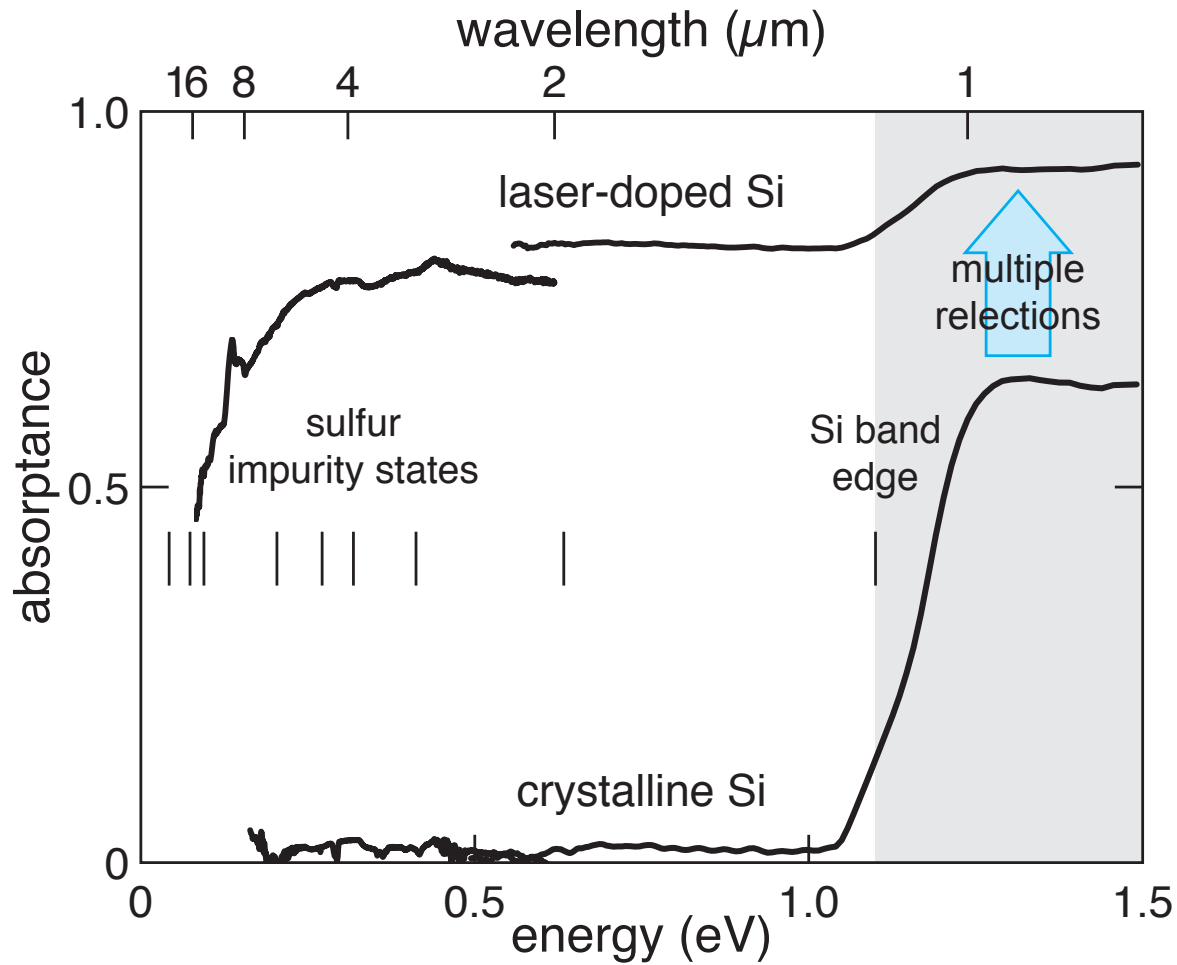
# laser-doped S:Si



1 properties

2 intermediate band

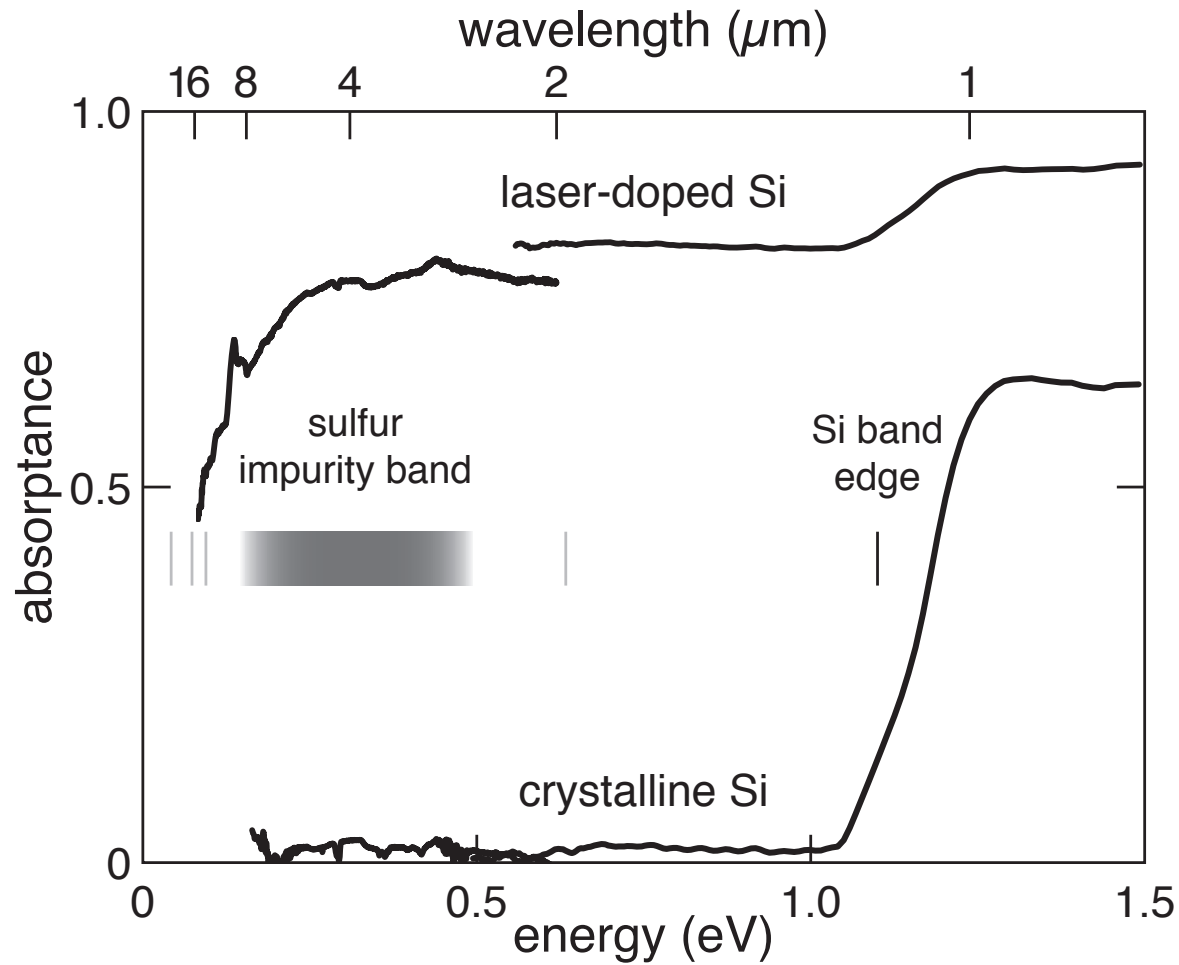
# laser-doped S:Si



1 properties

2 intermediate band

# laser-doped S:Si

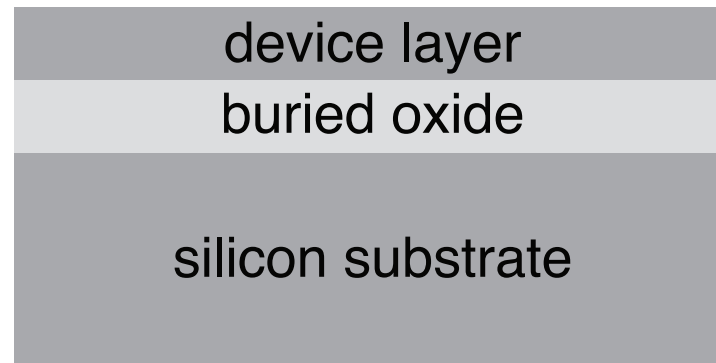


1 properties

2 intermediate band



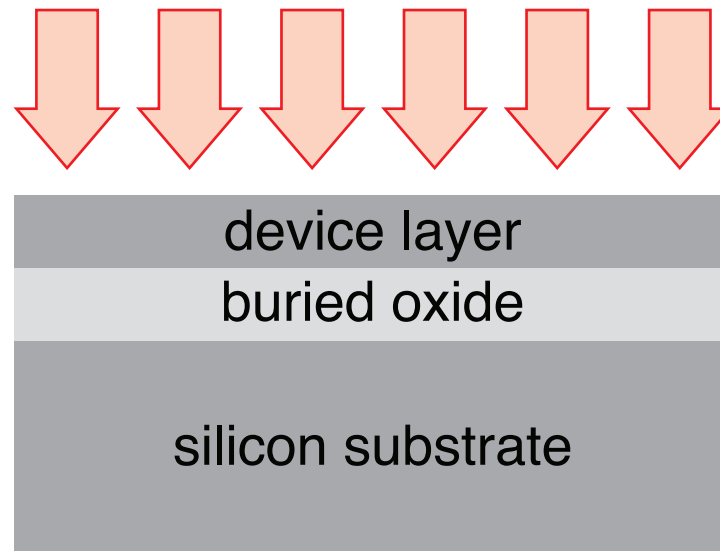
## isolate surface layer for Hall measurements



**1** properties

**2** intermediate band

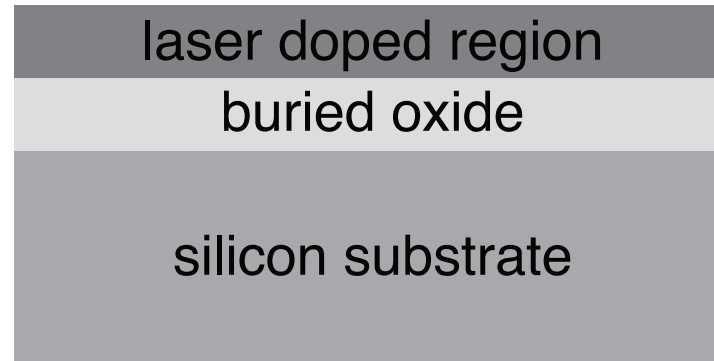
## isolate surface layer for Hall measurements



**1** properties

**2** intermediate band

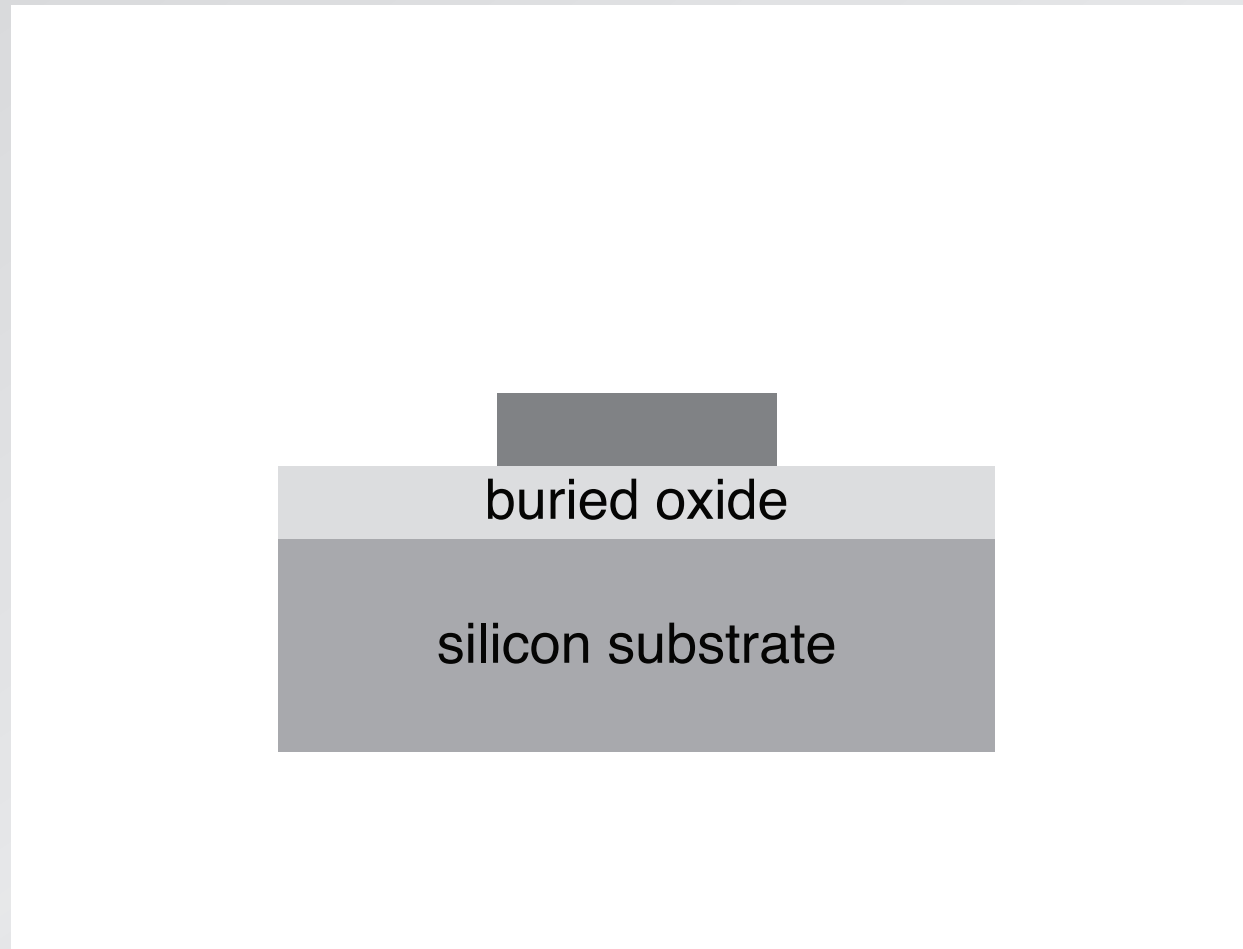
## isolate surface layer for Hall measurements



**1** properties

**2** intermediate band

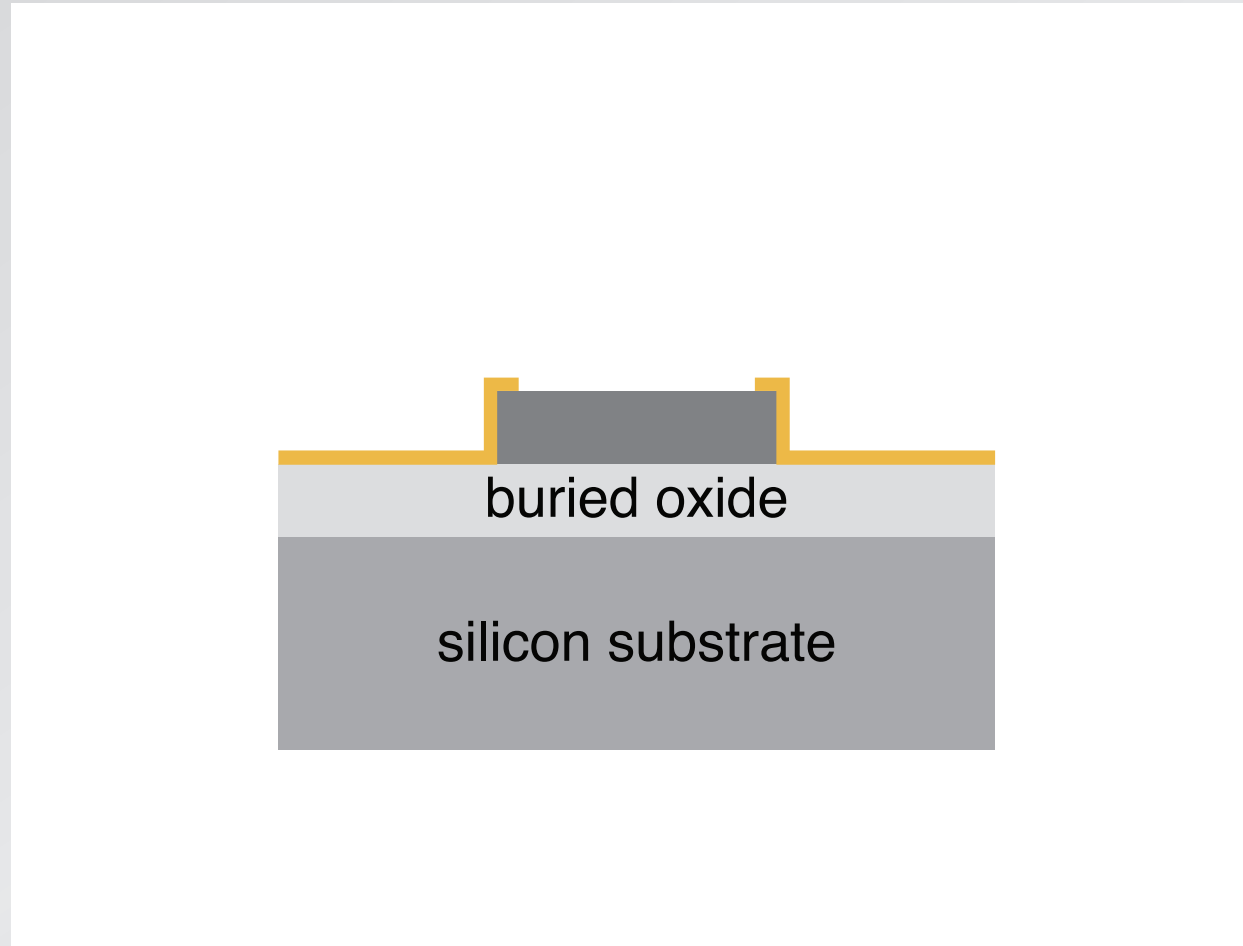
## isolate surface layer for Hall measurements



**1** properties

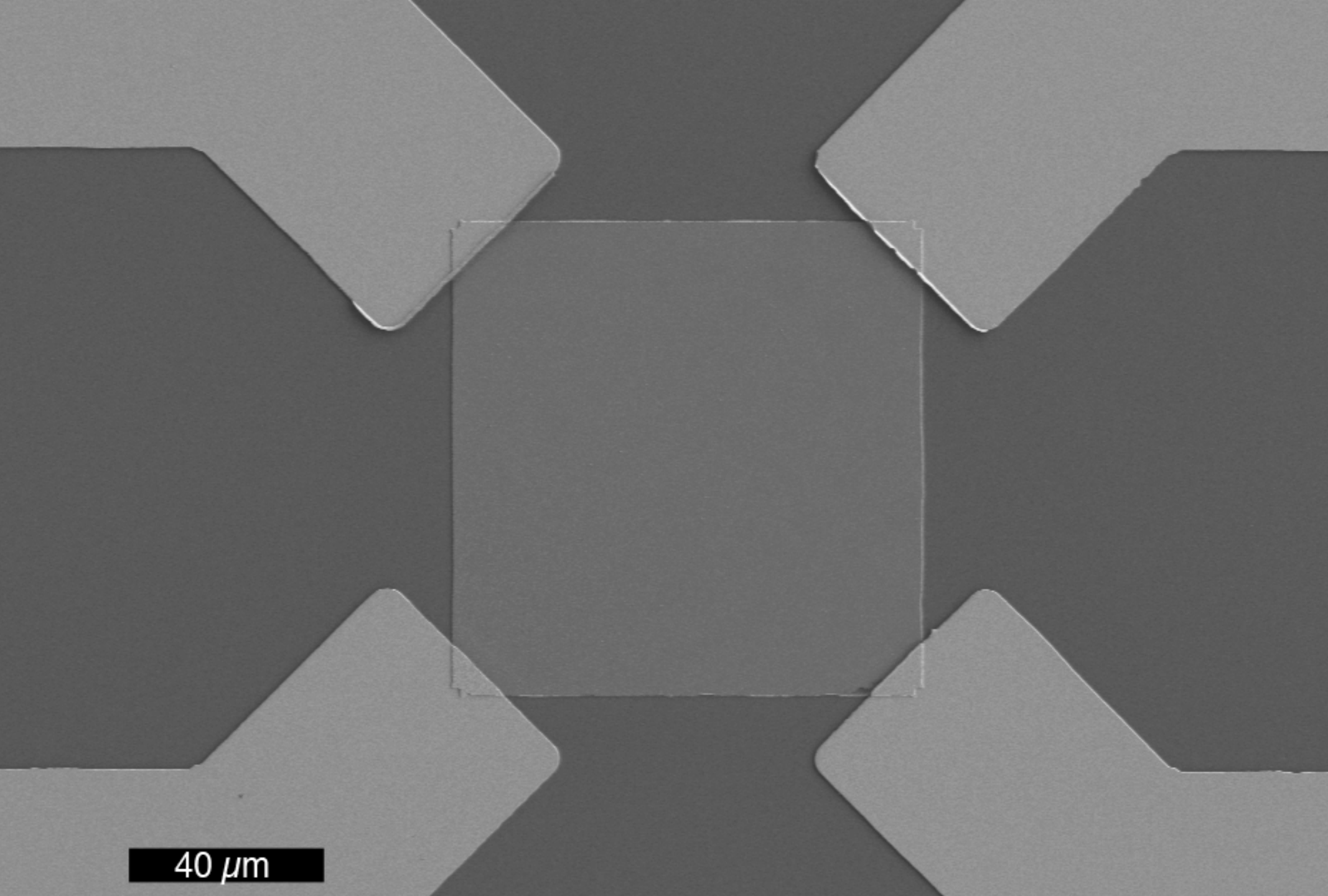
**2** intermediate band

## isolate surface layer for Hall measurements



**1** properties

**2** intermediate band

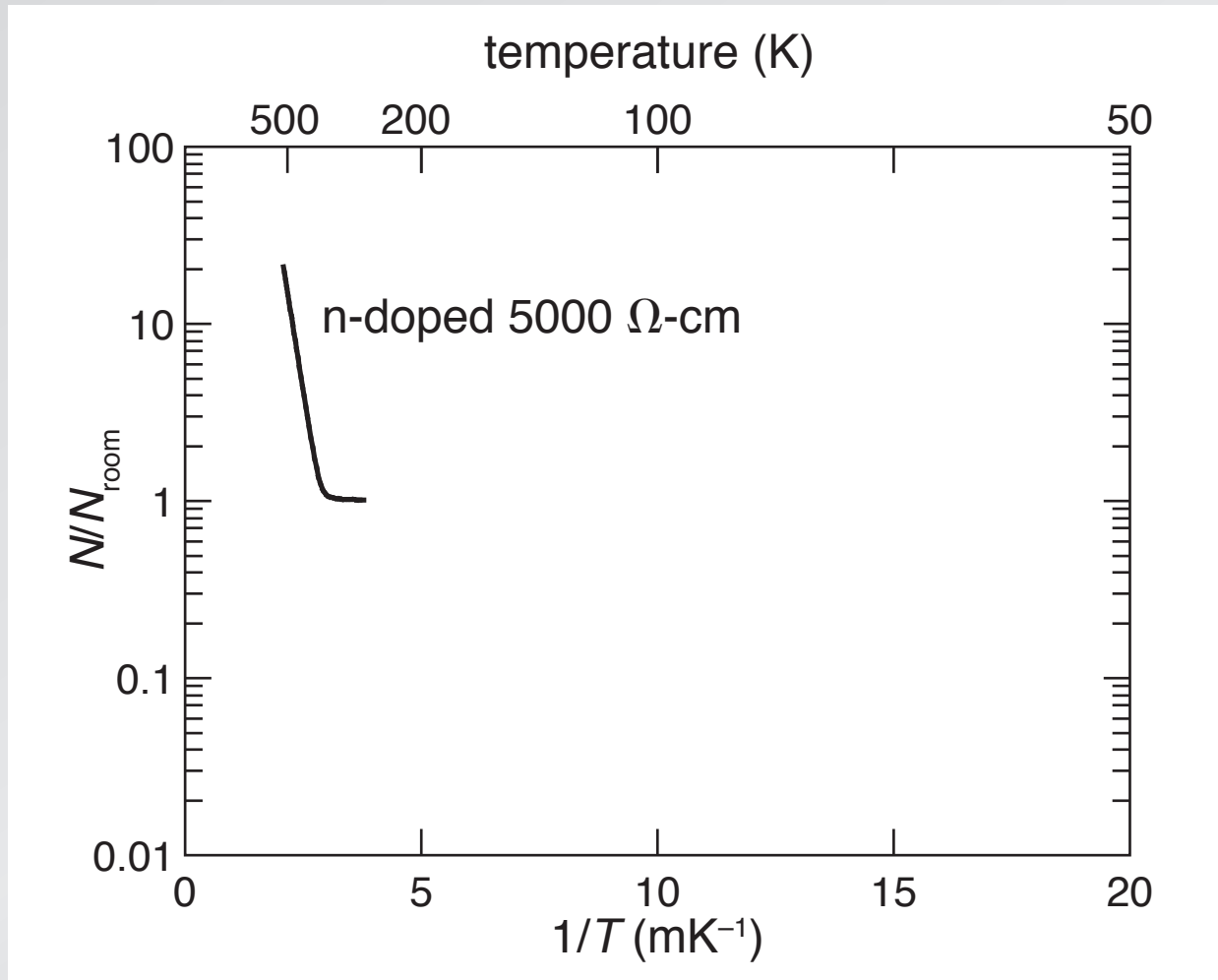


40  $\mu\text{m}$

**1** properties

**2** intermediate band

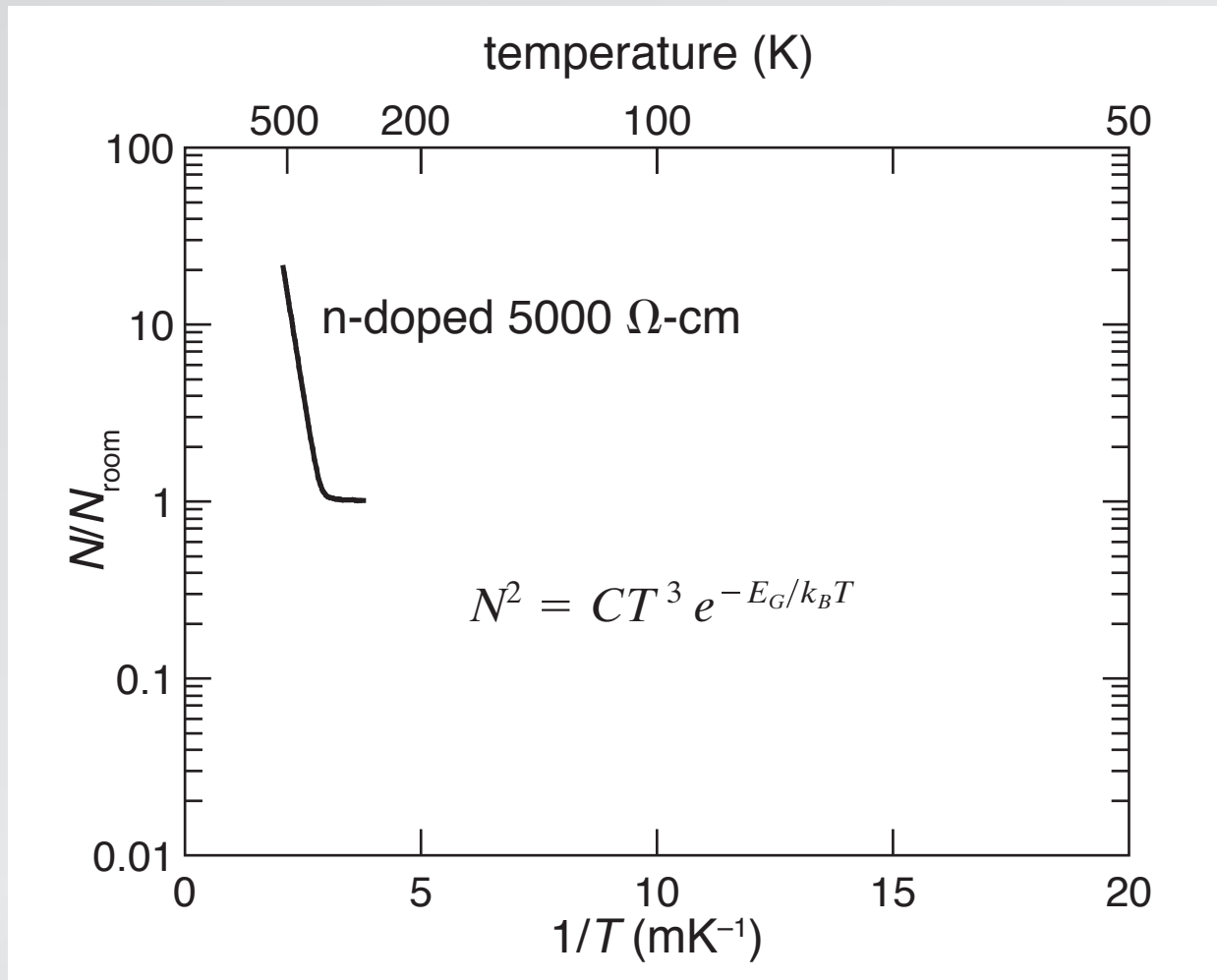
# Hall measurements



1 properties

2 intermediate band

# Hall measurements

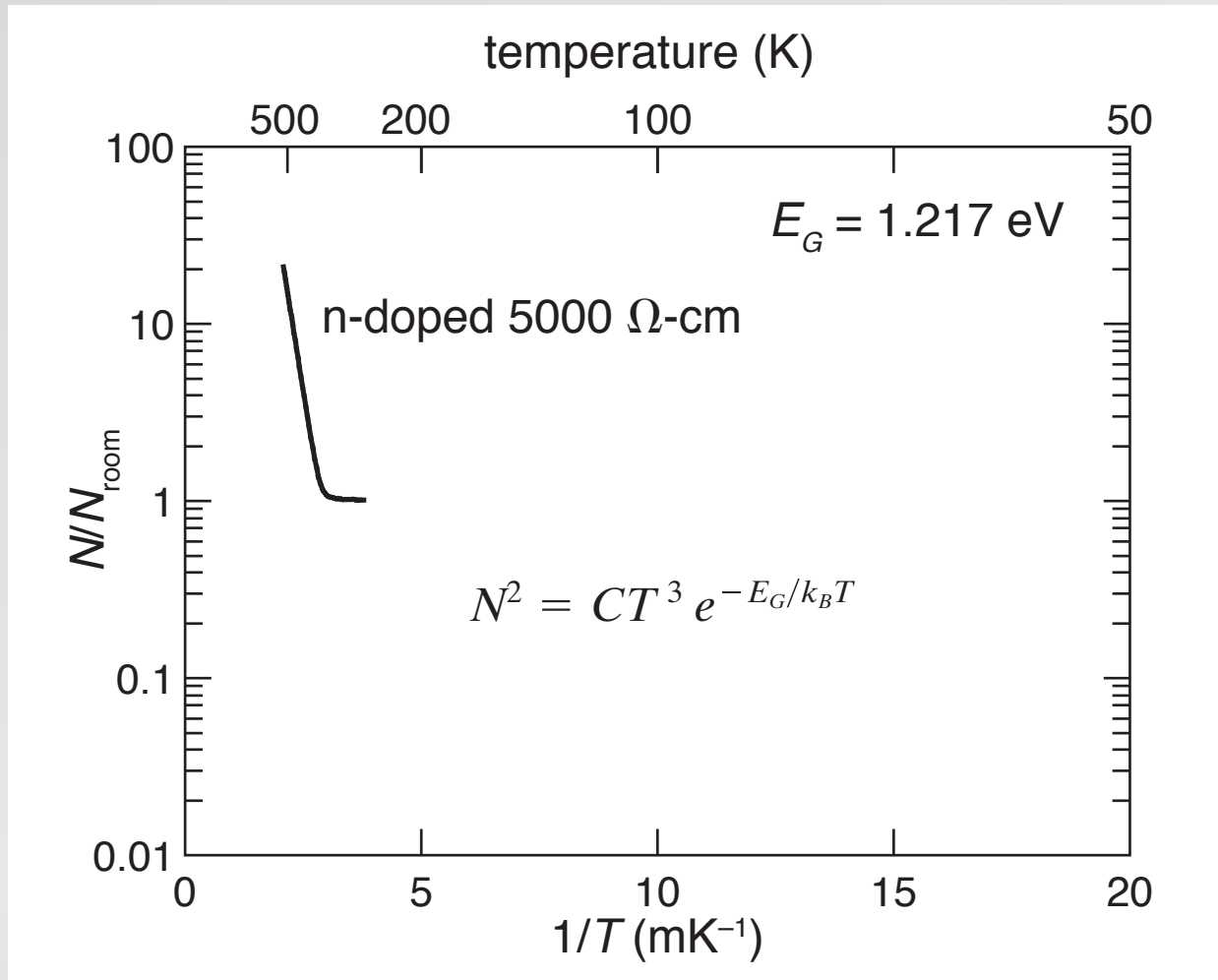


1 properties

2 intermediate band



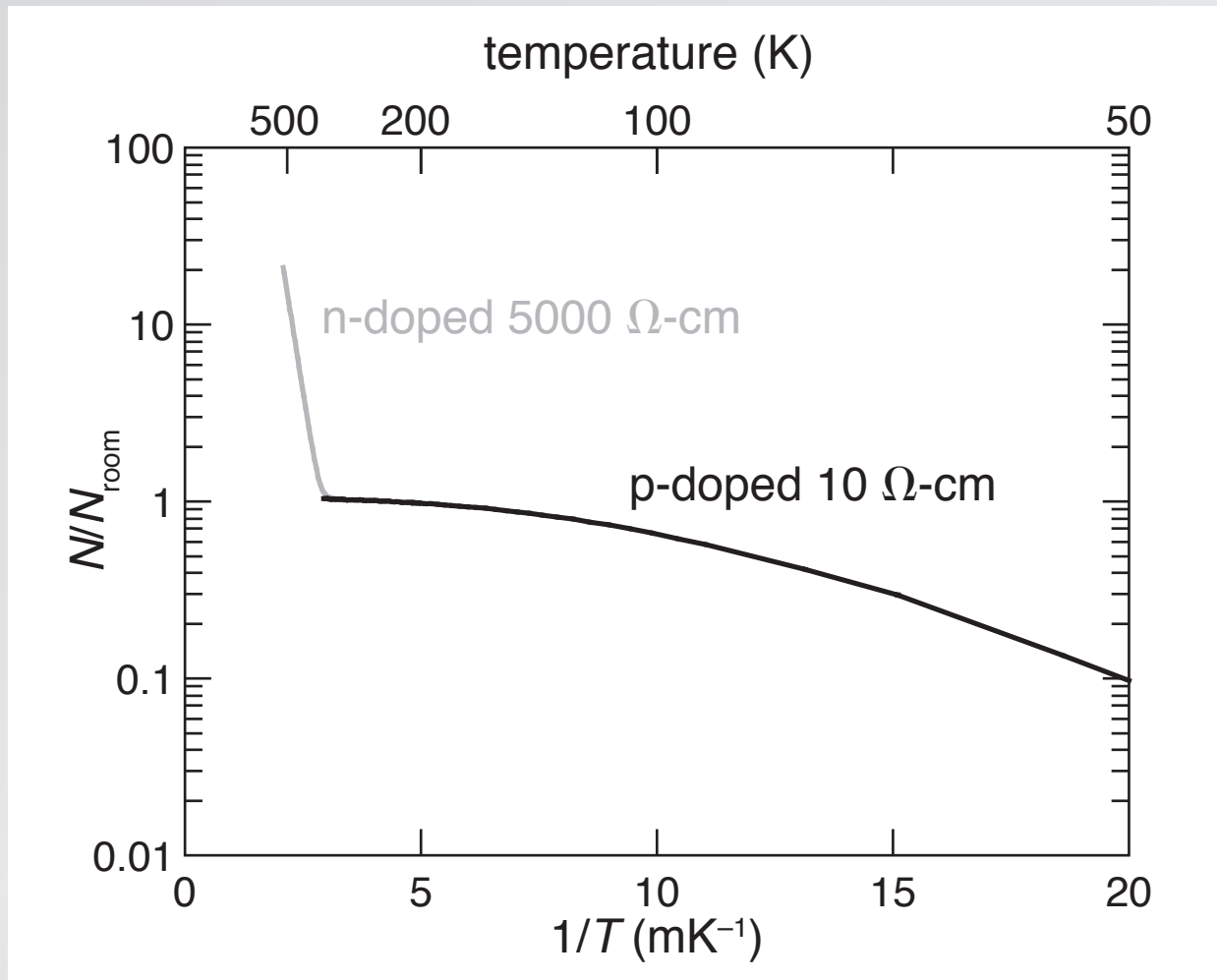
# Hall measurements



1 properties

2 intermediate band

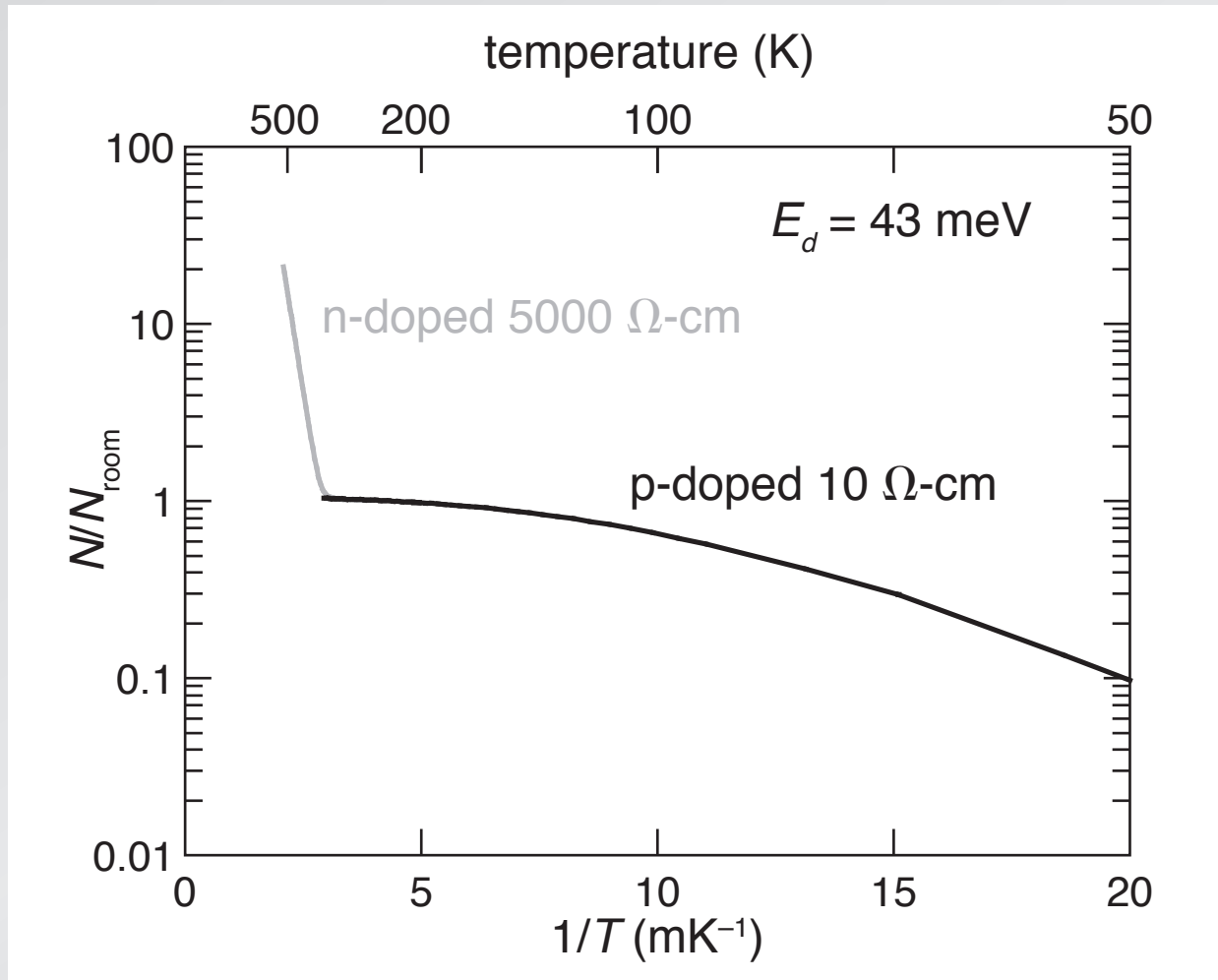
# Hall measurements



1 properties

2 intermediate band

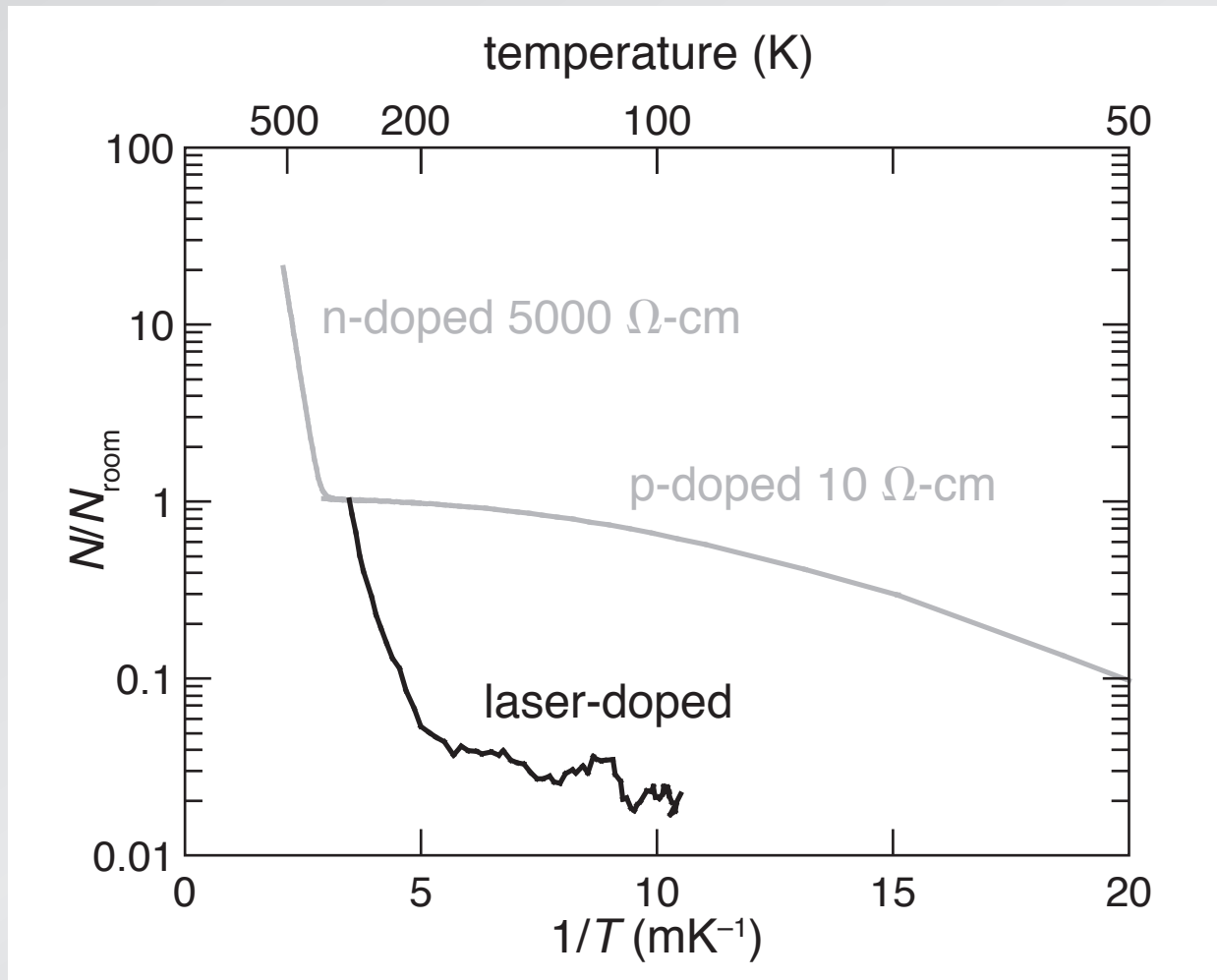
# Hall measurements



1 properties

2 intermediate band

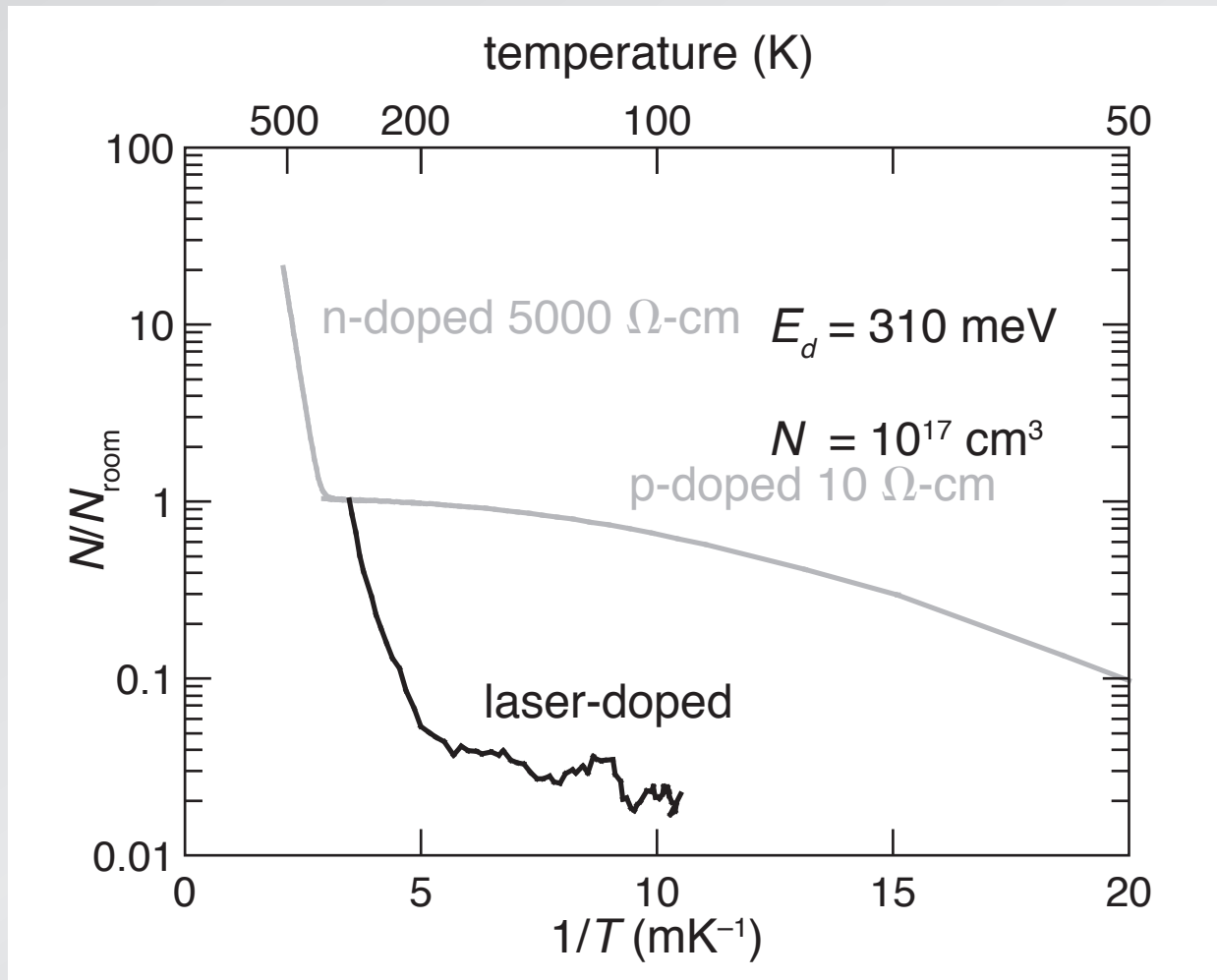
# Hall measurements



1 properties

2 intermediate band

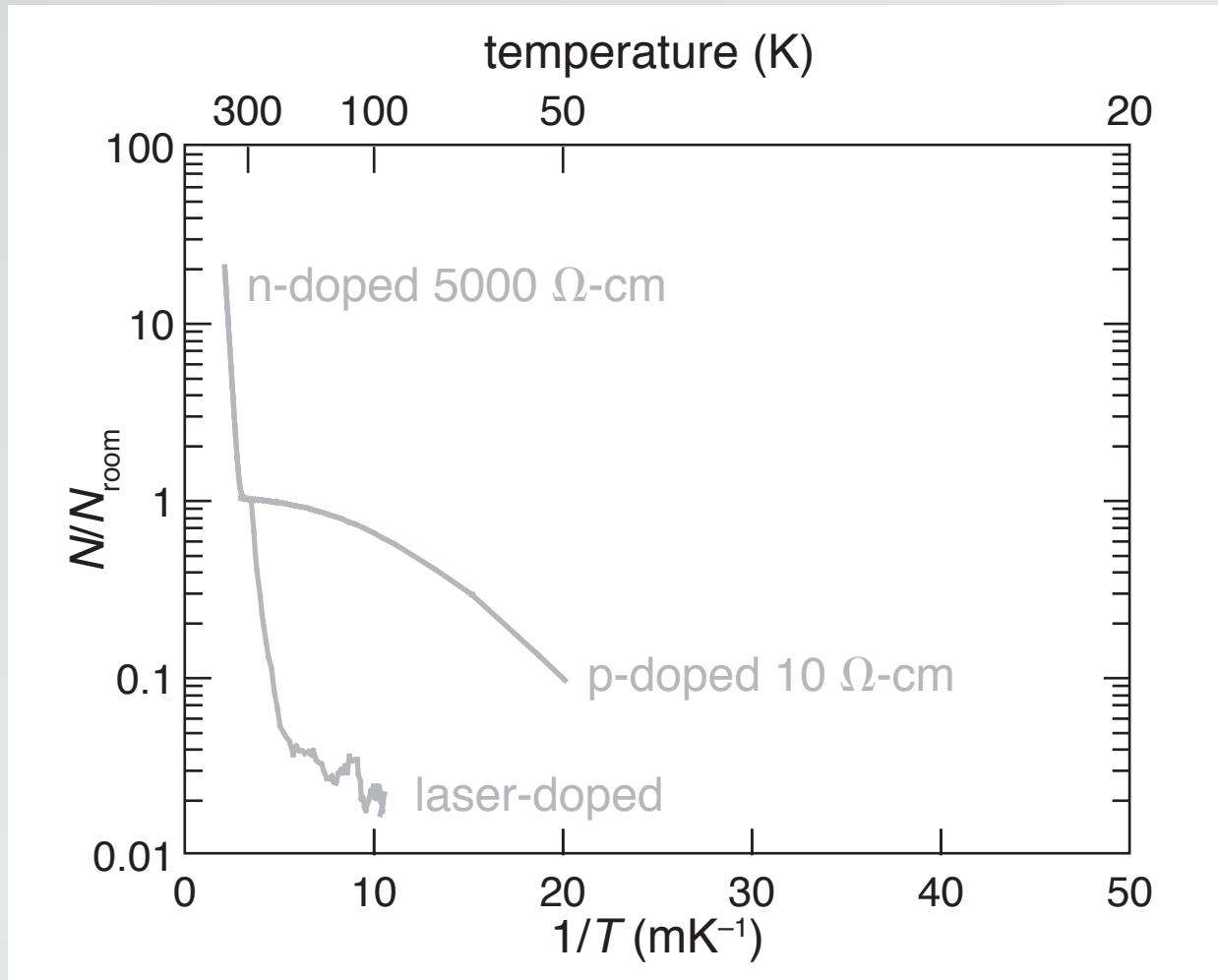
# Hall measurements



1 properties

2 intermediate band

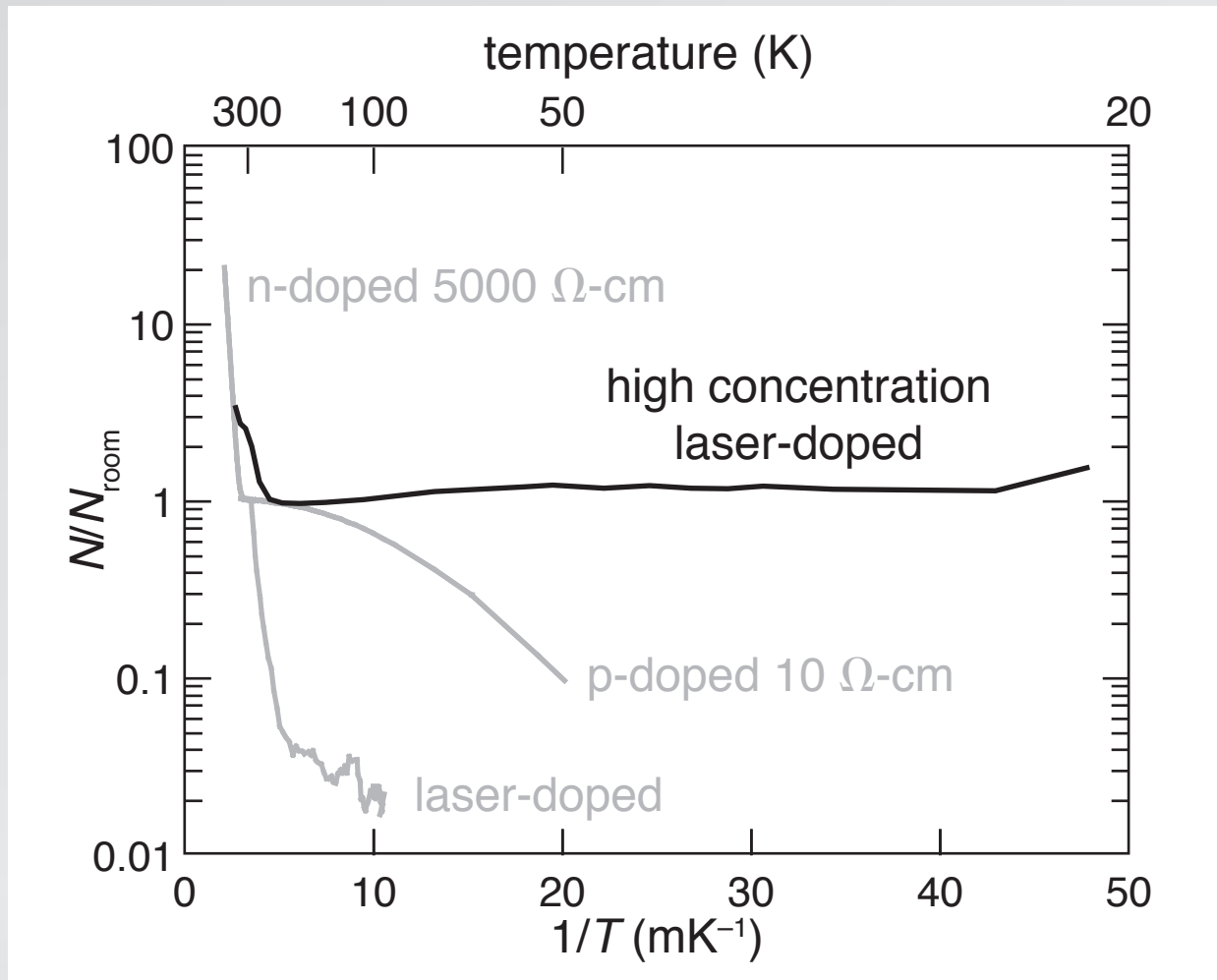
# Hall measurements



1 properties

2 intermediate band

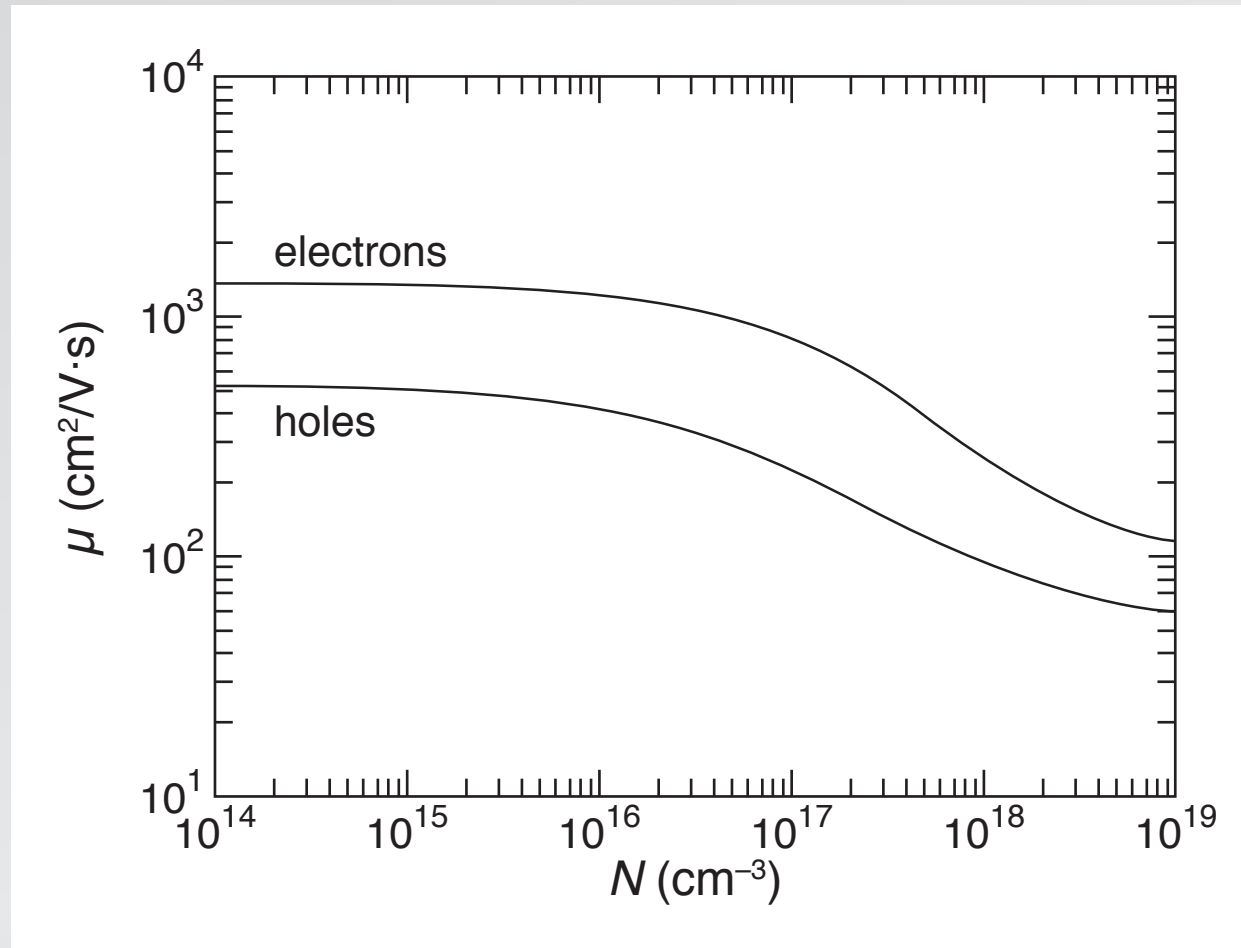
# Hall measurements



1 properties

2 intermediate band

## majority carrier mobility



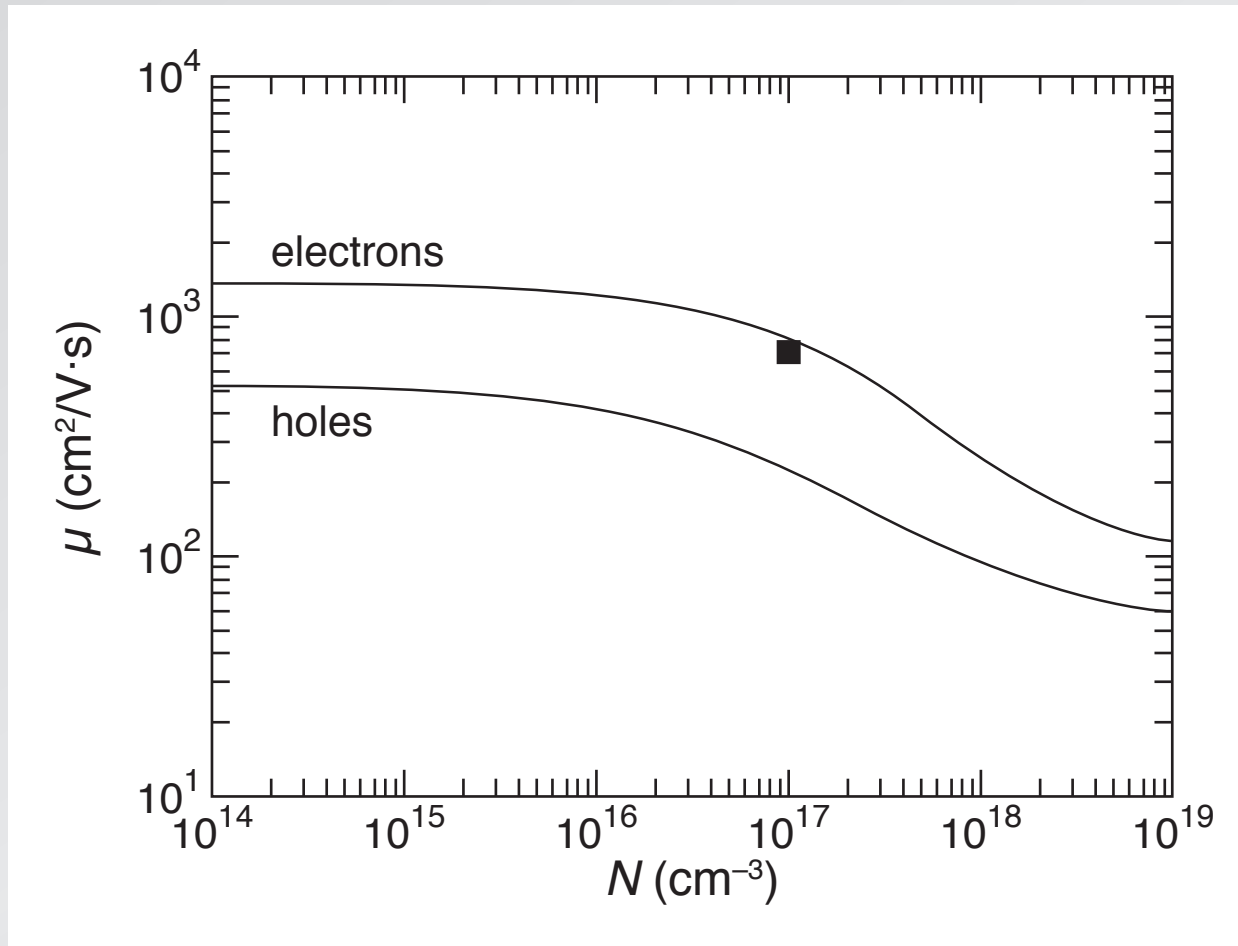
Caughey *et al.*, Proc. IEEE 55, 2192 (1967)

1 properties

2 intermediate band



# majority carrier mobility

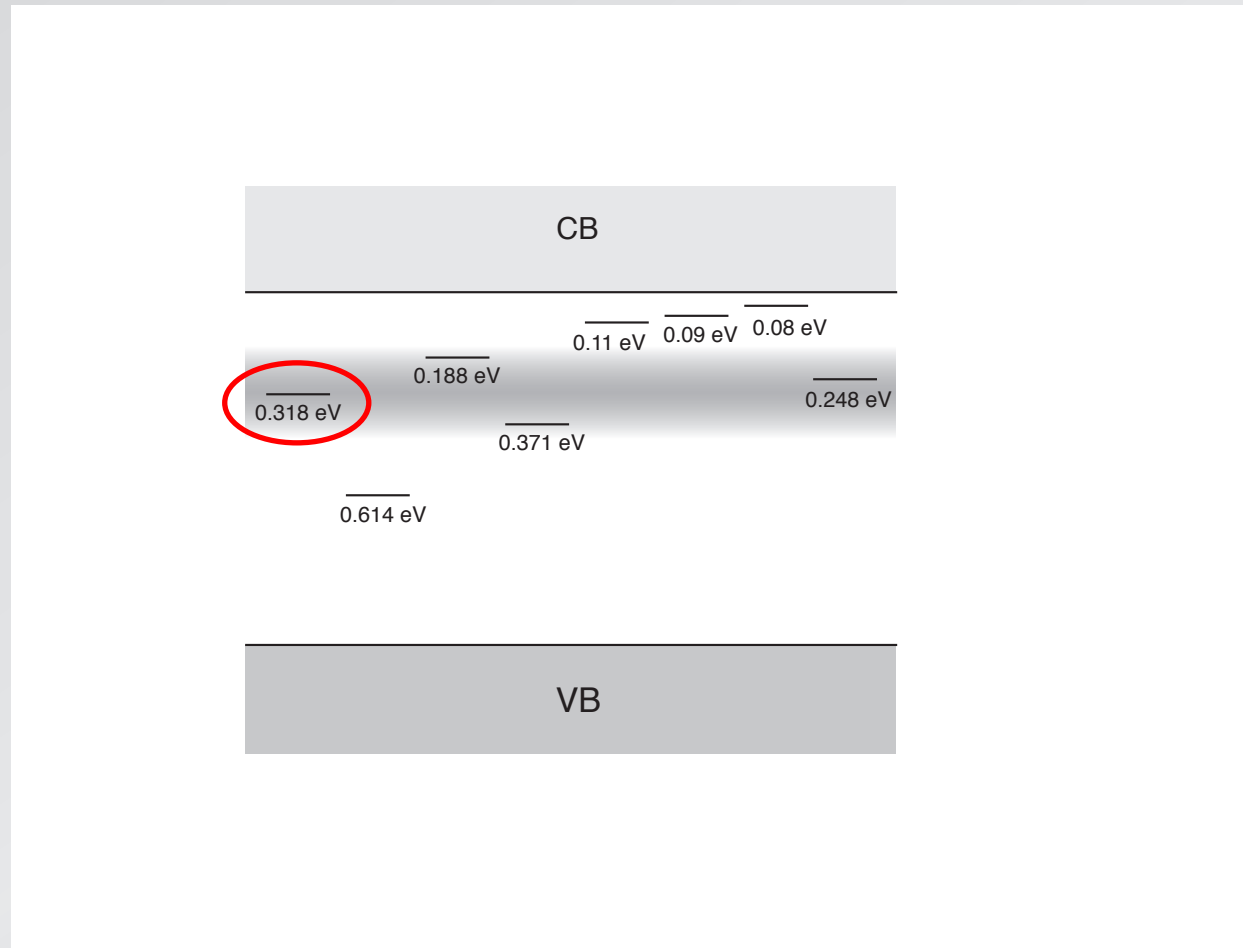


Caughey *et al.*, Proc. IEEE 55, 2192 (1967)

1 properties

2 intermediate band

# impurity (donor) band centered at 310 meV



1 properties

2 intermediate band

# Insulator-to-Metal Transition in Selenium-Hyperdoped Silicon: Observation and Origin

Elif Ertekin,<sup>1,\*</sup> Mark T. Winkler,<sup>2,†</sup> Daniel Recht,<sup>3</sup> Aurore J. Said,<sup>3</sup> Michael J. Aziz,<sup>3</sup>  
Tonio Buonassisi,<sup>2</sup> and Jeffrey C. Grossman<sup>1,2,‡</sup>

<sup>1</sup>Department of Materials Science and Engineering, Massachusetts Institute of Technology, Cambridge Massachusetts 02139, USA  
<sup>2</sup>Department of Mechanical Engineering, Massachusetts Institute of Technology, Cambridge Massachusetts 02139, USA  
<sup>3</sup>Harvard School of Engineering and Applied Sciences, Cambridge Massachusetts 02138, USA

(Received 14 October 2011; published 11 January 2012)

Hyperdoping has emerged as a promising method for designing semiconductors with unique optical and electronic properties, although such properties currently lack a clear microscopic explanation. Combining computational and experimental evidence, we probe the origin of sub-band-gap optical absorption and metallicity in Se-hyperdoped Si. We show that sub-band-gap absorption arises from direct defect-to-conduction-band transitions rather than free carrier absorption. Density functional theory predicts the Se-induced insulator-to-metal transition arises from merging of defect and conduction bands, at a concentration in excellent agreement with experiment. Quantum Monte Carlo calculations confirm the critical concentration, demonstrate that correlation is important to describing the transition accurately, and suggest that it is a classic impurity-driven Mott transition.

PACS numbers: 71.30.+h, 61.72.sd, 73.61.Cw, 78.20.Bh

DOI: 10.1103/PhysRevLett.108.026401

Of all the experimentally measurable physical properties of materials, electronic conductivity exhibits the largest variation, spanning a factor of  $10^{31}$  from the best metals to the strongest insulators [1]. Over the last century, the puzzle of why some materials are conductors and others insulators, and the mechanisms underlying the transformation from one to the other, have been carefully scrutinized; yet even after such a vast body of research over such a long period, the subject remains the object of controversy. In 1956, Mott introduced a model for the insulator-to-metal transition (IMT) in doped semiconductors, in which long-ranged electron correlations are the driving force [2]. Hyperdoping (doping beyond the solubility limit) creates a new materials playground to explore defect-mediated IMTs in semiconductors. In this Letter, we identify a defect-induced IMT in silicon hyperdoped with selenium to concentrations exceeding  $10^{20} \text{ cm}^{-3}$  (compared to the equilibrium solubility limit [3] of about  $10^{16} \text{ cm}^{-3}$ ) and we describe the detailed nature of the transition with both experimental and theoretical methods. Additionally, we

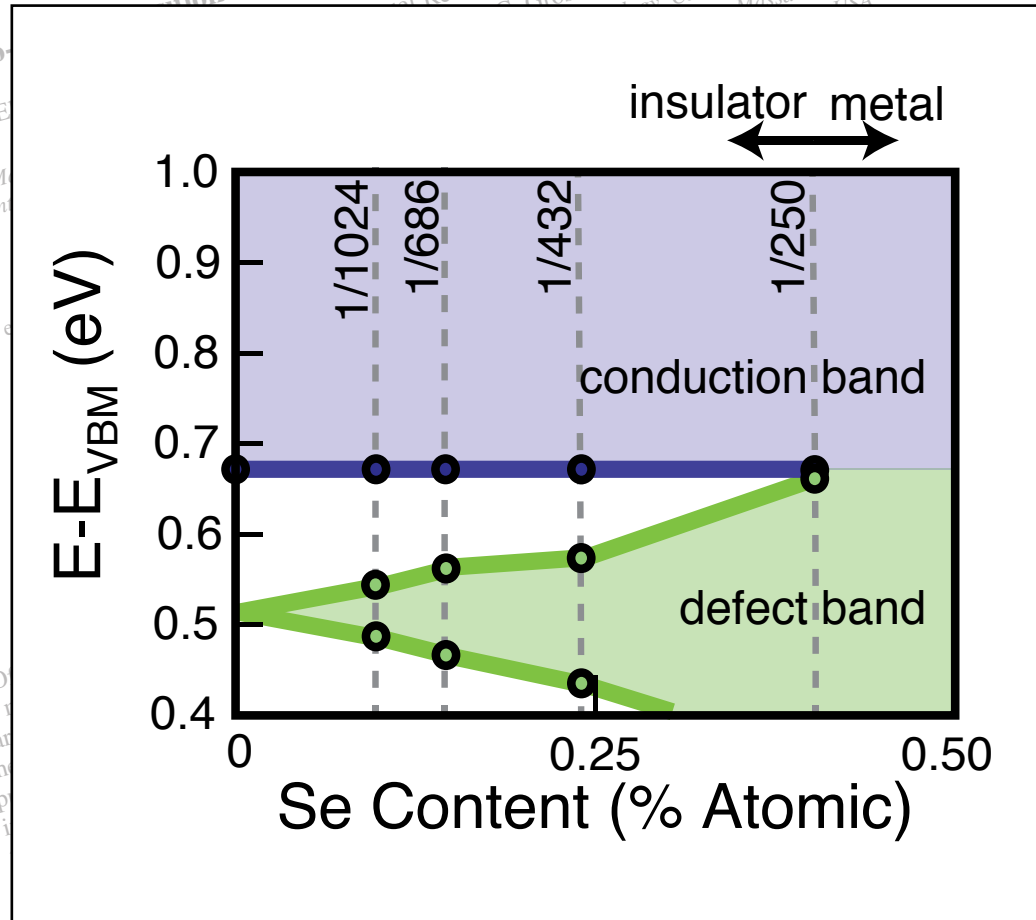
silicon appears to justify such interest. While isolated S and Se dopants are well-established deep double donors in silicon [3,14], the enhanced optical properties of hyperdoped silicon (in which these chalcogenic impurities are present at much higher concentrations) are not yet well understood. Further, unlike the prototypical system of phosphorus-doped silicon for which the IMT has been extensively studied and characterized [15,16], there are very few studies of an IMT resulting from deep defects such as chalcogens [17].

We prepared Se-doped silicon (Se:Si) samples using ion implantation followed by nanosecond pulsed-laser melting (PLM) and rapid resolidification. The PLM process enables chalcogen doping with concentrations exceeding 1% atomic; such samples exhibit unexplained optical properties including broad, featureless absorption of photons with energy lower than the band gap of silicon [9]. Silicon substrates (boron doped,  $\rho \approx 25 \text{ } \Omega \text{ cm}$ ) were ion implanted with Se to nominal doses of  $3 \times 10^{15}$  and  $1 \times 10^{16} \text{ cm}^{-2}$  using an ion beam energy of 176 keV. The implanted samples were exposed to four laser pulses (fluences of 1.7, 1.7, 1.7 and  $1.8 \text{ J cm}^{-2}$ ). This fluence regimen results in a slightly shallower dopant profile, and higher Se concentration, than reported previously [18]. The electrically isolated from the crystalline, extends approximately 350 nm between electrically isolated from the measured

1 properties

2 intermediate band

# DFT calculations



Ertekin *et al.*, Phys. Rev. Lett. 108, 026401 (2012)

1 properties

2 intermediate band

# Emergence of very broad infrared absorption band by hyperdoping of silicon with chalcogens

Ikurou Umezu,<sup>1</sup> Jeffrey M. Warrender,<sup>2</sup> Supakit Charnvanichborikarn,<sup>3</sup> Atsushi Kohno,<sup>4</sup>  
James S. Williams,<sup>3</sup> Malek Tabbal,<sup>5</sup> Dimitris G. Papazoglou,<sup>6,7</sup> Xi-Cheng Zhang,<sup>8,a)</sup>  
and Michael J. Aziz<sup>9</sup>

<sup>1</sup>Department of Physics, Konan University, Kobe 658-8501, Japan

<sup>2</sup>U.S. Army ARDEC-Benét Laboratories, Watervliet, New York 12189, USA

<sup>3</sup>Research School of Physics and Engineering, The Australian National University, Canberra, ACT 0200, Australia

<sup>4</sup>Department of Applied Physics, Fukuoka University, Fukuoka 814-0180, Japan

<sup>5</sup>Institute of Physics, American University of Beirut, Beirut 1107 2020, Lebanon

<sup>6</sup>71110 Heraklion, Greece

<sup>7</sup>Materials Science and Technology Department, University of Crete, P.O. Box 1527, 71003 Heraklion, Greece

<sup>8</sup>Department of Physics, Applied Physics and Astronomy, Rensselaer Polytechnic Institute, Troy, New York 12180, USA

<sup>9</sup>Harvard School of Engineering and Applied Sciences, Cambridge, Massachusetts 02138, USA

(Received 9 September 2012; accepted 29 April 2013; published online 3 June 2013)

We report the near through mid-infrared (MIR) optical absorption spectra, over the range 0.05–1.3 eV, of monocrystalline silicon layers hyperdoped with chalcogen atoms synthesized by ion implantation followed by pulsed laser melting. A broad mid-infrared optical absorption band emerges, peaking near 0.5 eV for sulfur and selenium and 0.3 eV for tellurium hyperdoped samples. Its strength and width increase with impurity concentration. Its strength decreases markedly with subsequent thermal annealing. The emergence of a broad MIR absorption band is consistent with the formation of an impurity band from isolated deep donor levels as the concentration of chalcogen atoms in metastable local configurations increases. © 2013 AIP Publishing LLC.  
[\[http://dx.doi.org/10.1063/1.4804935\]](http://dx.doi.org/10.1063/1.4804935)

## I. INTRODUCTION

Silicon hyperdoped with chalcogens can be synthesized by pulsed laser irradiation in a sulfur-bearing atmosphere,<sup>1,2</sup> ion implantation followed by pulsed laser melting,<sup>3,4</sup> or pulsed laser mixing.<sup>5</sup> This material has attracted interest because of its sub band gap absorption and has been studied as a candidate for infrared (IR) photodetectors<sup>6–8</sup> and efficient solar cells.<sup>9–11</sup> In addition, observations of carrier lifetime recovery for sufficiently high concentrations of titanium has aroused similar interest in this material.<sup>12,13</sup>

Hyperdoping has been shown to cause an intermediate bandgap<sup>4,10,14–16</sup> However, the bandgap

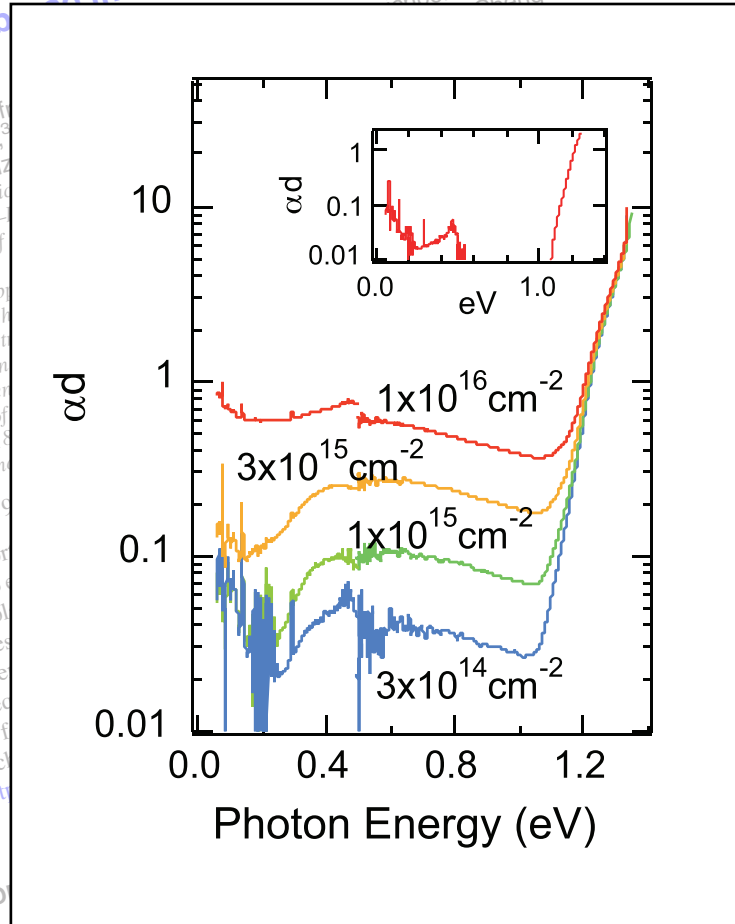
## II. EXPERIMENT

Double side polished p type (001) Si wafers, resistivity of 5–25  $\Omega$  cm, were ion implanted at room temperature with either 95 keV <sup>32</sup>S<sup>-</sup>, 176 keV <sup>80</sup>Se<sup>+</sup>, or 245 keV <sup>130</sup>Te<sup>+</sup> to doses of  $1 \times 10^{16}$  ions/cm<sup>2</sup>. The dose of <sup>32</sup>S<sup>-</sup> was varied from  $3 \times 10^{14}$  to  $1 \times 10^{16}$  ions/cm<sup>2</sup> and pre-amorphized by 85 keV Si<sup>-</sup> to doses of  $3 \times 10^{15}$  ions/cm<sup>2</sup>. Pulsed laser melting is not greater than  $1 \times 10^{15}$  ions/cm<sup>2</sup>. Pulsed laser melting was performed using a XeCl excimer laser beam (308 nm, 25 ns FWHM, 50 ns total duration). Each sample received three laser shots at 1.7 J/cm<sup>2</sup> followed by a fourth laser shot at 1.8 J/cm<sup>2</sup>. Time-resolved reflectivity of a 488 nm Ar<sup>+</sup> ion laser was used to measure the melt duration. The laser fluence was calibrated by comparing the melt duration with numerical solutions to the one-dimensional method<sup>18</sup> The details of the sample preparation method of chalcogen atoms observed by secondary ion mass spectrometry are reported elsewhere.<sup>3</sup> For the samples, the procedure is the same.

# Emergence of very broad infrared absorption band by hyperdoping of silicon

Ikuro Umezu,<sup>1</sup> Jeff James S. Williams,<sup>2</sup> and Michael J. Aziz<sup>3</sup>  
<sup>1</sup>Department of Physics, <sup>2</sup>U.S. Army ARDEC, <sup>3</sup>Research School of Physics, <sup>4</sup>Department of Physics, <sup>5</sup>Department of Physics, <sup>6</sup>Institute of Electronics, <sup>7</sup>Materials Science, <sup>8</sup>Department of Physics, <sup>9</sup>Harvard School of Engineering and Applied Sciences

Shrikant, Atsushi Kohno, Zhang



the range  
desized by  
ption band  
ed samples.  
arkedly with  
onsistent with  
concentration  
ublishing LLC.

ed p type (001) Si wafers, resistivity  
on implanted at room temperature with  
176 keV <sup>80</sup>Se<sup>+</sup>, or 245 keV <sup>130</sup>Te<sup>+</sup> to  
ions/cm<sup>2</sup>. The dose of <sup>32</sup>S<sup>-</sup> was varied  
x 10<sup>16</sup> ions/cm<sup>2</sup> and pre-amorphized by  
ses of 3 x 10<sup>15</sup> ions/cm<sup>2</sup> when the <sup>32</sup>S<sup>-</sup>  
than 1 x 10<sup>15</sup> ions/cm<sup>2</sup>. Pulsed laser melt-  
ing was performed using a XeCl excimer laser beam  
(308 nm, 25 ns FWHM, 50 ns total duration). Each sample  
received three laser shots at 1.7 J/cm<sup>2</sup> followed by a fourth  
laser shot at 1.8 J/cm<sup>2</sup>. Time-resolved reflectivity of a  
488 nm Ar<sup>+</sup> ion laser was used to measure the melt dura-  
tion with numerical solutions to the one-dimensional method  
The laser fluence was calibrated by comparing the melt dura-  
tion with numerical solutions to the one-dimensional method  
of chalcogen atoms observed by secondary  
18 The details of the sample preparation method  
reported elsewhere.<sup>3</sup> For  
samples,

Umezu et al., J. Appl. Phys. 113, 213501 (2013)

1 properties

2 intermediate band

# Understanding the Viability of Impurity-Band Photovoltaics: A Case Study of S-doped Si

by

Joseph Timothy Sullivan

Submitted to the Department of Mechanical Engineering  
on May 18, 2013, in partial fulfillment of the  
requirements for the degree of  
Doctor of Philosophy

## Abstract

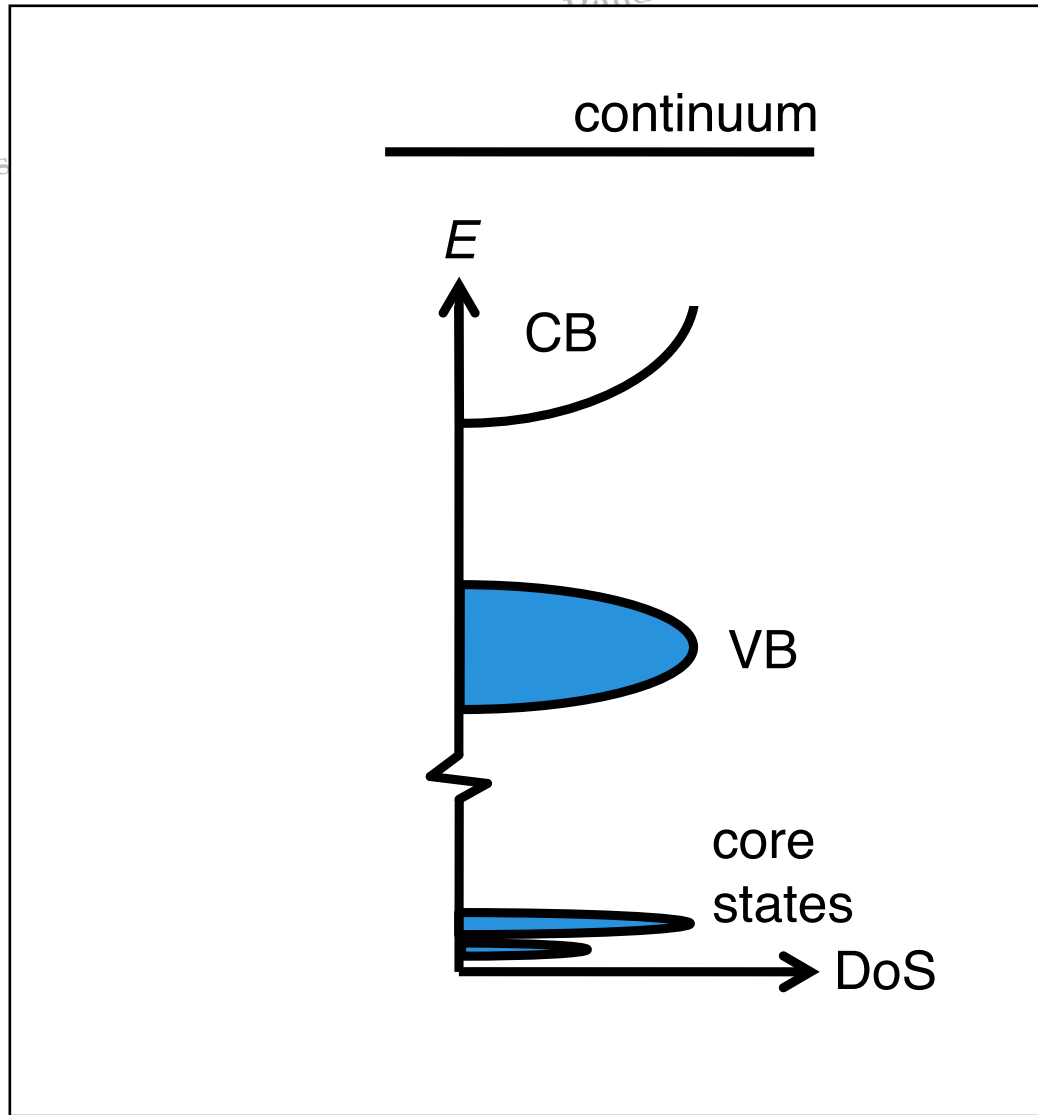
This thesis explores the electronic structure, optical properties, and carrier lifetimes in silicon that is doped with sulfur beyond the equilibrium solid solubility limit, with a focus on applications as an absorber layer for an impurity-band photovoltaic device. The concept of an impurity-band material envisions the creation of a band of electronic states by incorporating high concentrations of deep-level dopants, which enable the generation of free carriers using photons with energy less than that of the band gap of the host semiconductor. The investigations reported in this thesis provide a framework for the appropriate selection of impurity-band candidate materials. The thesis is divided into three primary sections, one for each of three experimental techniques, respectively.

First, the electronic band structure is studied using synchrotron-based x-ray emission spectroscopy. These spectra provide the first insights into how the electronic structure changes as the sulfur concentration is increased across the metal-insulator transition, and how the electronic structure is linked to the anomalously high sub-band gap absorption. A discrete change in local electronic structure is seen that corresponds to the macroscopic change in electronic behavior. Additionally, a direct correlation is seen between sulfur-induced states and the sub-band gap absorption. The optical properties are studied using Fourier transform infrared spectroscopy. The complex index of refraction is performed using numerical transmission and reflection measurements. Analysis of the position of the sulfur-induced states within the metal-insulator transition, and the different sulfur concentrations and their effect on the sub-band gap absorption, are also presented.

1 properties

2 intermediate band

Unders



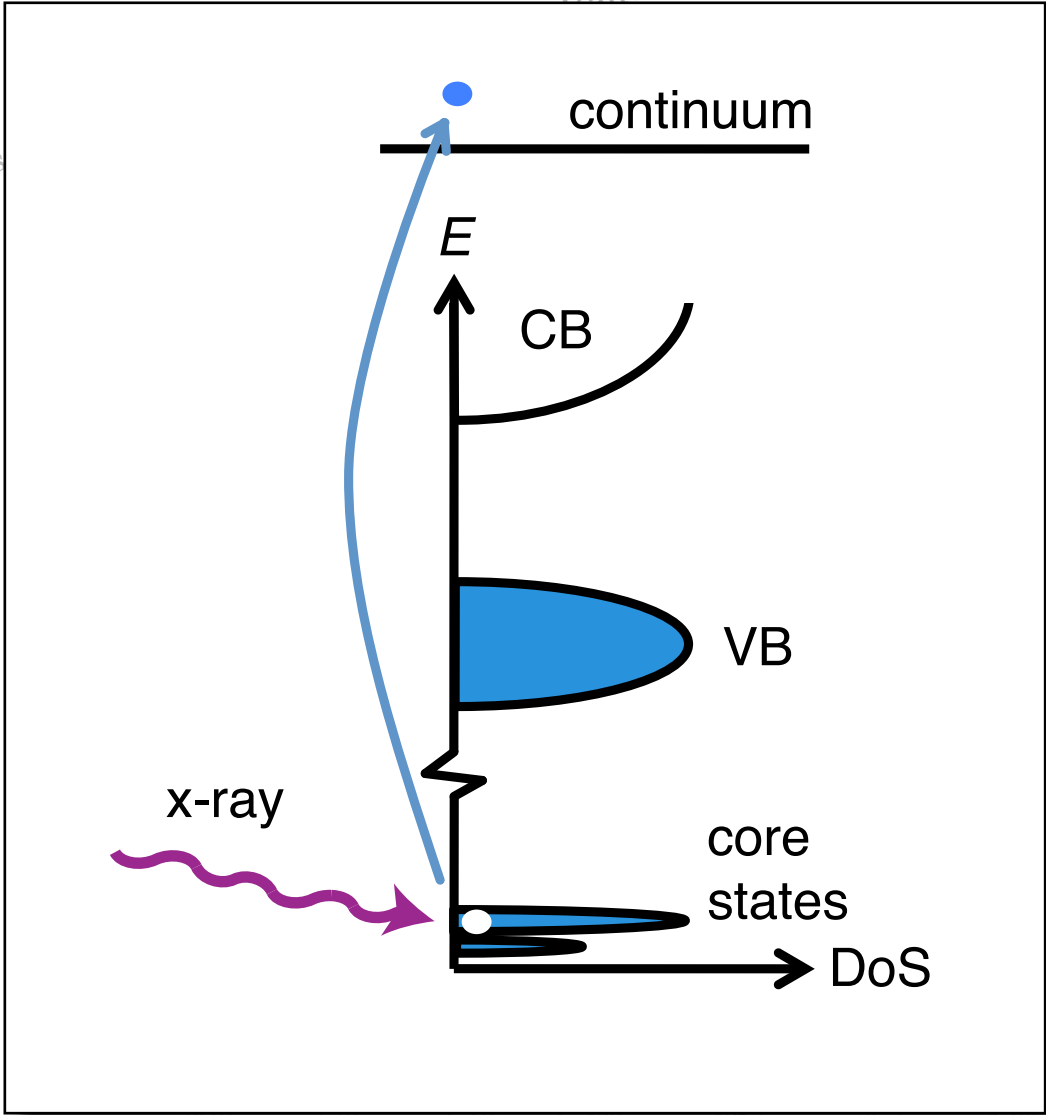
J. Sullivan, Ph.D. Thesis, MIT (2013)

1 properties

2 intermediate band



Unders

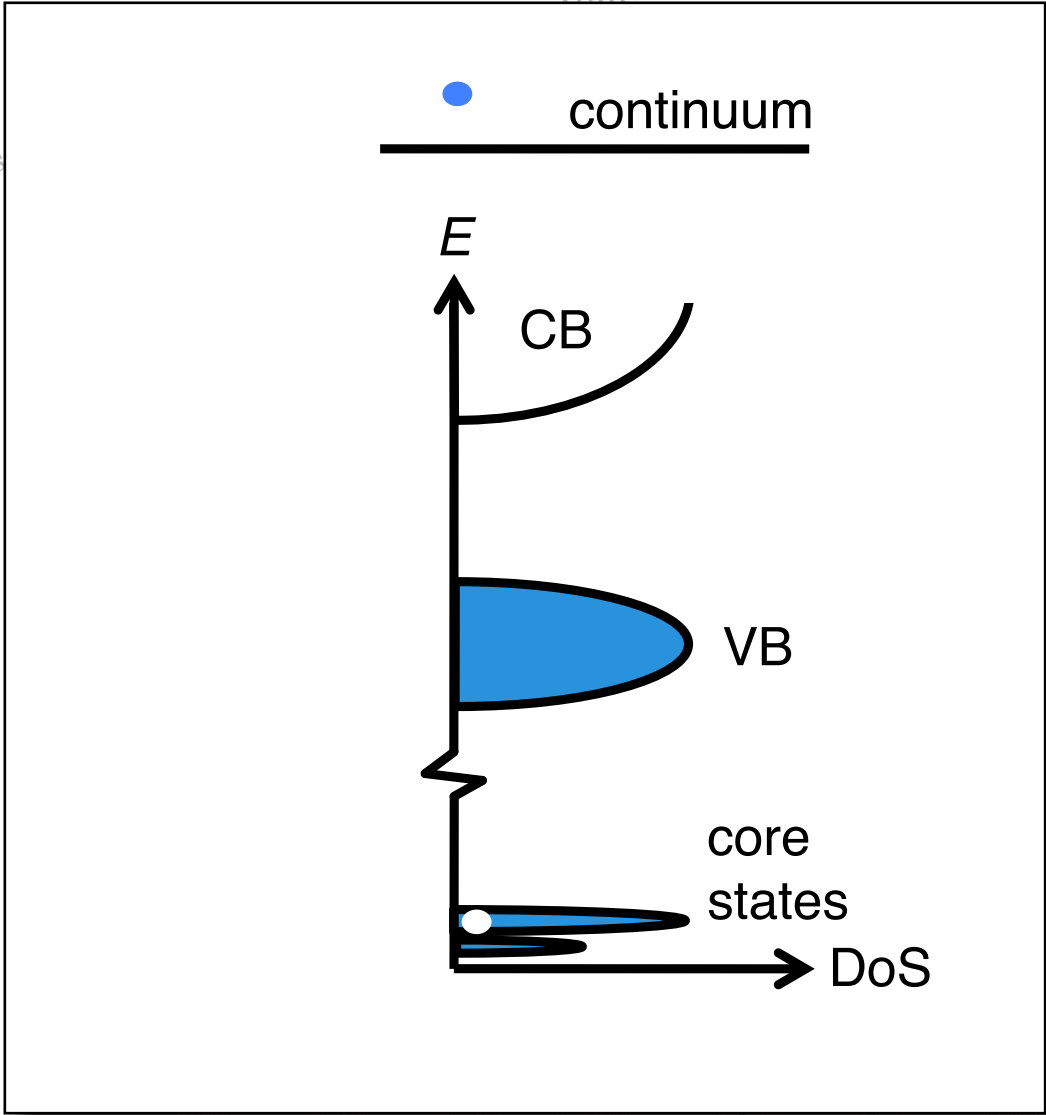


J. Sullivan, Ph.D. Thesis, MIT (2013)

1 properties

2 intermediate band

Unders

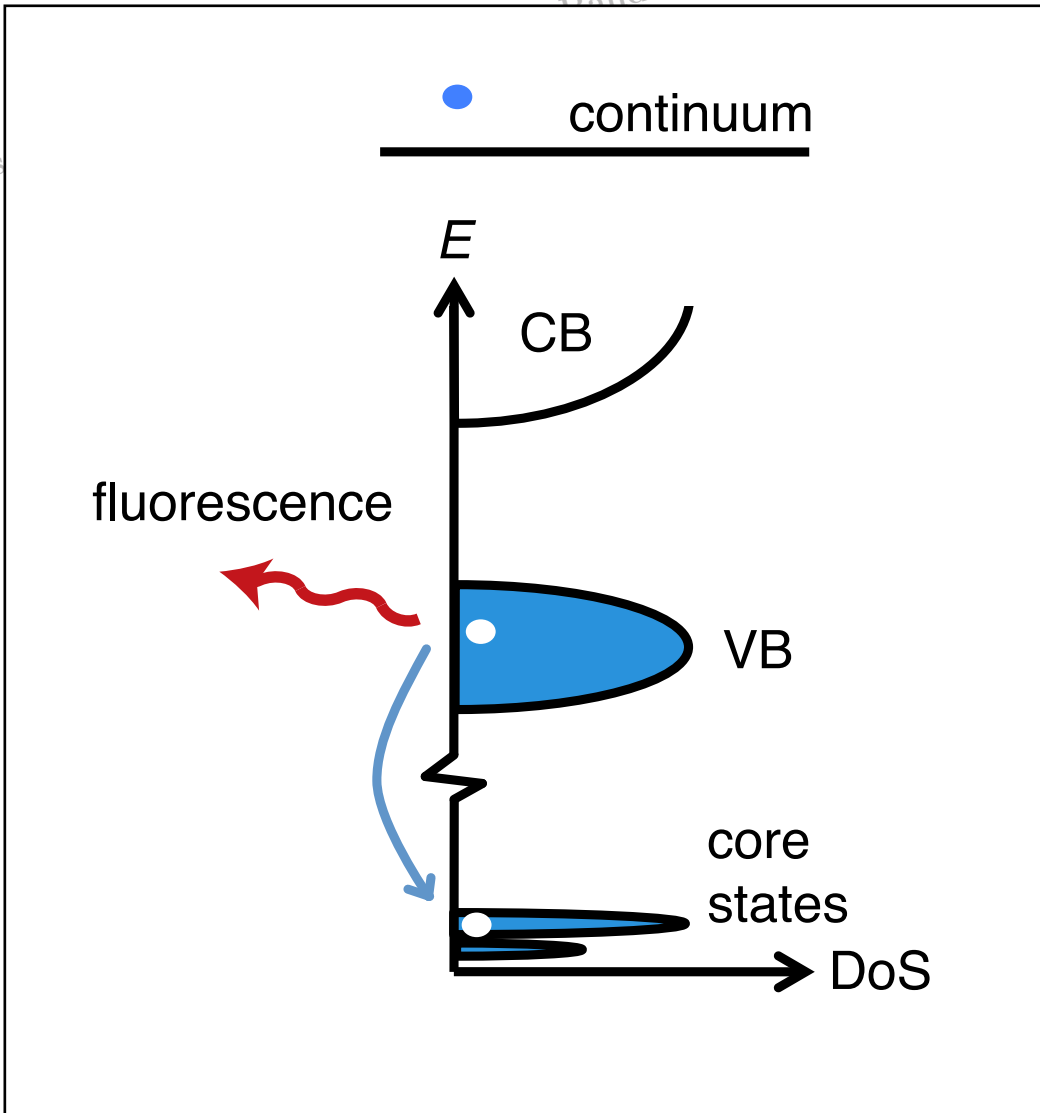


J. Sullivan, Ph.D. Thesis, MIT (2013)

1 properties

2 intermediate band

Unders

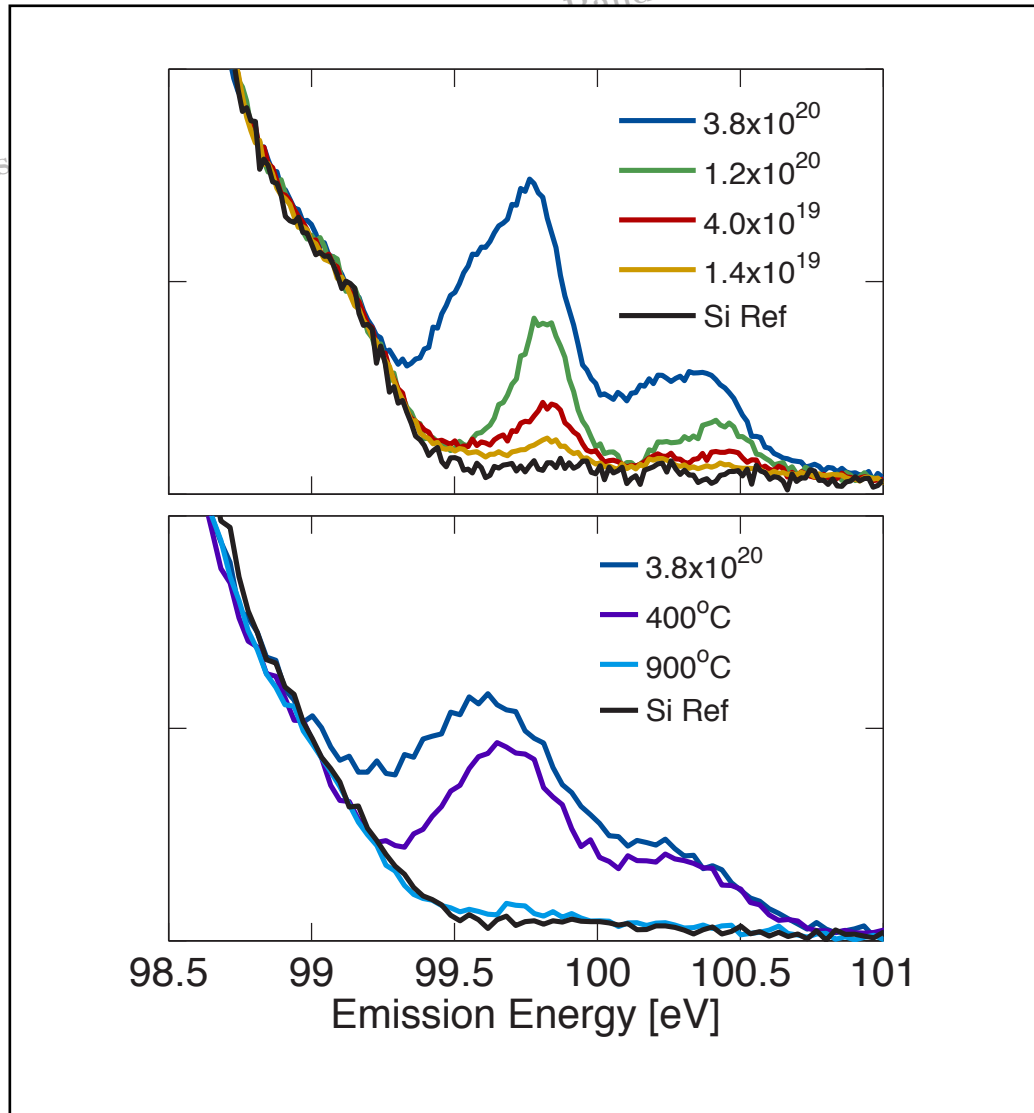


J. Sullivan, Ph.D. Thesis, MIT (2013)

1 properties

2 intermediate band

Unders



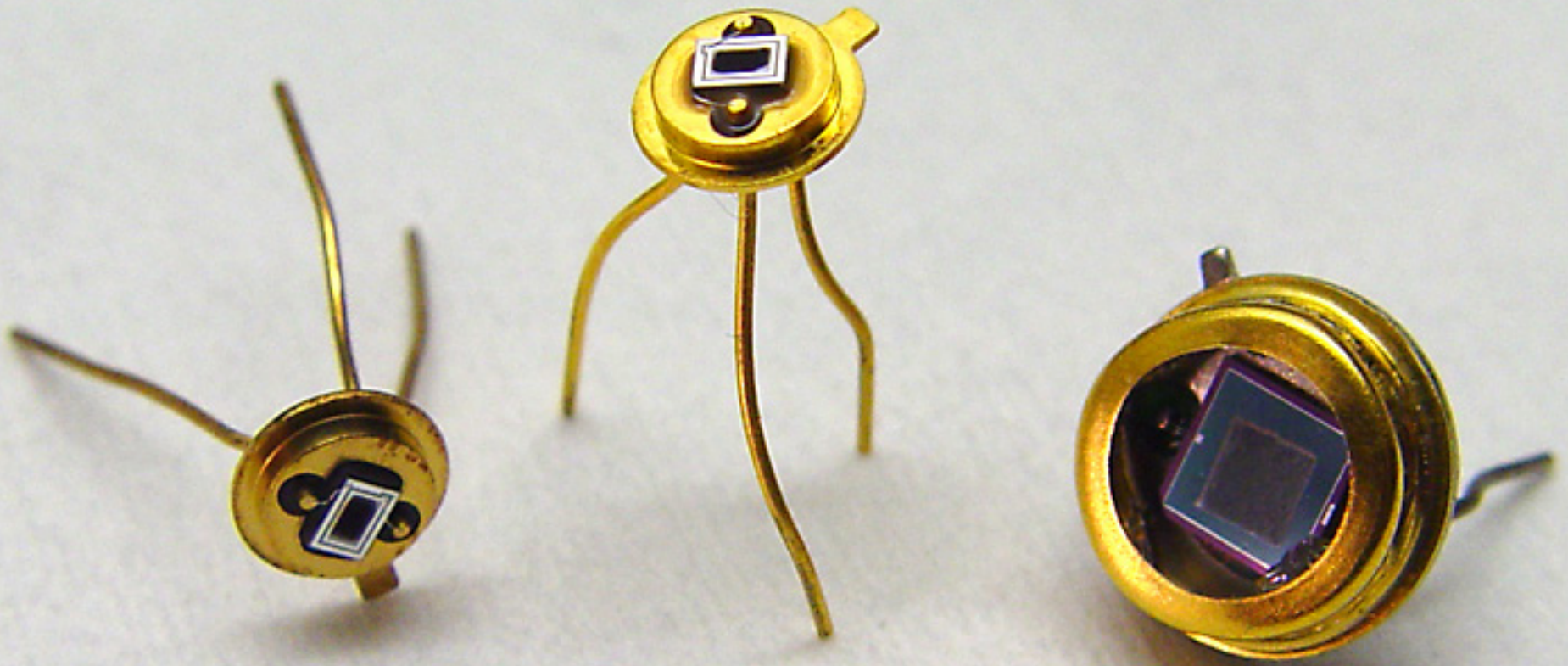
J. Sullivan, Ph.D. Thesis, MIT (2013)

1 properties

2 intermediate band

## Things to keep in mind

- IR absorption rolls off around 8  $\mu\text{m}$
- consistent evidence of intermediate band formation
- IB forms at 0.1% at. doping, broadens at higher doping
- IB merges with CB at 0.4% at. yielding metallic behavior

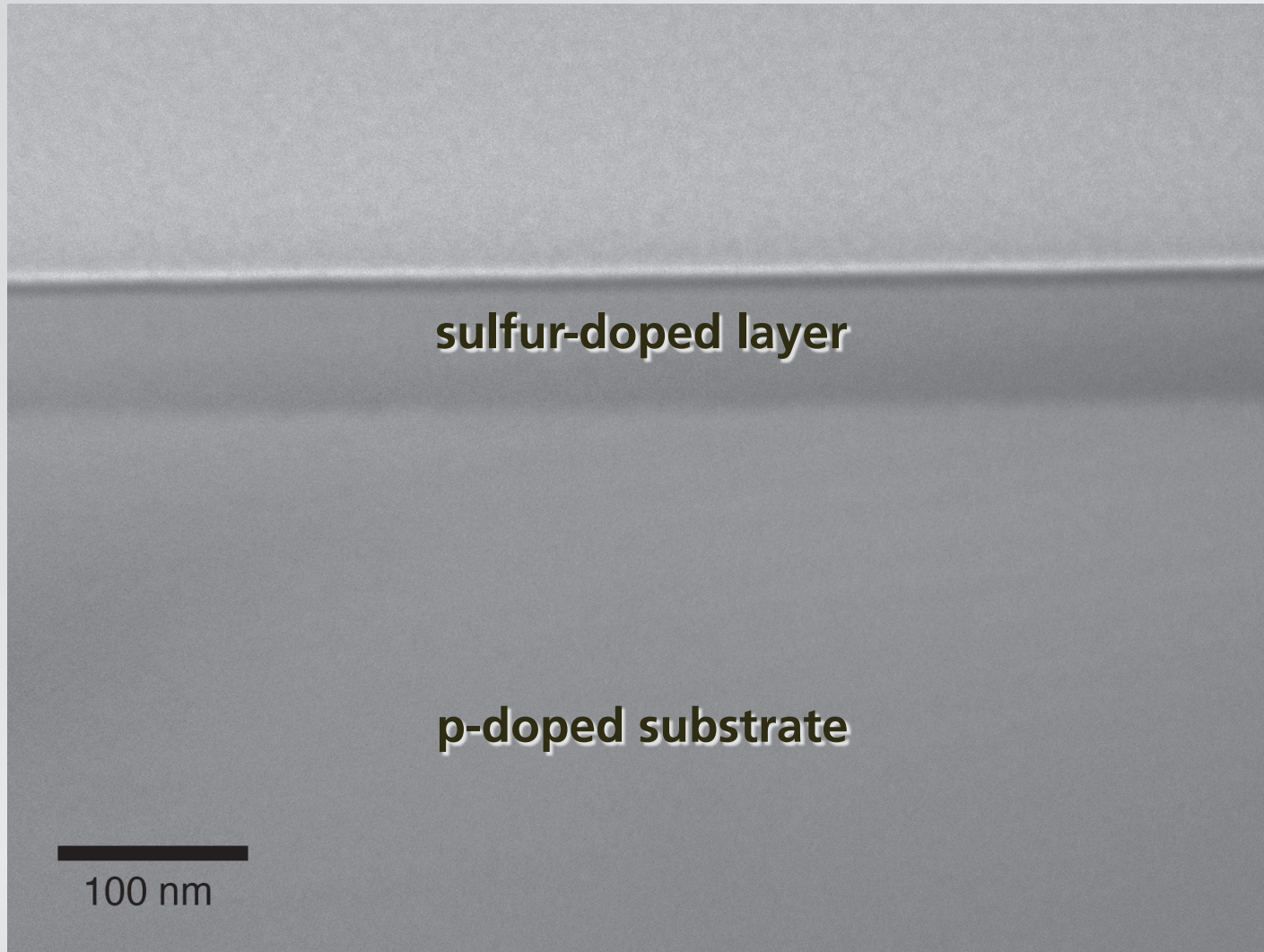


**1** properties

**2** intermediate band

**3** devices

should have shallow junction below surface

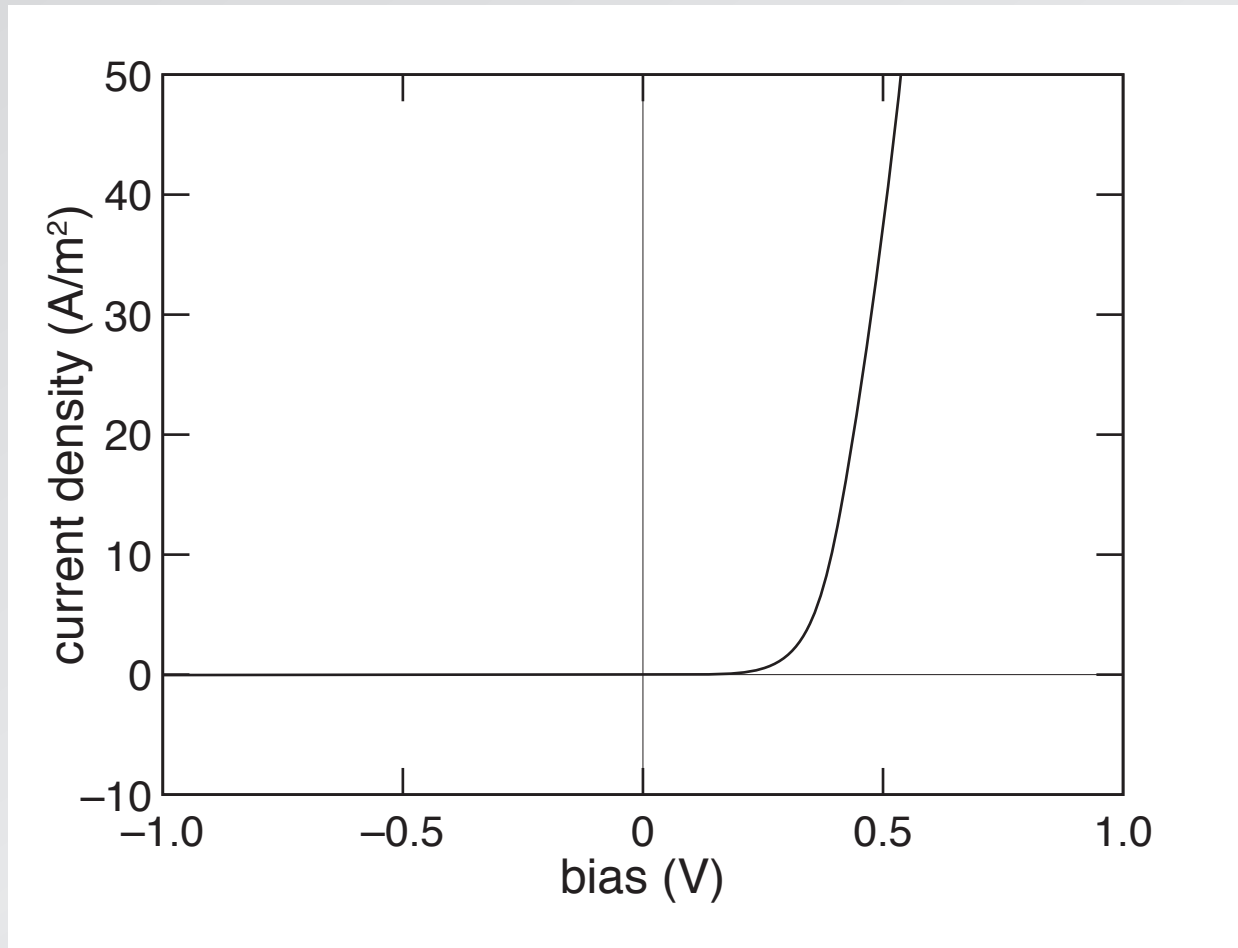


1 properties

2 intermediate band

3 devices

## excellent rectification (after annealing)



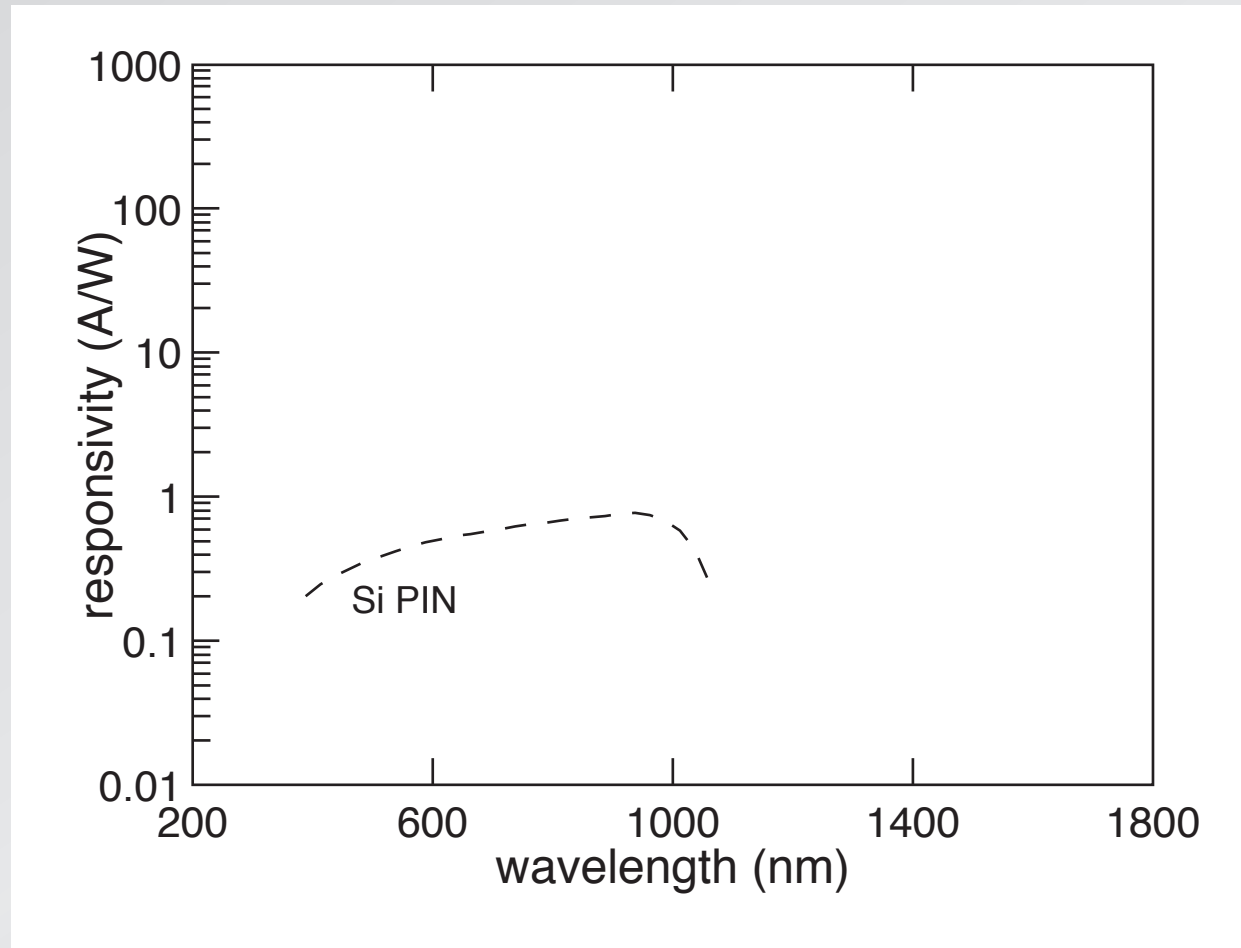
1 properties

2 intermediate band

3 devices



# responsivity

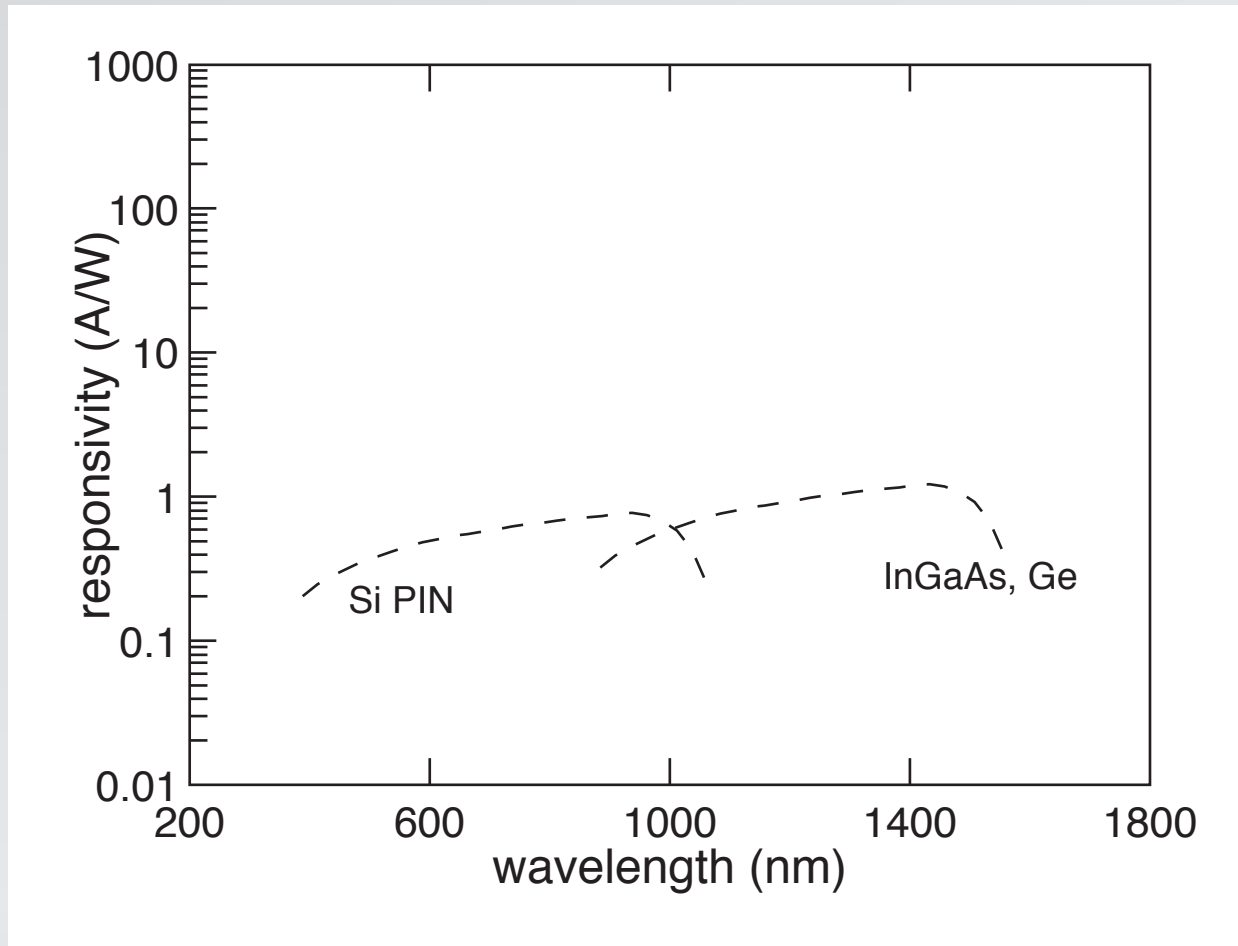


1 properties

2 intermediate band

3 devices

# responsivity

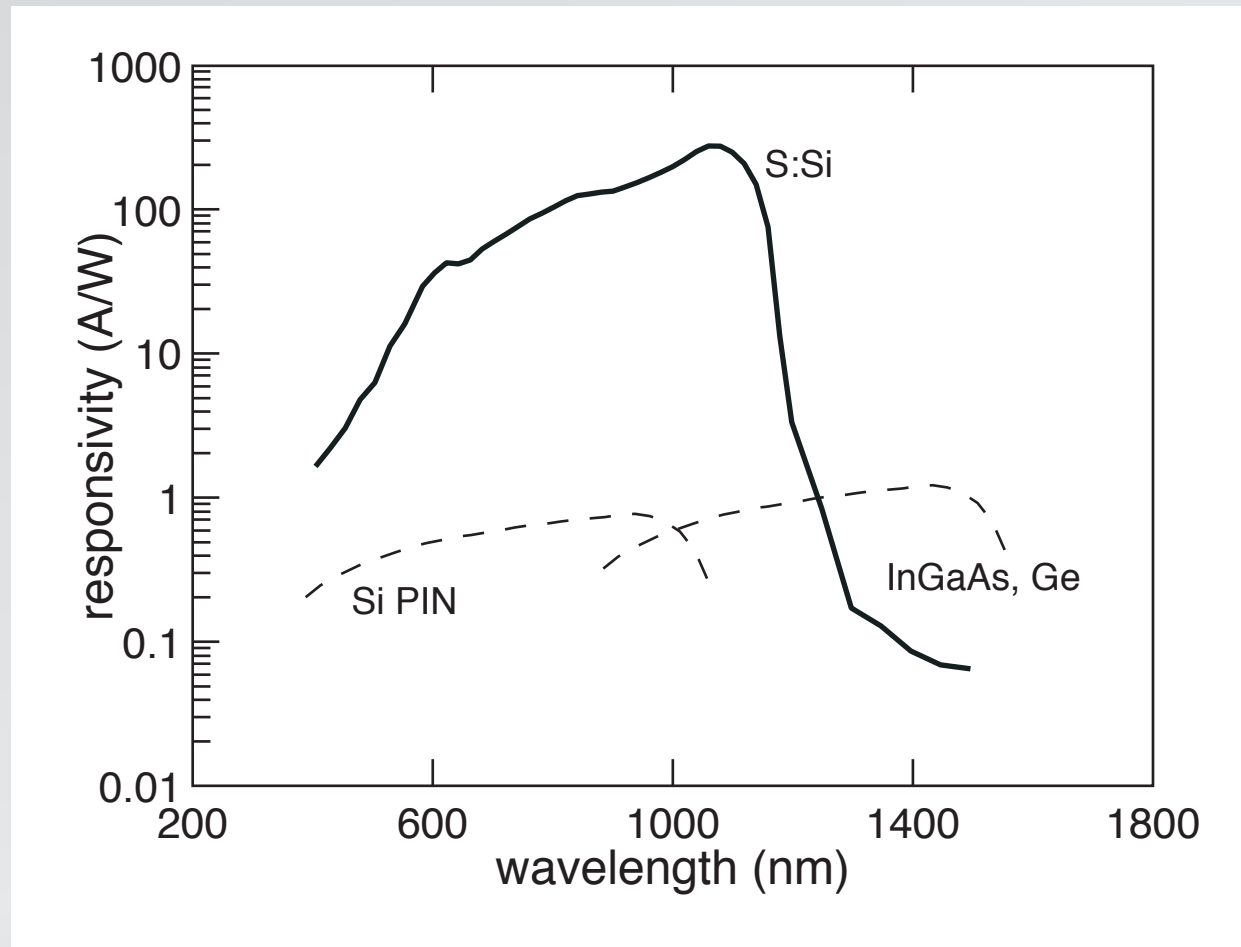


1 properties

2 intermediate band

3 devices

# responsivity

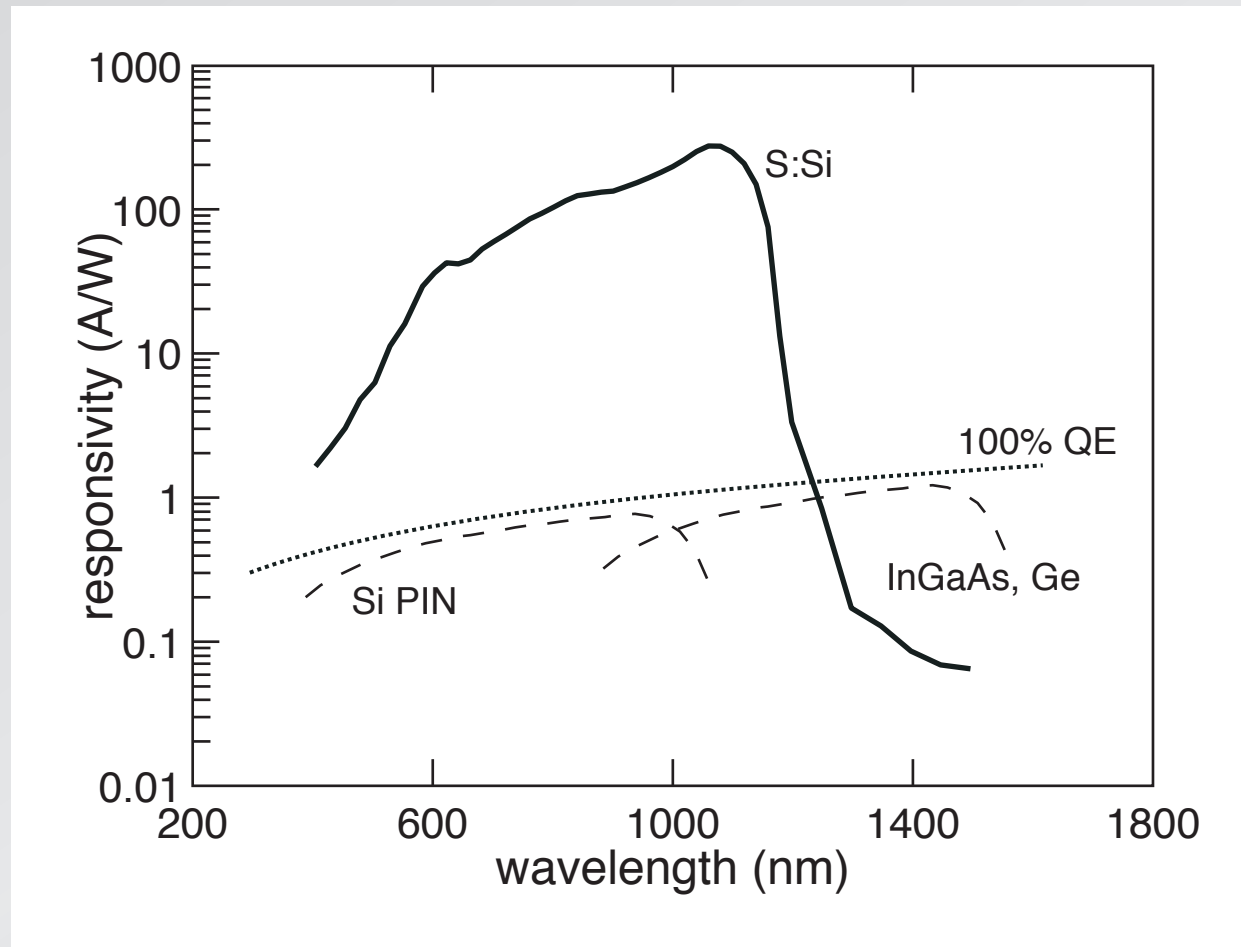


1 properties

2 intermediate band

3 devices

# responsivity

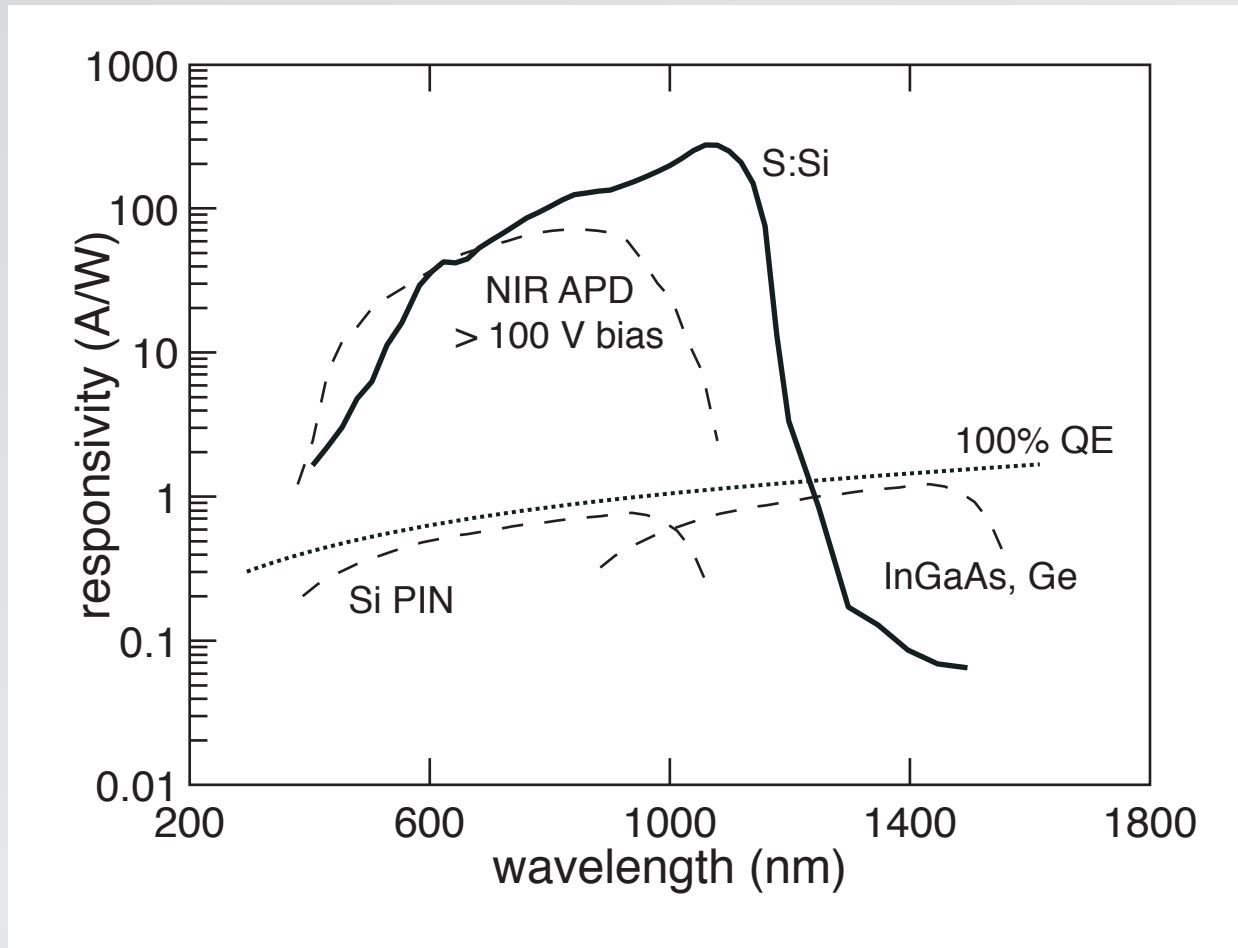


1 properties

2 intermediate band

3 devices

# responsivity



1 properties

2 intermediate band

3 devices

- **enhanced sensitivity**
- **extended IR response**

**near-IR is next wave in imaging!**

**1** properties

**2** intermediate band

**3** devices



# gesture recognition

image: fastcolabs.com

**1** properties

**2** intermediate band

**3** devices





# night vision

wikimedia.org

**1** properties

**2** intermediate band

**3** devices

# biometrics



image: kusic.ca

**1** properties

**2** intermediate band

**3** devices

# robotics

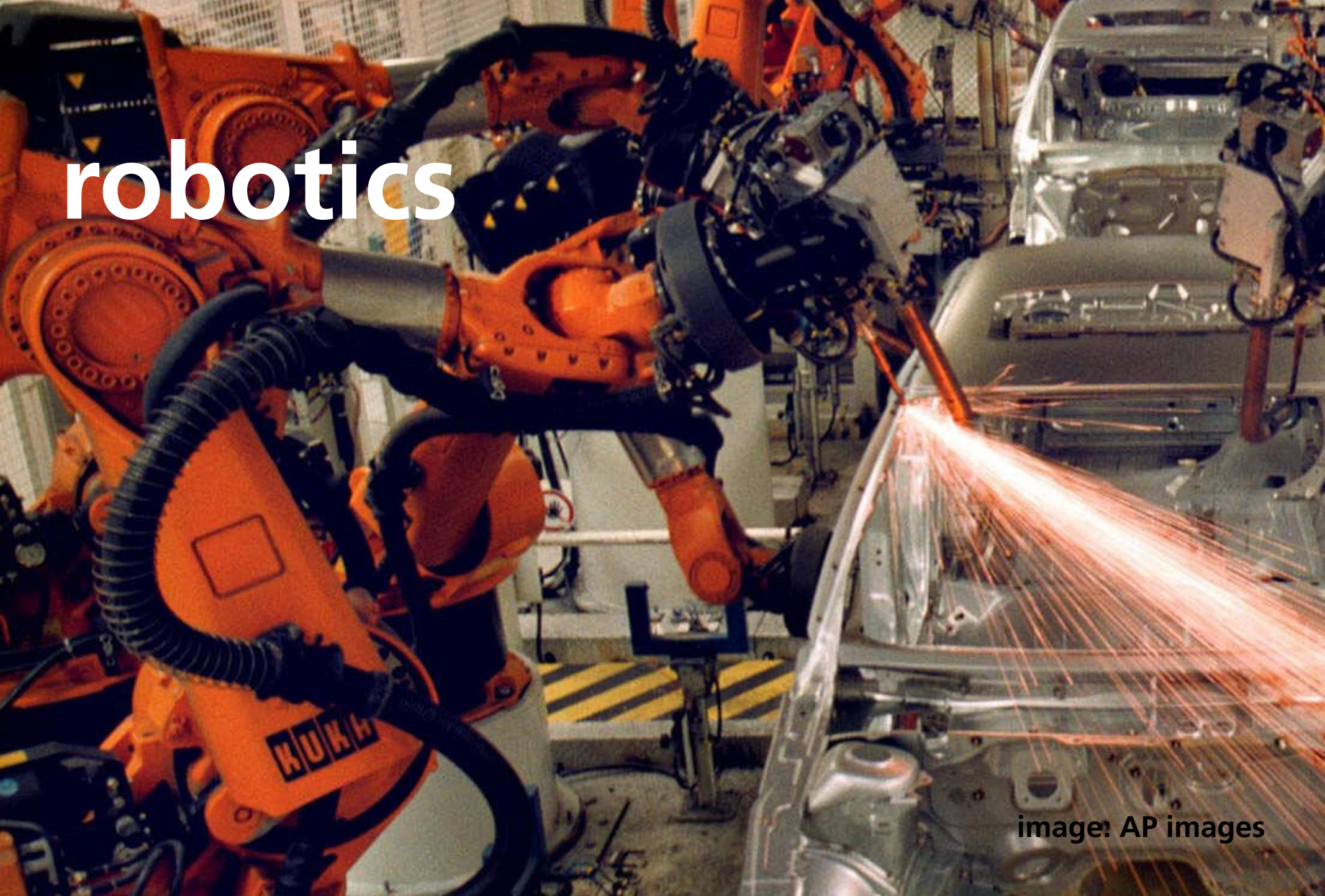
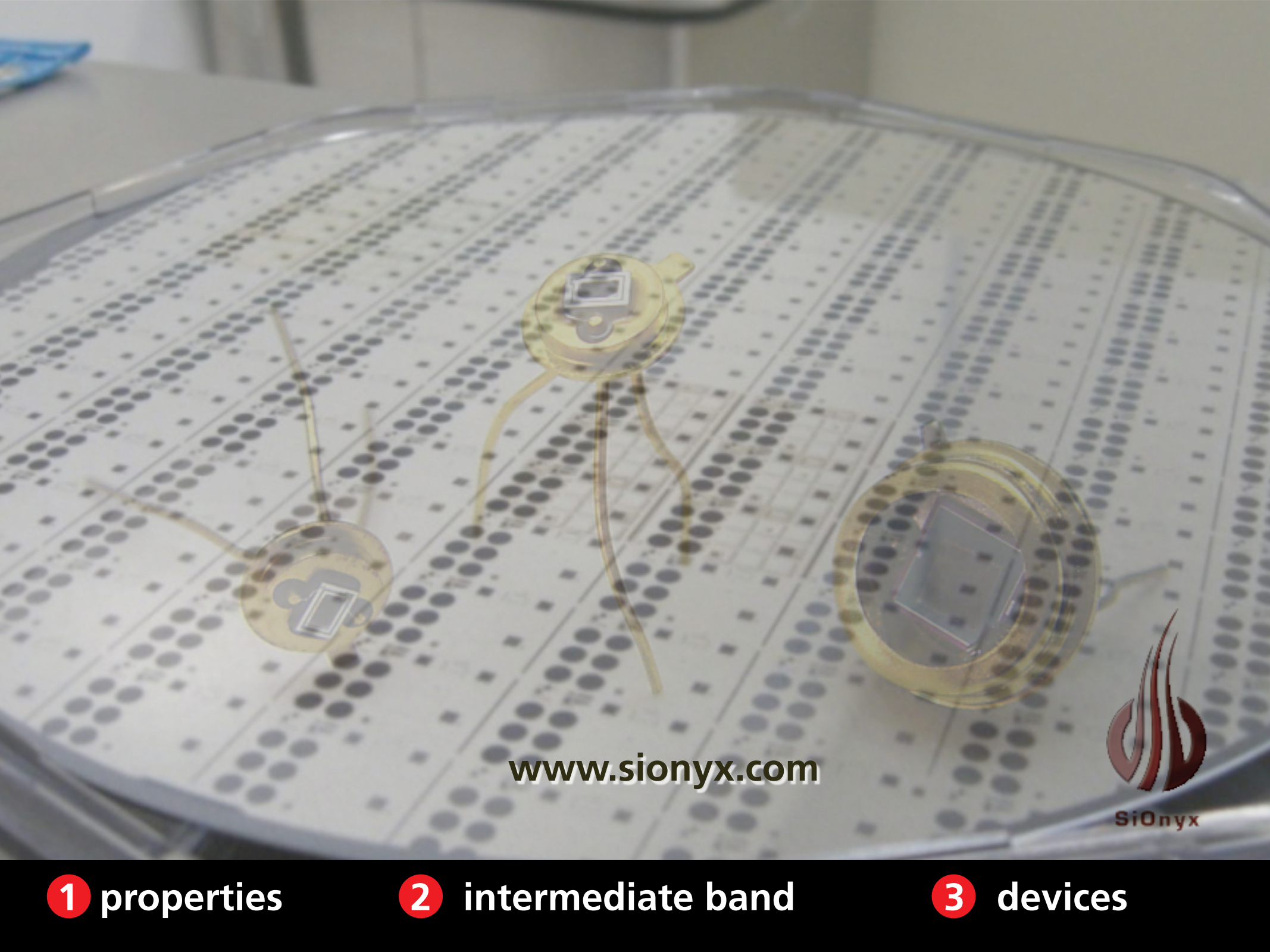


image: AP images

1 properties

2 intermediate band

3 devices



[www.sionyx.com](http://www.sionyx.com)

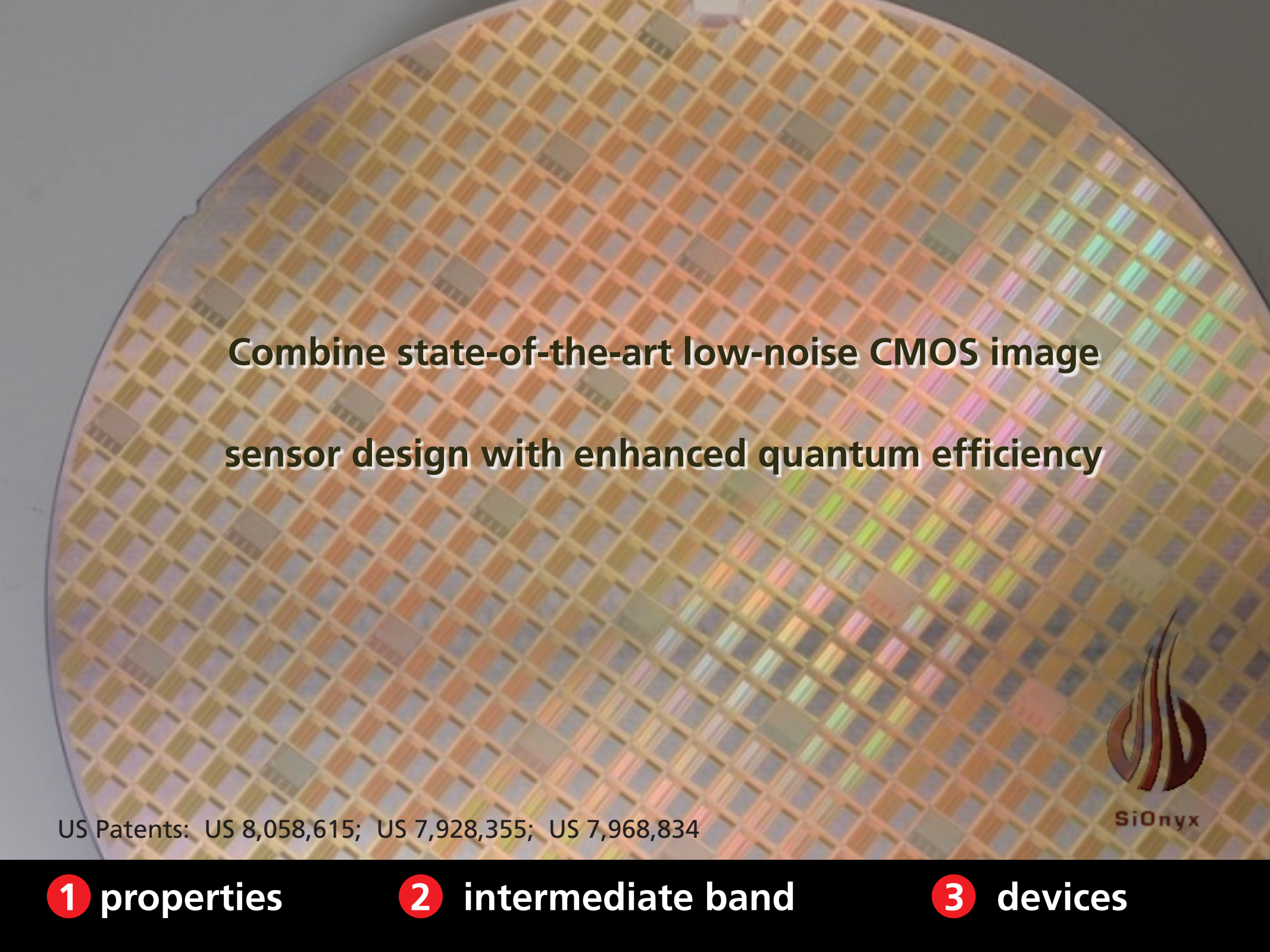


SiOnyx

**1** properties

**2** intermediate band

**3** devices



**Combine state-of-the-art low-noise CMOS image sensor design with enhanced quantum efficiency**



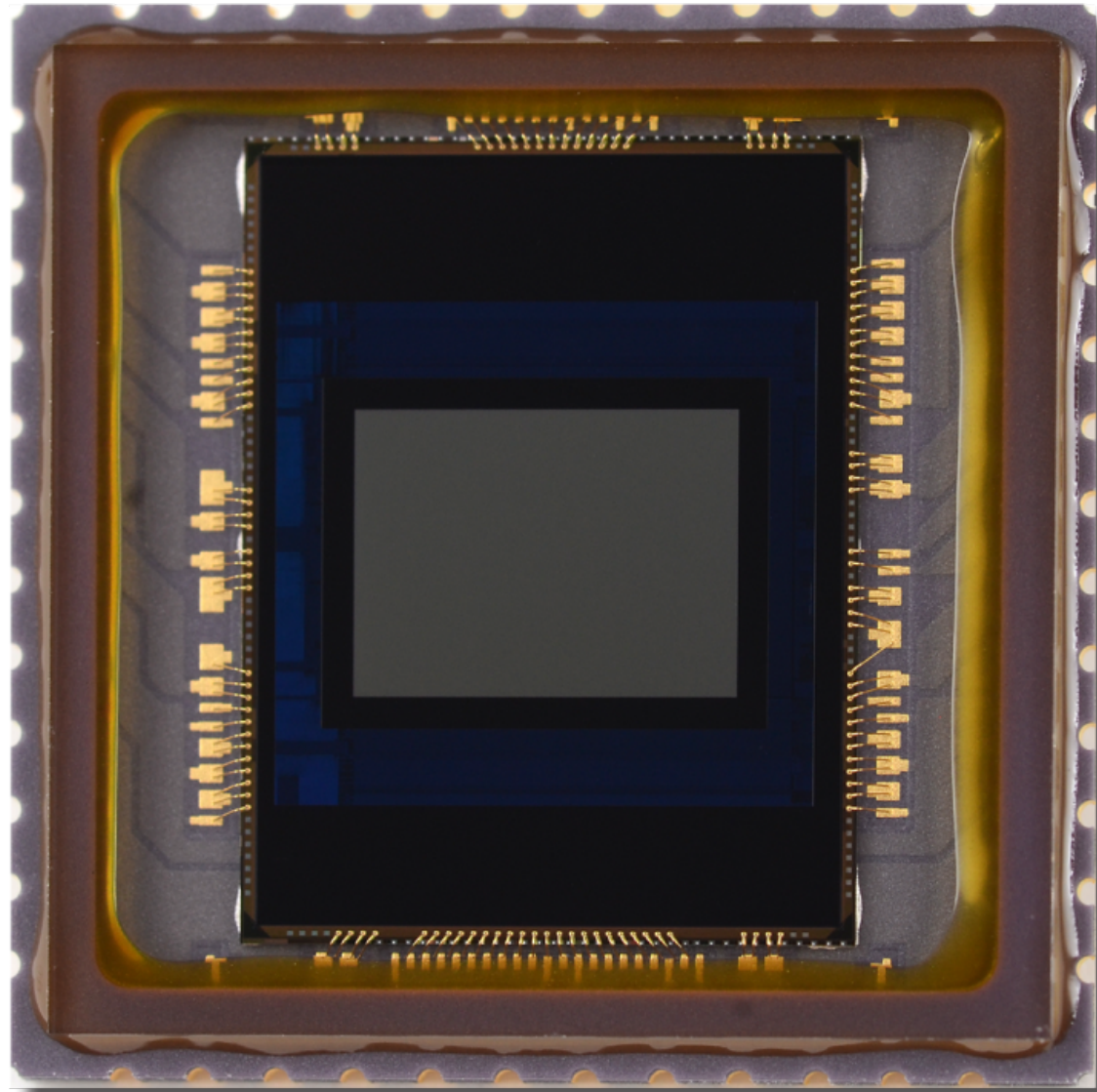
SiOnyx

US Patents: US 8,058,615; US 7,928,355; US 7,968,834

**1** properties

**2** intermediate band

**3** devices



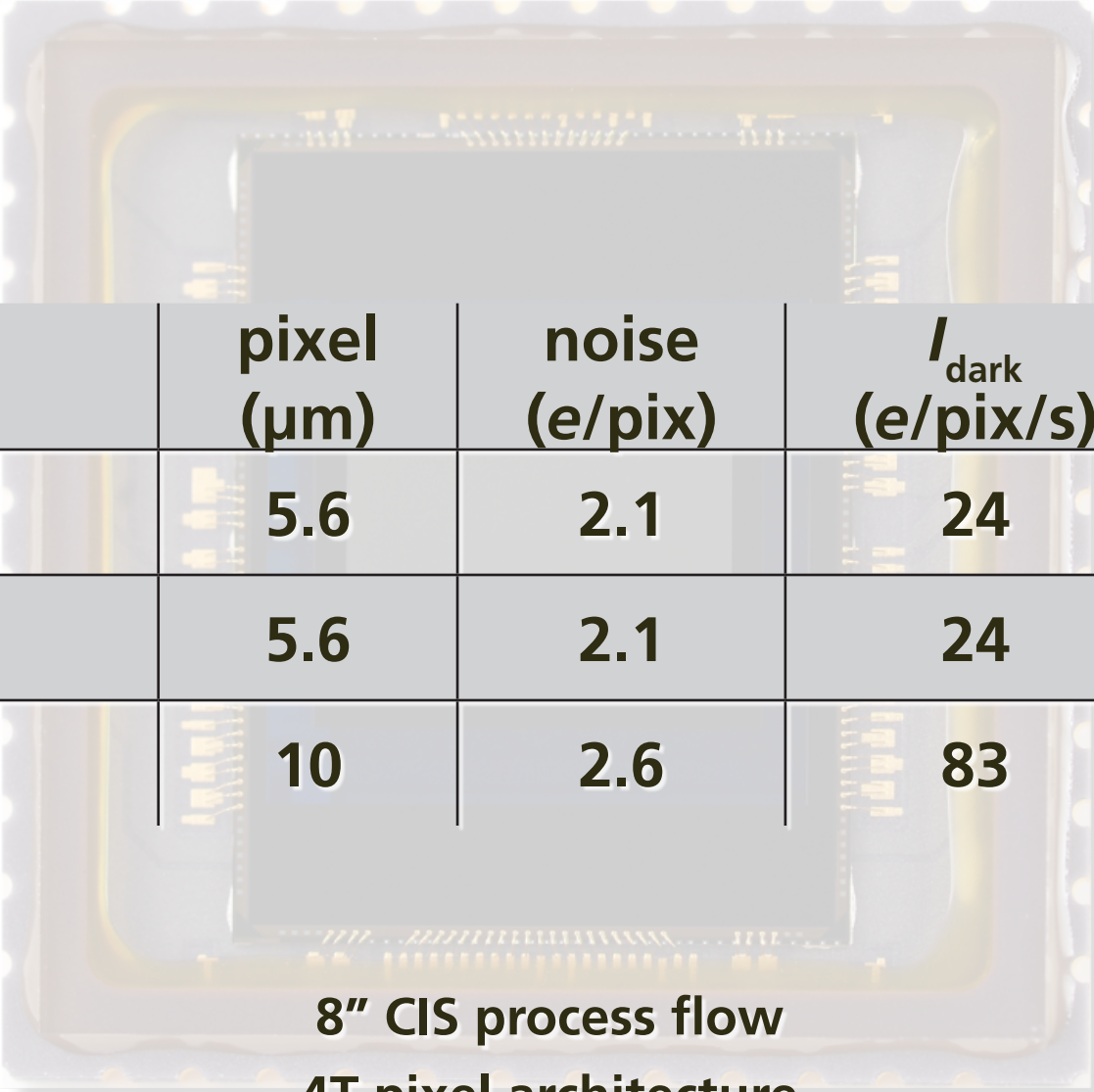
SiOnyx

US Patents: US 8,058,615; US 7,928,355; US 7,968,834

**1** properties

**2** intermediate band

**3** devices



Resolution	pixel ( $\mu\text{m}$ )	noise (e/pix)	$I_{\text{dark}}$ (e/pix/s)	$P$ (mW)
872 x 654	5.6	2.1	24	300
1280 x 720	5.6	2.1	24	360
1280 x 1024	10	2.6	83	400

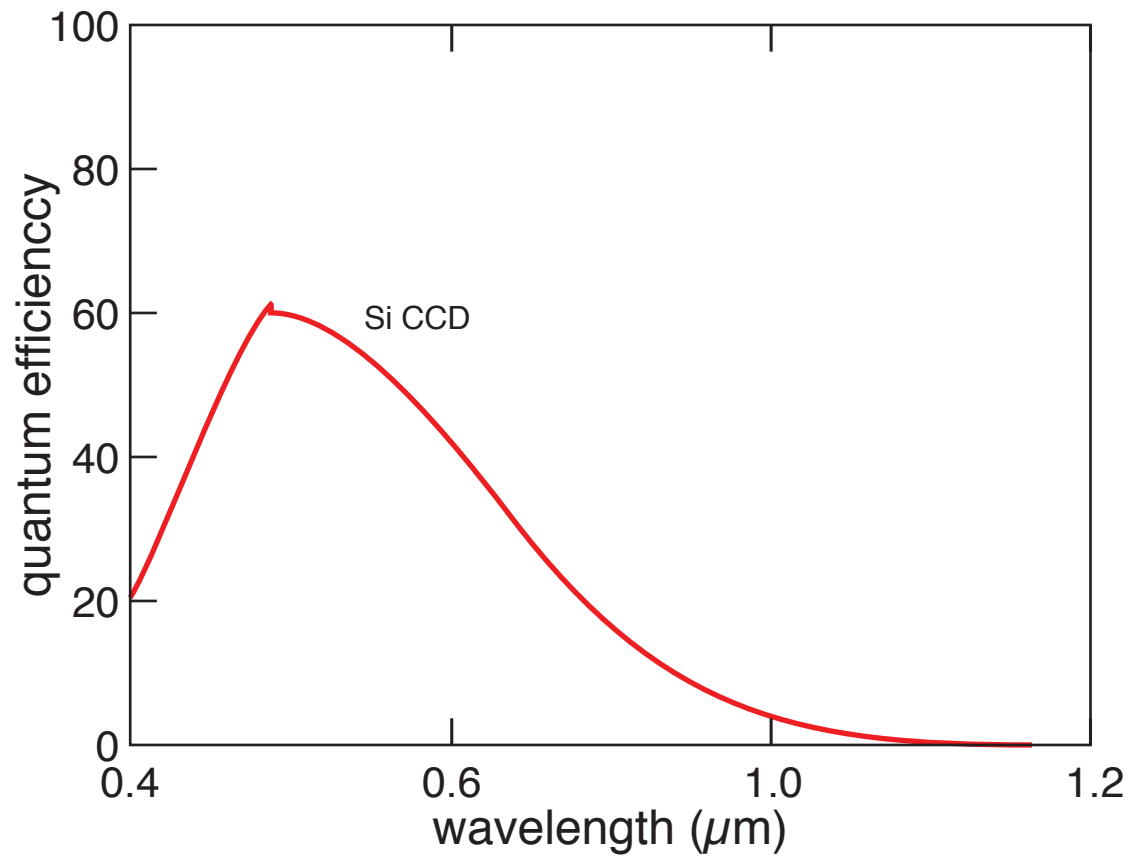
8" CIS process flow  
4T pixel architecture



1 properties

2 intermediate band

3 devices

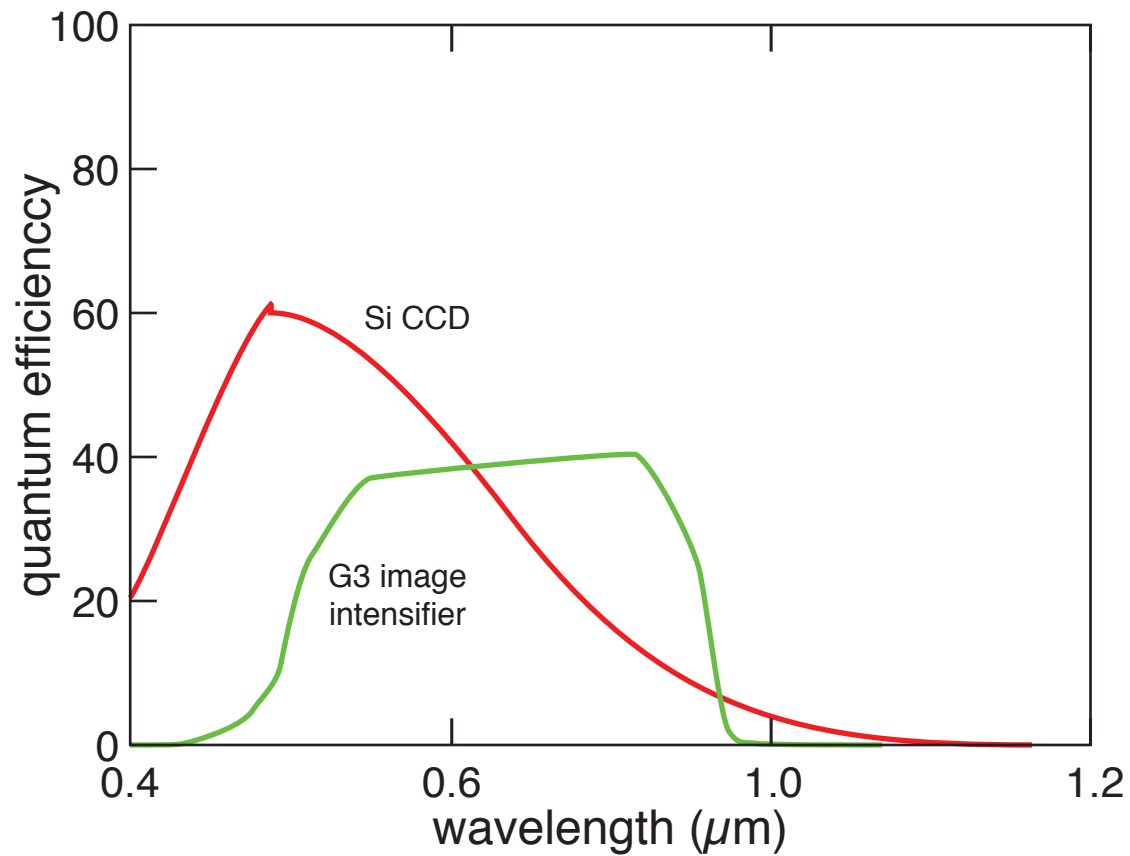


**1** properties

**2** intermediate band

**3** devices

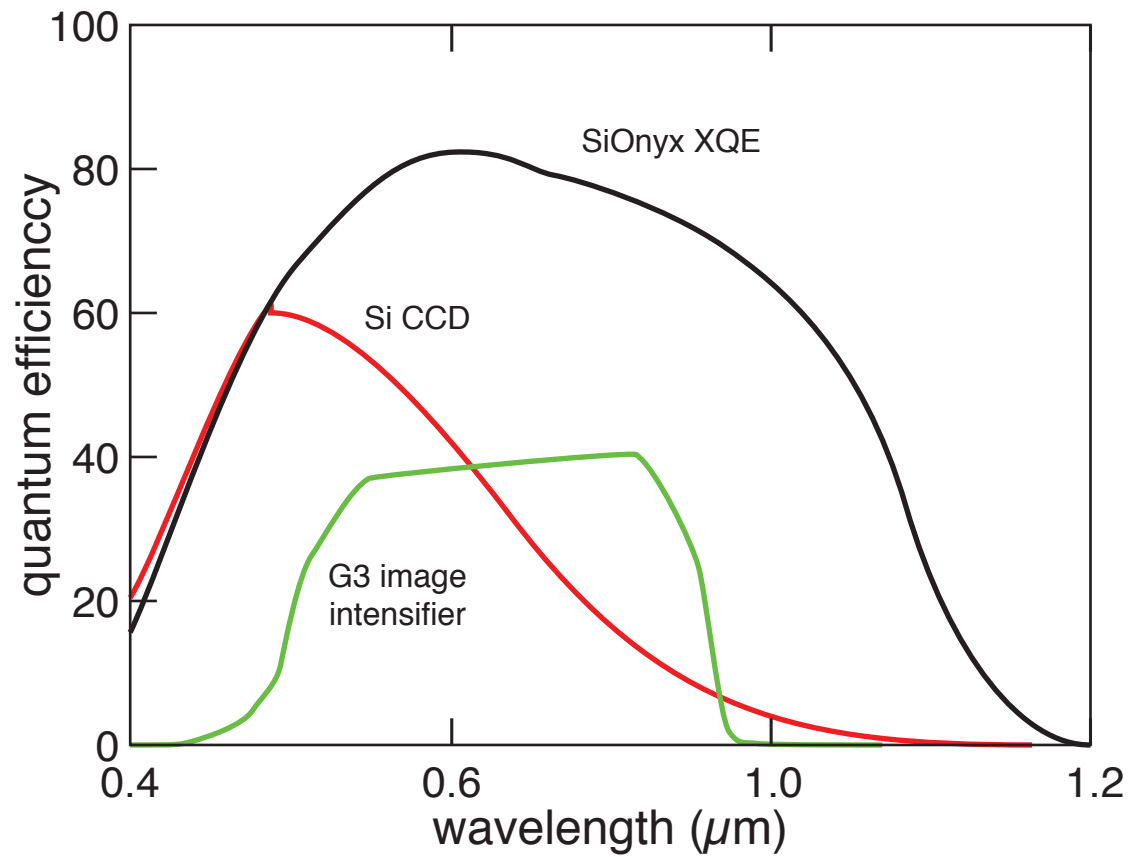




1 properties

2 intermediate band

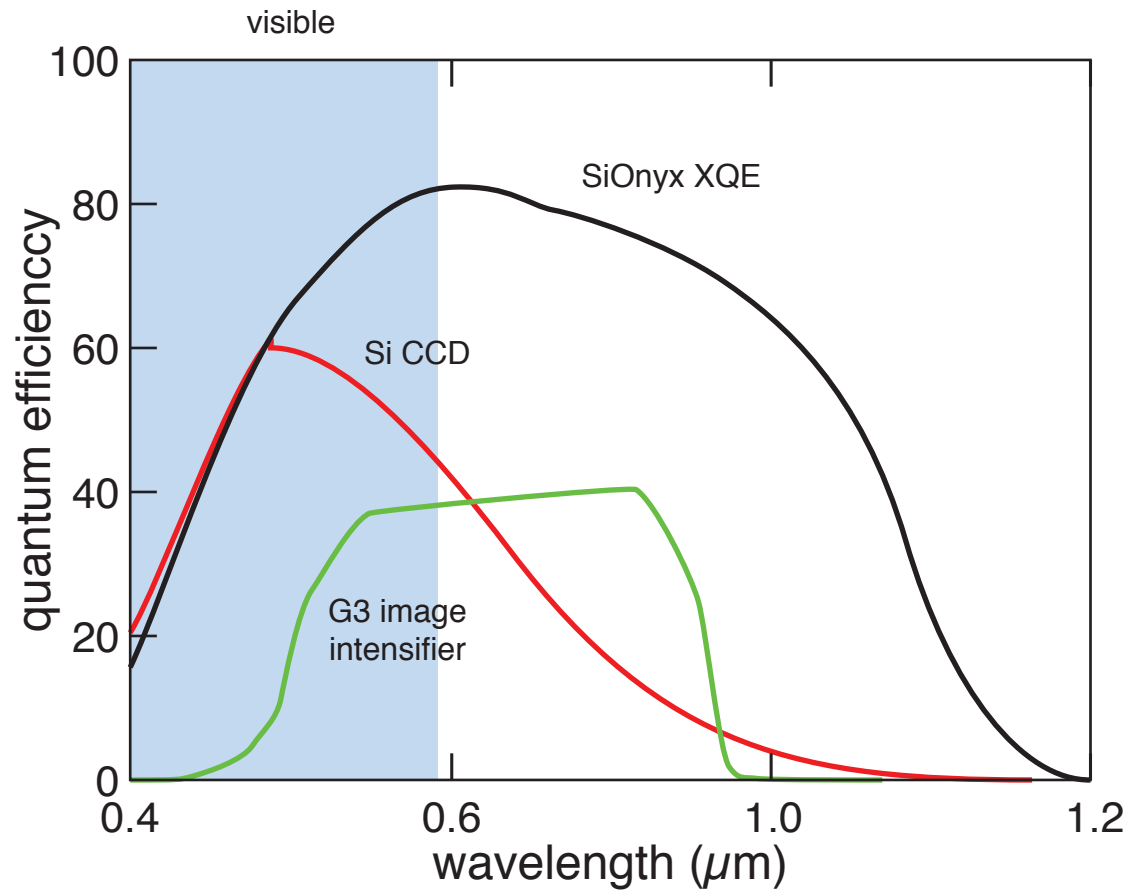
3 devices



1 properties

2 intermediate band

3 devices



**1** properties

**2** intermediate band

**3** devices

no compromises in visible



Sony color CCD



**1** properties

**2** intermediate band

**3** devices

## no compromises in visible



Sony color CCD



SiOnyx XQE sensor

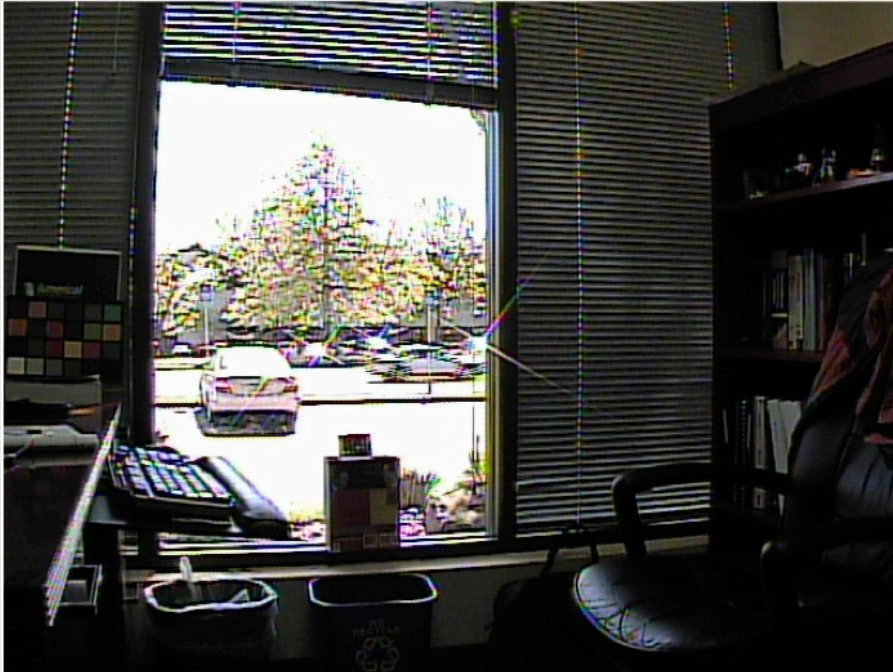


1 properties

2 intermediate band

3 devices

90+ dB dynamic range



Sony color CCD

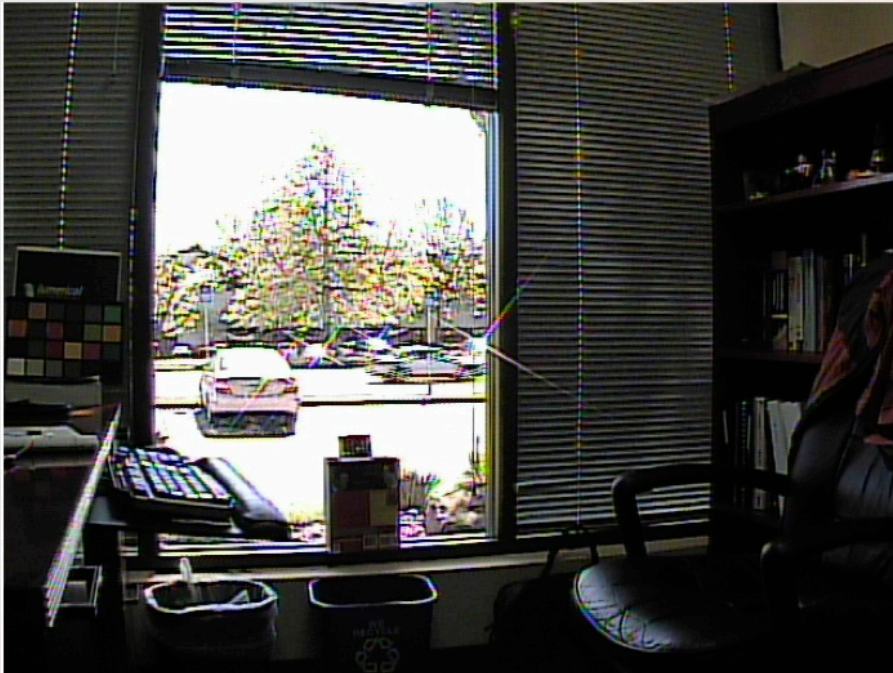


**1** properties

**2** intermediate band

**3** devices

# 90+ dB dynamic range



Sony color CCD



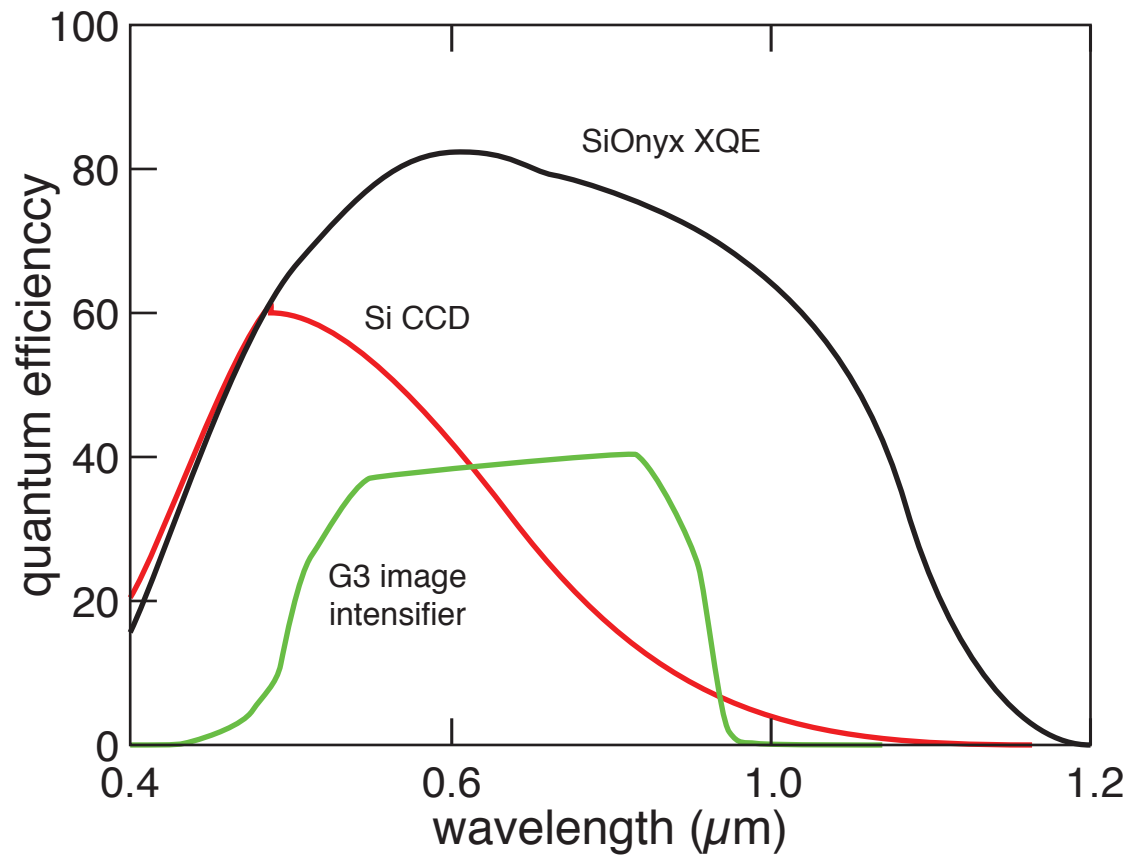
SiOnyx X1 sensor



**1** properties

**2** intermediate band

**3** devices

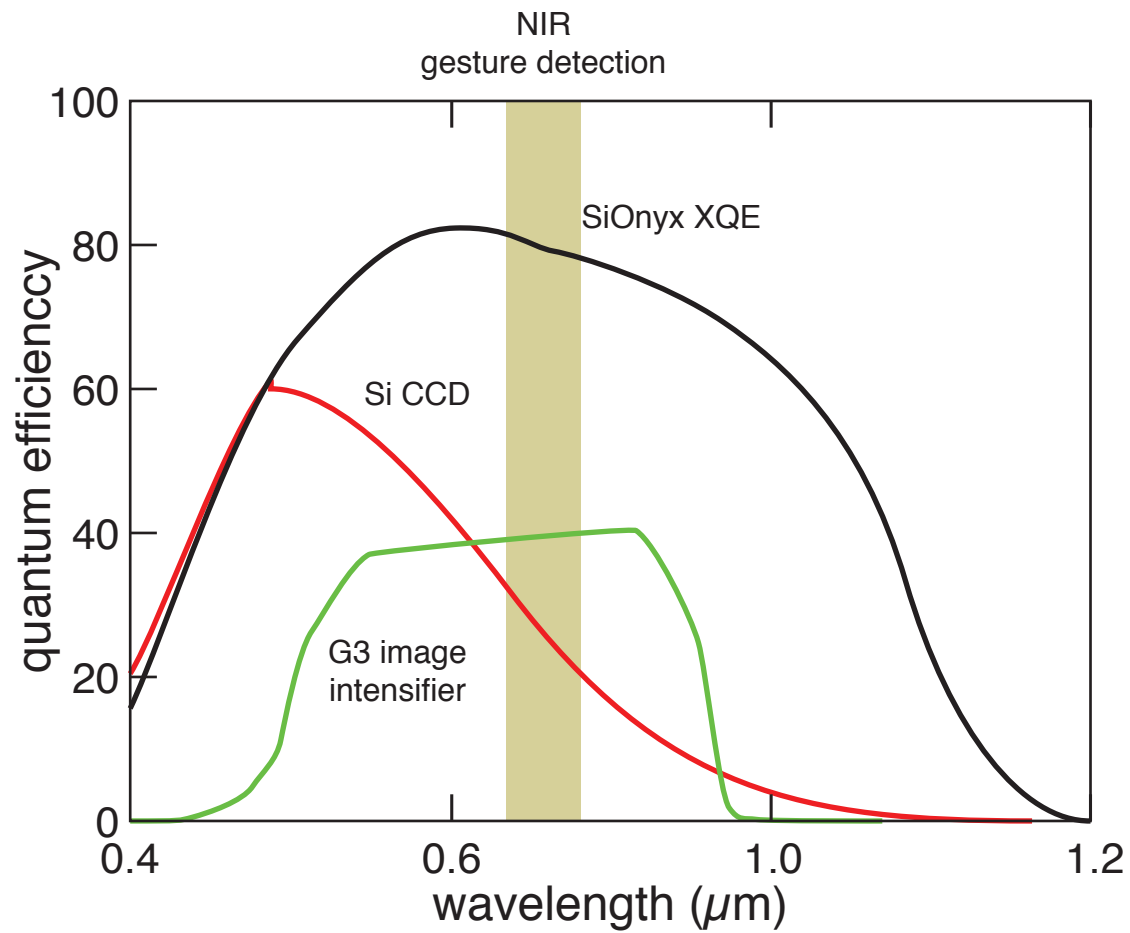


1 properties

2 intermediate band

3 devices

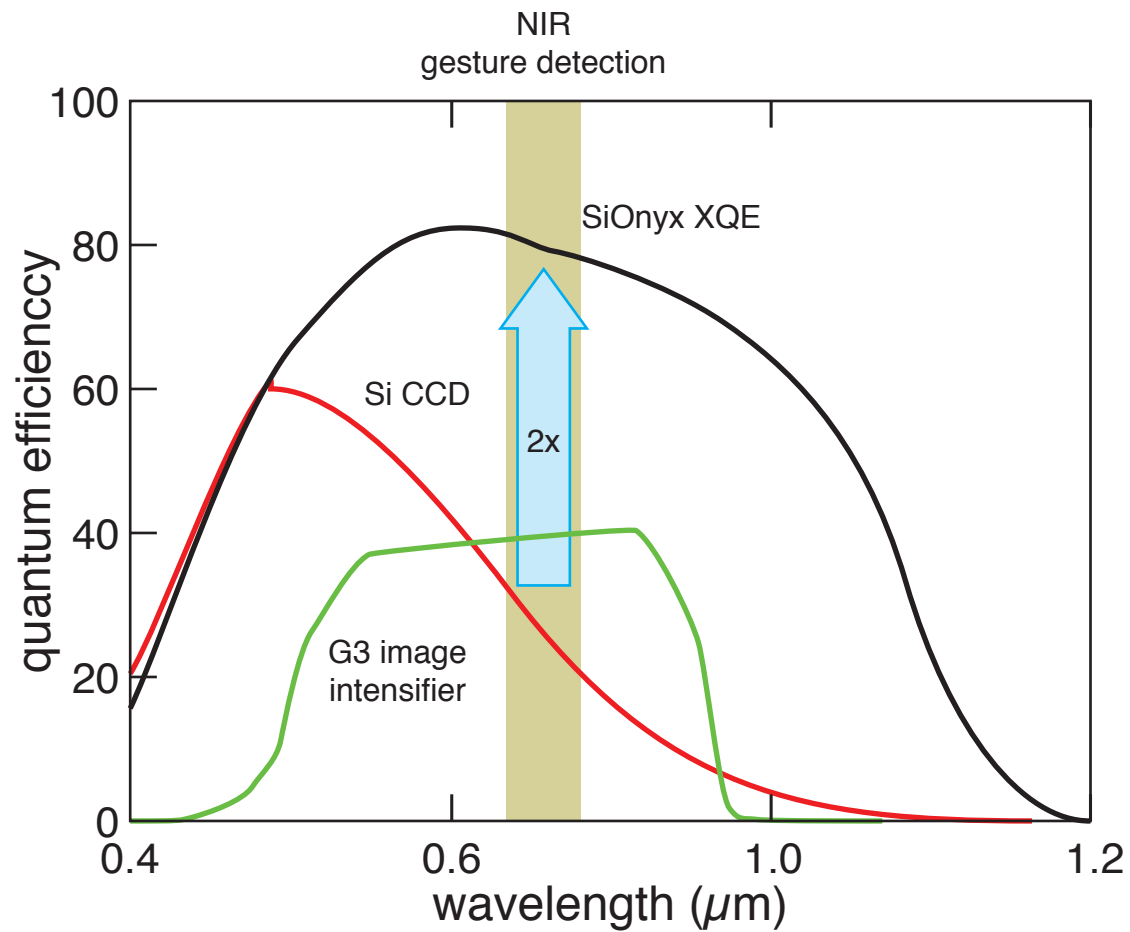




1 properties

2 intermediate band

3 devices



**1** properties

**2** intermediate band

**3** devices

# 3D imaging for gesture user interface (850 nm)

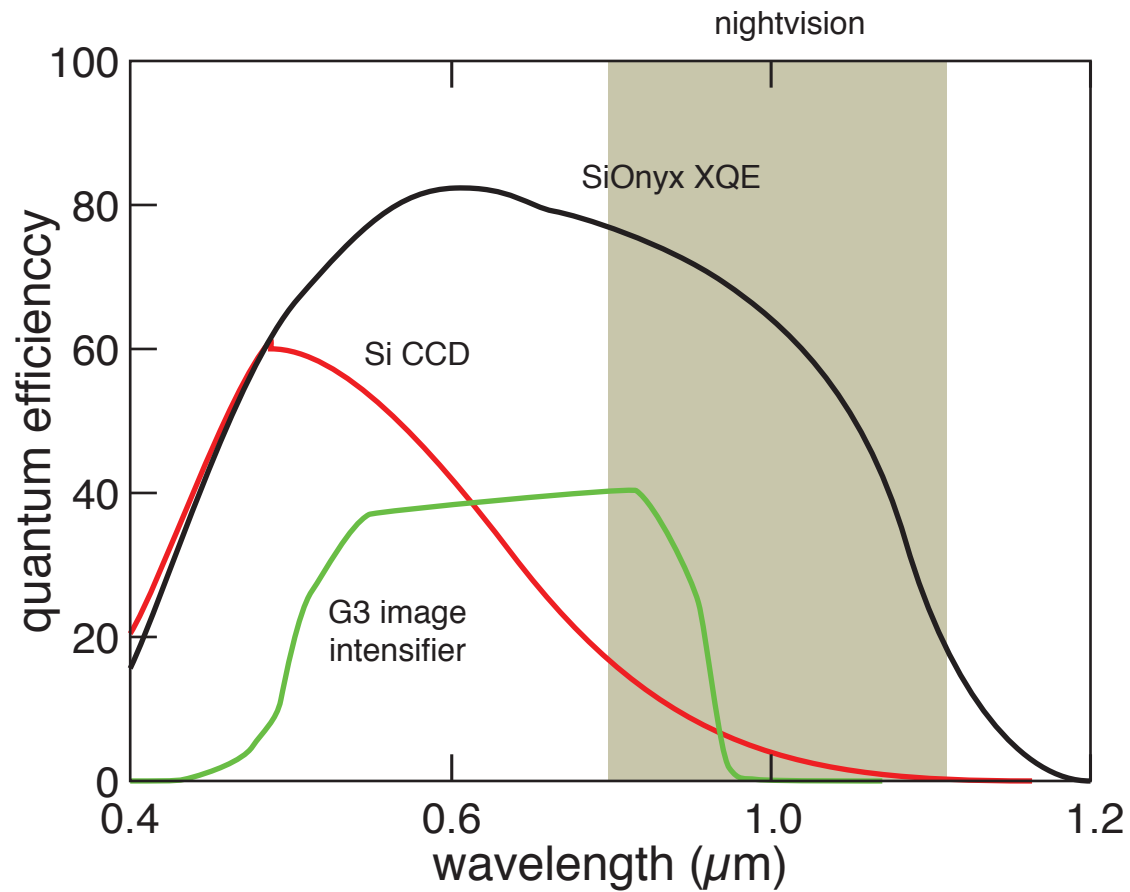


SiOnyx XQE



standard CCD

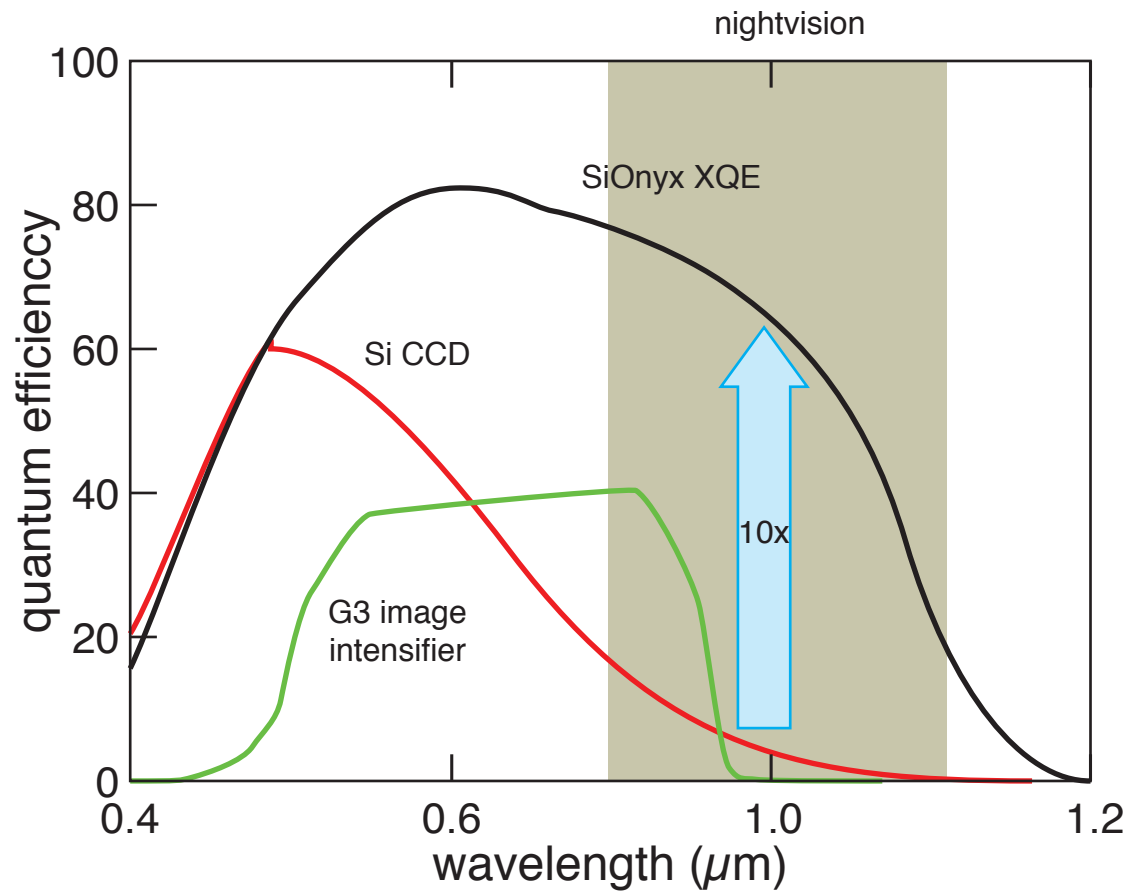




1 properties

2 intermediate band

3 devices

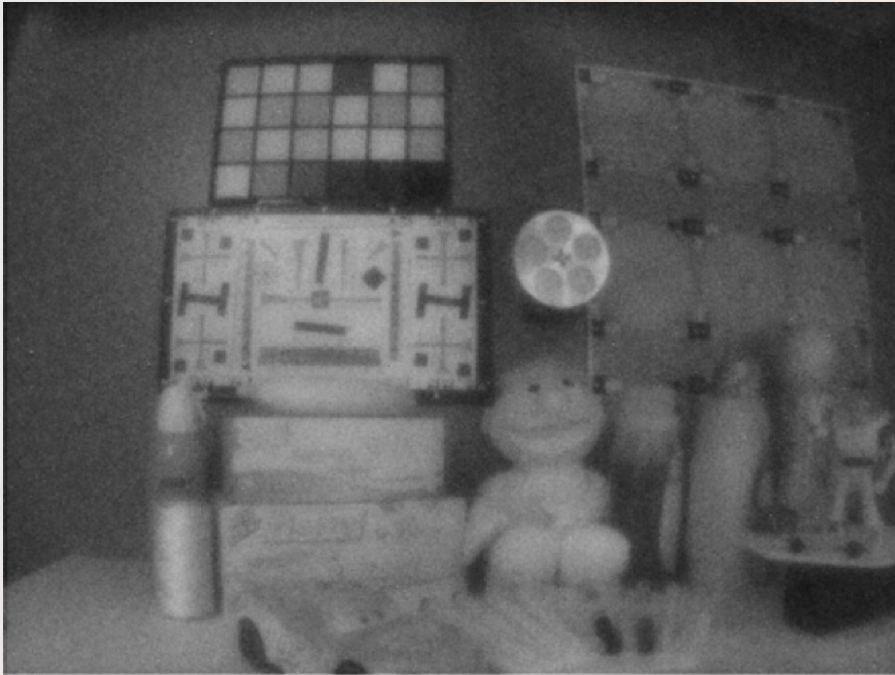


**1** properties

**2** intermediate band

**3** devices

## dark room 1050 illumination



SiOnyx (F1.4, 33 ms, 24x)

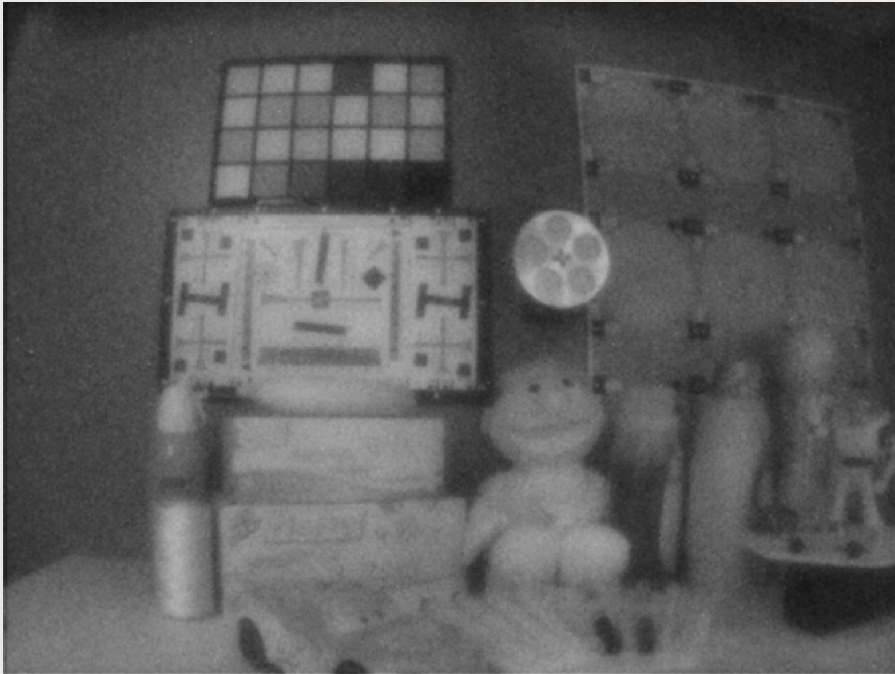


**1** properties

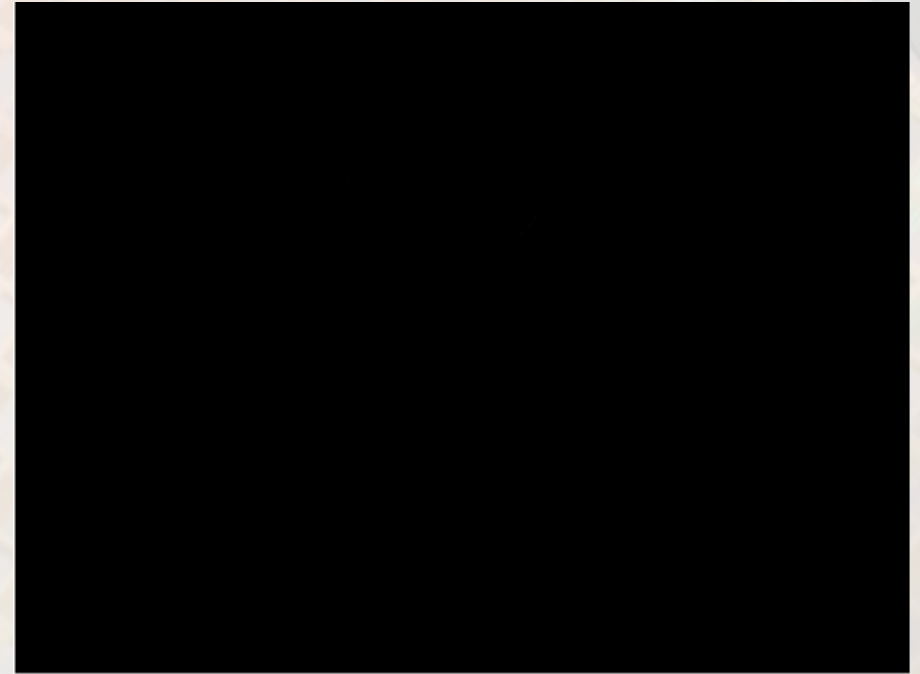
**2** intermediate band

**3** devices

# dark room 1050 illumination



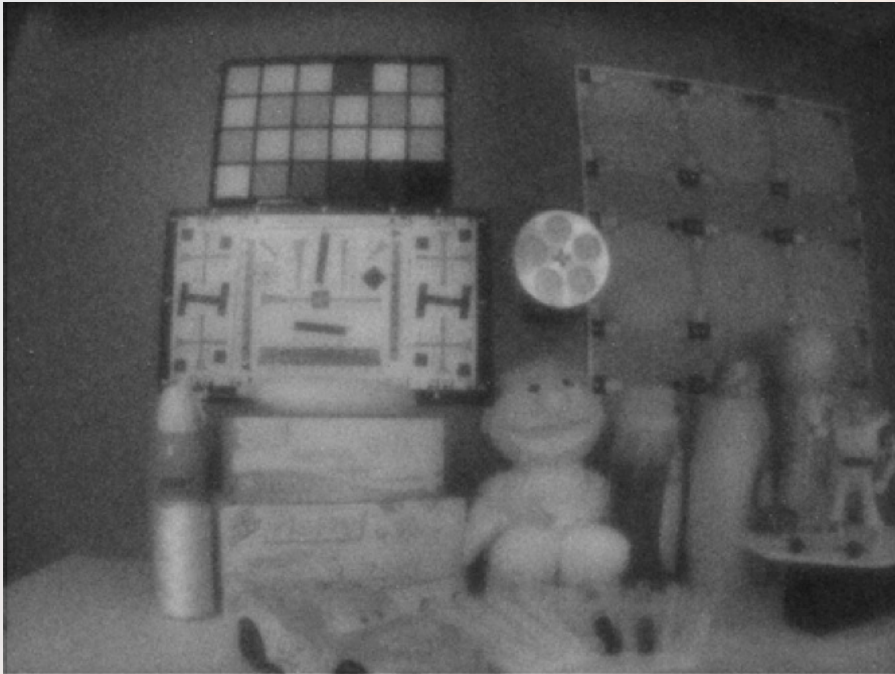
SiOnyx (F1.4, 33 ms, 24x)



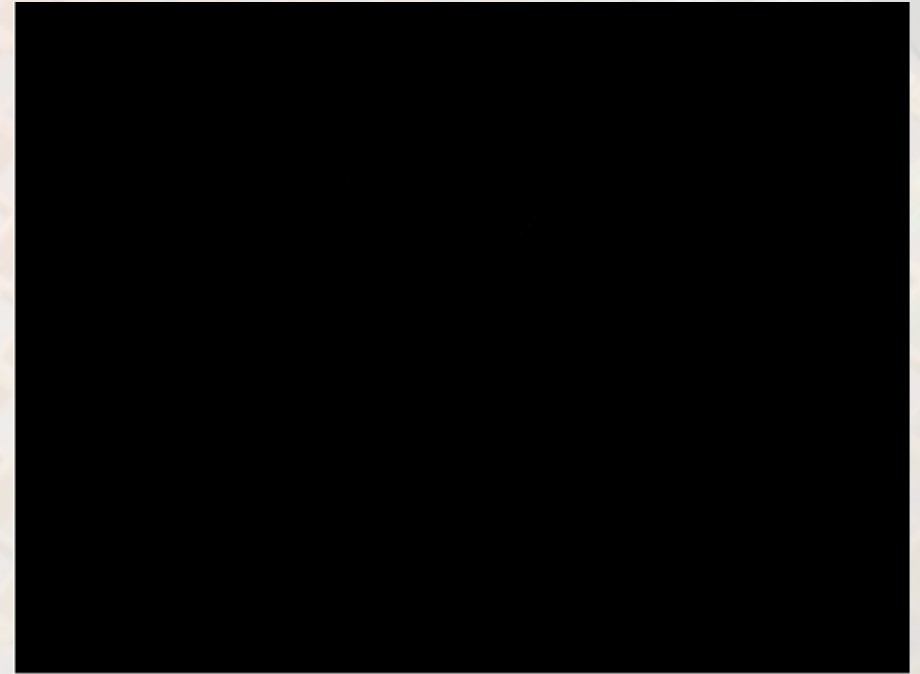
reference (F1.4, 33 ms, 24x)



# dark room 1050 illumination



SiOnyx (F1.4, 33 ms, 24x)



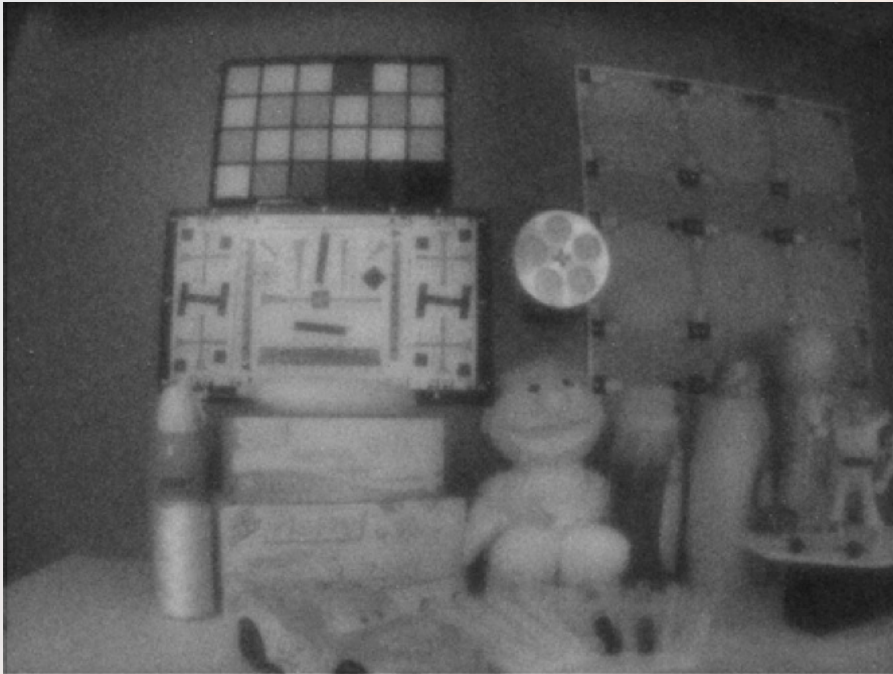
reference (F1.4, 33 ms, 24x)

no image processing





# dark room 1050 illumination



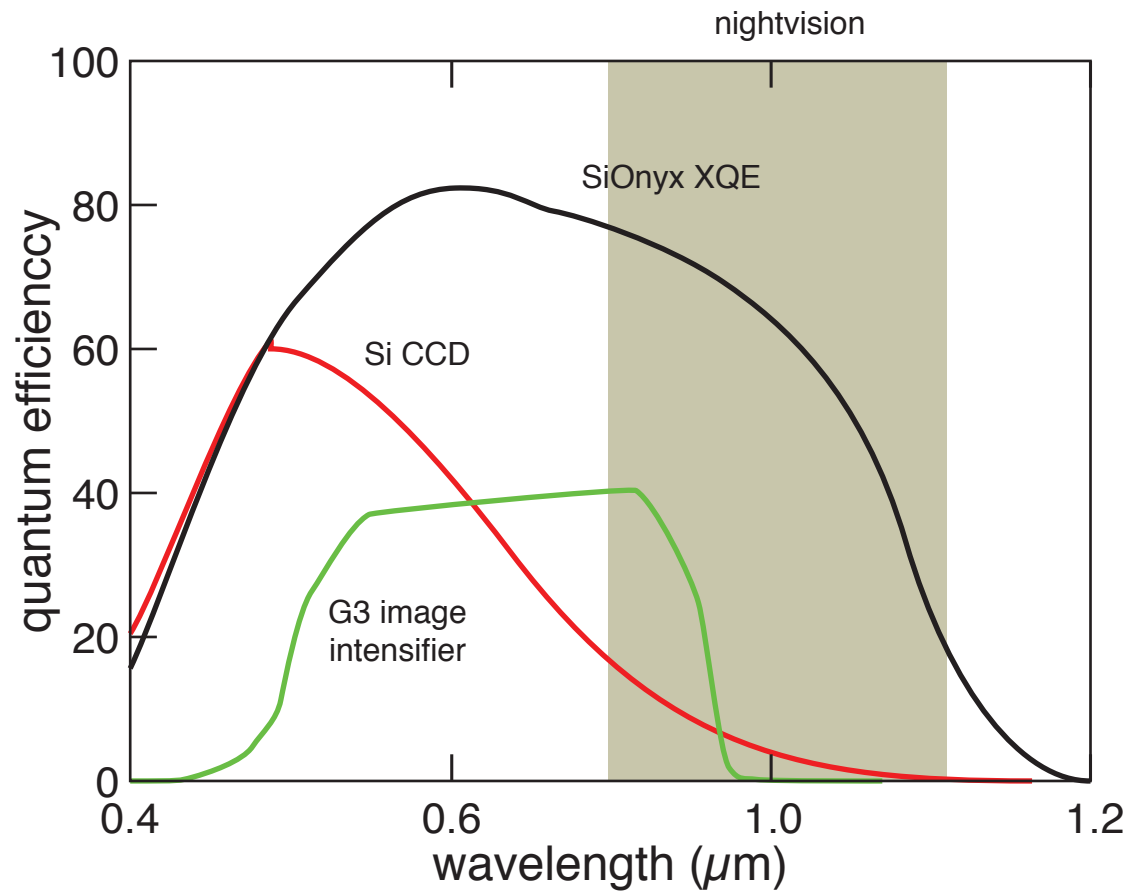
SiOnyx (F1.4, 33 ms, 24x)



reference (F1.4, 33 ms, 24x)  
**2x DIGITAL GAIN ADDED**

no image processing

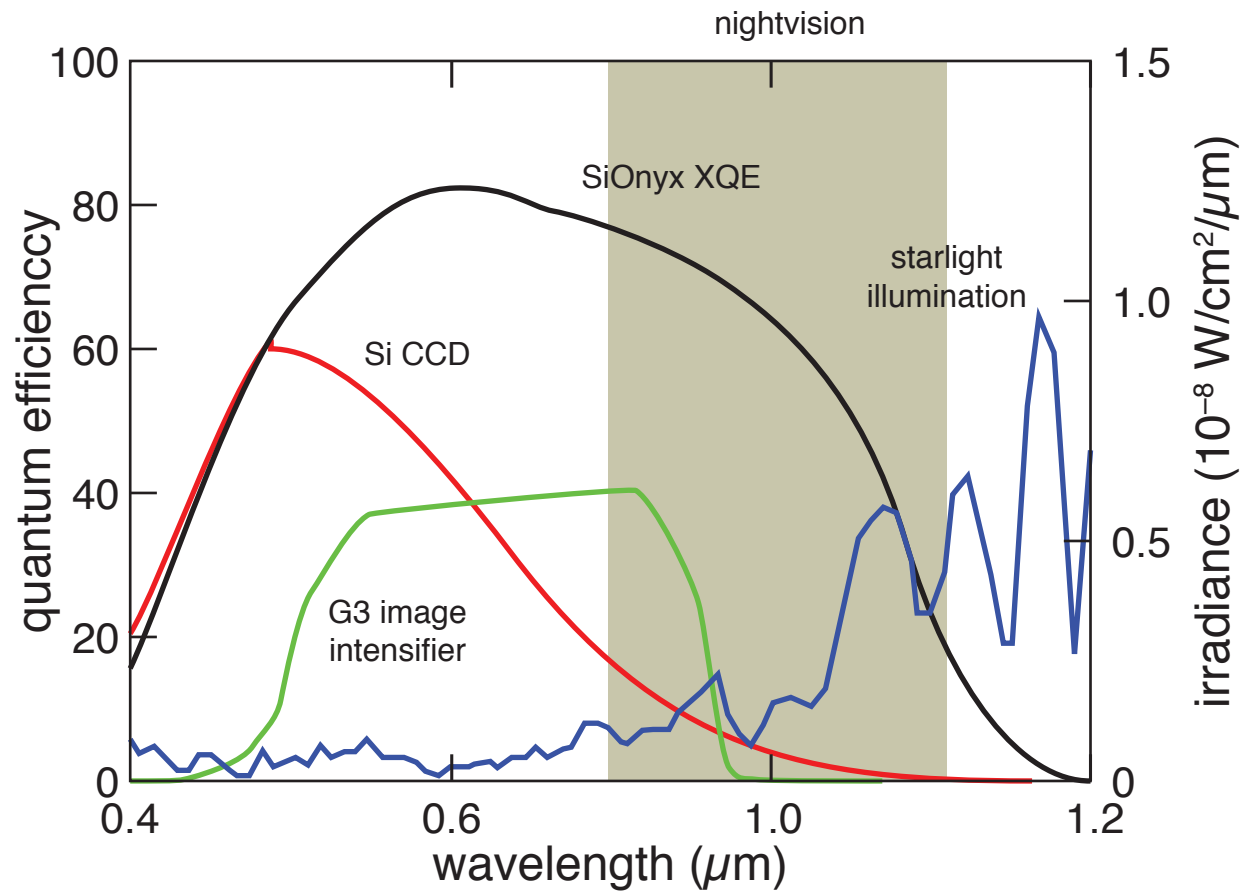




1 properties

2 intermediate band

3 devices



1 properties

2 intermediate band

3 devices

## Things to keep in mind

- can turn b:Si absorption into carrier generation

## Things to keep in mind

- can turn b:Si absorption into carrier generation
- very high responsivity in VIS and NIR

## Things to keep in mind

- can turn b:Si absorption into carrier generation
- very high responsivity in VIS and NIR
- disruptive improvement in Si imaging

## Things to keep in mind

- can turn b:Si absorption into carrier generation
- very high responsivity in VIS and NIR
- disruptive improvement in Si imaging
- potential benefits in solar energy harvesting



## Summary

- new doping process
- new class of material
- new types of devices

**1** properties

**2** intermediate band

**3** devices



A collection of colorful, star-patterned paper scraps is scattered on a white surface. The scraps are in various shades of blue, cyan, and purple, each featuring a pattern of small white stars. Some scraps are partially overlapping, and a few are plain white. The background is a soft, out-of-focus white.

**What is different about this process?**

**1** properties

**2** intermediate band

**3** devices



**Compare femtosecond laser doping to:**

- **inclusion during growth**
- **thermal diffusion**
- **ion implantation**

**1** properties

**2** intermediate band

**3** devices



**Funding:**

**Army Research Office**

**DARPA**

**Department of Energy**

**NDSEG**

**National Science Foundation**

**for more information and a copy of this presentation:**

**[ericmazur.com](http://ericmazur.com)**

**Follow me!**



**[eric\\_mazur](https://twitter.com/eric_mazur)**

**[sionyx.com](http://sionyx.com)**



**SiOnyx**